LES METAL·LOPROTEINASES DE MATRIU EXTRACEL·LULAR EN LA ISQUÈMIA CEREBRAL

Tesi doctoral presentada per

Sònia Solé i Tost

Barcelona, Maig del 2005

RESUM DE RESULTATS

Els resultats que s'han obtingut es presenten organitzats en forma d'articles que responen a les preguntes que ens hem plantejat en els objectius tal i com s'indica a continuació :

1) Article nº 1:

Estimation of gelatinase content in rat brain: effect of focal ischemia.

Planas AM**,** Solé S, Justicia C, Rodríguez-Farré E.

Biochem Biophys Res Comm 278: 803-807 (2000).

En aquest treball es va posar a punt la tècnica de la zimografia que permet detectar l'activitat de les gelatinases. Es va estimar el contingut de gelatinases (MMP-2 i MMP-9) en el cervell de la rata a nivell basal en 0.44 ng/mg de proteina, i es va veure que les gelatinases augmenten la seva activitat 1.7 vegades a les 4 hores després d'una isquèmia cerebral focal transitòria en la rata.(Objectiu 1).

2) Article nº 2:

Expression and activation of matrix metalloproteinase-2 and –9 in rat brain after transient focal cerebral ischaemia.

Planas AM, Solé S, Justicia C

Neurobiology of Disease 8: 834-846 (2001).

En aquest article es va determinar el patró espacial i temporal d'expressió i activació de les gelatinases després de la isquèmia, i se'n va localitzar l'origen cel·lular (*Objectiu 1*). Es va determinar que la MMP-9 presenta un pic a les 24 hores i està associada a les neurones i als tractes de fibres mielinitzades, mentre que la MMP-2 té un augment d'activitat a les 4 hores i un increment enorme als 4 dies, localitzant-se principalment en la micròglia reactiva.

3) Article nº 3:

Certain forms of matrix metalloproteinase-9 accumulate in the extracellular space after microdyalysis probe implantation and middle cerebral artery occlusion/reperfusion.

Planas AM, Justicia C, Solé S, Fríguls B, Cervera A, Adell A i Chamorro A .

Journal of Cerebral Blood Flow and Metabolism 22: 918-925 (2002).

En aquest article s'analitzà mitjançant la tècnica de la microdiàlisi in vivo si les gelatinases s'alliberen a l'espai extracel·lular després de la isquèmia (*Objectiu 2*).

Veiem que la isquèmia provoca un alliberament a l'espai extracel·lular de dímers i de la proforma de la MMP-9, però no de la forma de 88 KD observada prèviament en el teixit. Aquest augment està relacionat amb la infiltració de neutròfils de la sang al teixit lesionat després de la isquèmia.

4) Article nº 4:

Neutrophil infiltration increases matrix metalloproteinase-9 in the ischemic brain after occlusion/reperfusion of the middle cerebral artery in rats.

Justicia C, Panés J, Solé S, Cervera A, Deulofeu R, Chamorro A and Planas AM. *Journal of Cerebral Blood Flow and Metabolism* 23: 1430-1440. (2003).

En aquest treball s'intenta determinar si els neutròfils contribueixen significativament a l'augment de la MMP-9 que s'observa en el cervell postisquèmic i si participen en l'increment del volum de l'infart a les 24 hores (*Objectiu 3*) .Hem inhibit l'entrada de neutròfils al teixit isquèmic per mitjà de dues estratègies: la inducció de la neutropènia i el bloqueig de les proteines ICAM-1 mitjançant l'administració sistèmica d' anticossos.

Els resultats d'aquest estudi mostren que els neutròfils infiltrats són una important font de MMP-9 després de la isquèmia focal transitòria; que són els responsables de l'augment de la proforma de MMP-9 de 95-kDa que es troba al cervell (lliure al medi extracel·lular), però no modifiquen l'augment de la forma endògena de la MMP-9 de 88-kDa; i que la infiltració de neutròfils al teixit isquèmic no contribueix significativament a incrementar el volum de l'infart cerebral a les 24 hores en el nostre model.

5) Article nº 5:

Activation of matrix metalloproteinase-3 and agrin cleavage in cerebral ischaemia / reperfusion.

Solé S, Petegnief V, Gorina R, Chamorro A, Planas AM.

Journal of Neuropathology and Experimental Neurology. (2004).

Els resultats presentats en aquest article corresponen a *l'Objectiu 4.*

En aquest article veiem que la isquèmia cerebral produeix una activació de la MMP-3 a les 24 hores i als 4 dies postisquèmia, localitzant-se en neurones a les 24 hores, en la microvasculatura, en la microglia reactiva/macròfags a partir del 4 dies i en els oligodendròcits augmentada als 14 dies postisquèmia .En cultius cel·lulars, l'expressió de MMP-3 s'observa en neurones i, en menor mesura, en oligodendròcits madurs, però no en progenitors d'oligodendròcits, astròcits o

micròglia. La zimografia de caseïna ens revela activitat de la MMP-3 en els cultius de neurones.

Trobem un substrat de la MMP-3, l'agrina, localitzada en les neurones, en els astròcits reactius als 7 dies, en acúmuls al voltant dels vasos sanguinis als 4 dies i en les vesícules de fagocitosi de la microglia reactiva als 4 i als 14 dies. En cultius cel·lulars l'agrina s'expressa en neurones i astròcits .

Veiem que la MMP-3 degrada in vitro l'agrina neuronal present en homogenats de cervell .

També observem que després de la isquèmia (als 1, 4 i 7 dies) disminueix el contingut d'agrina de la membrana cel·lular i es genera una forma de pes molecular més baix de la forma neuronal de l'agrina, deguda segurament a proteolisi per la MMP-3.

6) Article nº 6:

Matrix Metalloproteinase-9 in mitotic human neuroblastoma SH-SY5Y cells.

Solé S, Sanfeliu C, Chamorro A, Planas AM (2004).

Els resultats presents en aquest article corresponen a *l'objectiu 5* i sugereixen que la MMP-9, o una proteïna molt semblant a la MMP-9, podria tenir un paper en la divisió cel·lular en els cultius de cèl·lules de neuroblastoma (línia SHSY5Y) .

Veiem que les cèl·lules en mitosi presenten una immunoreactivitat més alta (estudis en citometria de flux) i un increment de l'activitat gelatinasa (estudis de zimografia in situ), així com una expressió precisa, dinàmica i ben orquestrada d'aquesta proteïna en les diferents etapes de la divisió cel·lular.

Per altra banda, el creixement cel·lular es veu afectat per l'ús d'inhibidors de les MMPs, sense afectar-ne la viabilitat (estudis de creixement dels cultius) i augmenta el percentatge de cél·lules que estan en fase S i G2 reduint-se el de les que estan en G1 (estudis realitzats per citometria de flux).

Per últim observem que l'estimulació del creixement cel·lular amb el factor de creixement transformant (TGF-ζ) és depenent de l'activació de la MMP-9 cel·lular.

Article nº 1:

Estimation of gelatinase content in rat brain: effect of focal ischemia.

Planas AM, Solé S, Justicia C, Rodríguez-Farré E.

Departament de Farmacologia i Toxicologia, Institut d'Investigacions Biomèdiques de Barcelona, CSIC-IDIBAPS.

Publicat en la revista: *Biochem Biophys Res Comm* **278**: 803-807 (2000).

EL TEXT DE L'ARTICLE FIGURA COM A ANNEX_ARTICLE_1

Article nº 2:

Expression and activation of matrix metalloproteinase-2 and –9 in rat brain after transient focal cerebral ischaemia.

Planas AM, Solé S, Justicia C

Departament de Farmacologia i Toxicologia, Institut d'Investigacions Biomèdiques de Barcelona, CSIC-IDIBAPS.

Publicat en la revista: *Neurobiology of Disease 8: 834-846* (2001).

EL TEXT DE L'ARTICLE FIGURA COM A ANNEX_ARTICLE_2

Article nº 3:

Certain forms of matrix metalloproteinase-9 accumulate in the extracellular space after microdyalysis probe implantation and middle cerebral artery occlusion/reperfusion.

Planas AM, Justicia C, Solé S, Fríguls B, Cervera A, Adell A i Chamorro A

Departament de Farmacologia i Toxicologia i Departament de Neuroquímica de l' Institut d'Investigacions Biomèdiques de Barcelona, CSIC-IDIBAPS.
Servei de Neurologia de l'Hospital Clínic, IDIBAPS.

Publicat en la revista: *Journal of Cerebral Blood Flow and Metabolism* **22**: 918-925 (2002)

Journal of Cerebral Blood Flow & Metabolism
22:918–925 © 2002 The International Society for Cerebral Blood Flow and Metabolism
Published by Lippincott Williams & Wilkins, Inc., Philadelphia

Certain Forms of Matrix Metalloproteinase-9 Accumulate in the Extracellular Space After Microdialysis Probe Implantation and Middle Cerebral Artery Occlusion/Reperfusion

*Anna M. Planas, *Carles Justicia, *Sònia Solé, *Bibiana Friguls, ‡Álvaro Cervera, †Albert Adell, and ‡Ángel Chamorro

**Departament de Farmacologia i Toxicologia, †Departament de Neuroquímica, IIBB-CSIC, and ‡Servei de Neurología del Hospital Clínic, IDIBAPS, Barcelona, Spain*

Summary: Matrix metalloproteinases (MMPs) are activated in focal cerebral ischemia. The activation of MMP-9 is involved in blood–brain barrier breakdown and tissue remodeling. The MMPs are released to the extracellular space, but the form and fate of secreted enzymes in brain are unknown. Using microdialysis *in vivo*, the authors studied whether ischemia-induced MMP-9 in brain tissue was related to free MMP-9 in the extracellular fluid. A microdialysis probe was placed into the right striatum and microdialysis was initiated 24 hours later in controls (n = 7). One hour prior to microdialysis, a group of rats (n = 7) was subjected to 1-hour occlusion of the right middle cerebral artery, followed by reperfusion. Dialysates were collected at discrete time points up to 24 hours, and subjected to zymography and Western blot analysis. The MMP-9 was released after ischemia and accumulated in the extracellular space at 24 hours ($P < 0.05$). Free MMP-9 forms include mainly the 95-kd proform, and, to a lesser extent, dimers and cleaved active forms (70 kd), but not the 88-kd form found in tissue. Probe implantation and microdialysis increased free MMP-9 in the dialysate. This increase was concomitant with neutrophil infiltration after the mechanical lesion, as myeloperoxidase was found by means of Western blot analysis in the brain hemisphere subjected to microdialysis ($P < 0.005$), and immunohistochemistry revealed the presence of myeloperoxidase stain surrounding the site of probe implantation. The results suggest that certain forms of MMP-9 are released and accumulate in the extracellular space after brain injury, and that vascular alterations and neutrophil recruitment elicit MMP-9 activation in the brain after focal ischemia and trauma. **Key Words:** *In vivo* microdialysis—Focal ischemia—Neutrophils—Brain—Stroke—Injury.

Acute cerebral ischemia alters the cellular environment and affects neural cell viability through multiple alterations. Both the extracellular matrix and the extracellular fluid are part of the neural cell environment. The former maintains cells and tissues together and is a dynamic space suitable for intercellular communication. It consists of a complex network of macromolecules, mainly made of proteoglycans, that intensely interacts with cell membranes and blood vessels and that has regulatory and modulator properties (Bovolenta and Fernaud-Espinosa, 2000; Yamaguchi, 2000).

The extracellular matrix of the brain is not very extensive, compared with that in other tissues, because of the high cellular density and abundance of cell processes, but it is needed for the formation of perineuronal nets (Celio et al., 1998), in synaptic clefts (Yamaguchi, 2000), and around the endothelial wall of blood vessels (Yurchenco and Schittny, 1990). The basal lamina, which is located between the outer vessel wall and the surrounding astrocytic processes, is a specialized matrix that gives structural support to blood vessels and ensures integrity of the blood–brain barrier. Several zinc- and calcium-dependent matrix metalloproteinases (MMPs), like MMP-2 and MMP-9 (gelatinase A and B, respectively), degrade components of the basal lamina, causing disruption of the blood brain–barrier (Mun-Bryce and

Received January 7, 2002; final version received April 2, 2002; accepted April 2, 2002.

This study was supported by a grant from FIS (00/0957). S. Solé and B. Friguls received fellowships from the IDIBAPS and the University of Barcelona, respectively. Á. Cervera was supported by the Fundació Clínic.

Address correspondence and reprint requests to Dr. Anna M. Planas, Departament de Farmacologia i Toxicologia IIBB-CSIC, IDIBAPS Rosselló, 161, planta 6, E-08036 Barcelona, Spain; e-mail: ampfat@iibb.csic.es

Rosenberg, 1998; Rosenberg et al., 1992, 1995). Microvascular basal lamina antigens disappear after cerebral ischemia (Hamann et al., 1995) and there is evidence that MMP-9 and MMP-2 are involved in blood–brain barrier breakdown after ischemia (Gasche et al., 1999; Rosenberg et al., 1998). Matrix metalloproteinases increase in the brain after ischemia in animal models (Fujimura et al., 1999; Gasche et al., 1999; Heo et al., 1999; Planas et al., 2000, 2001; Romanic et al., 1998; Rosenberg et al., 1994, 1996, 2001) and in humans (Clark et al., 1997). Increase of MMP-9 in brain is associated with hemorrhagic transformation (Heo et al., 1999), and increase of MMP-9 in plasma is predictive of hemorrhagic transformation after cardioembolic stroke (Montaner et al., 2001). Pharmacologic inhibition of MMPs reduces thrombolytic-induced hemorrhage after thromboembolic middle cerebral artery (MCA) occlusion in rabbits (Lapchak et al., 2000), decreases infarct volume after focal ischemia in rodents (Asahi et al., 2000; Romanic et al., 1998), and prevents oxidative stress-associated blood–brain barrier disruption after transient MCA occlusion in mice (Gasche et al., 2001). Also, deletion of the MMP-9 gene reduces infarct volume after ischemia (Asahi et al., 2000).

Matrix metalloproteinases contribute to signaling between the extracellular environment and cells, and to tissue degradation after brain lesion (Bruno et al., 1998; Lukes et al., 1999; Mun-Bryce and Rosenberg, 1998), as they degrade myelin basic protein (Gijbels et al., 1993) and other neural proteins and peptides (Backstrom and Tökés, 1995). Furthermore, MMPs are involved in various diseases of the central nervous system (Kieseier et al., 1999; Lukes et al., 1999; Yong et al., 2001). Cells synthesize MMPs as proforms, with the catalytic side hidden from substrates. Upon activation, they can suffer proteolytic cleavage, which exposes their active sites (Springman et al., 1990; Woesser, 1991). Matrix metalloproteinase 9 is released from the producer cells to degrade components of the extracellular matrix, although the extracellular release of MMP-9 in the brain following ischemia is unknown. In the present study, we aimed to test whether MMP-9 is released and accumulates in the extracellular fluid after ischemia *in vivo,* to determine its time course, and to identify the released MMP forms. This information will contribute to a better understanding of the mechanism of MMP-9 activation in the brain, which will lead to further designs of inhibitory drugs. Microdialysis is a tool for sampling interstitial compound concentration within the local brain tissue environment where the microdialysis probe is inserted (Adell and Artigas, 1997). We used *in vivo* microdialysis in the rat to measure MMP-9 in dialysates as an indicator of the release to the extracellular fluid within the 24 hours that follow MCA occlusion with reperfusion.

MATERIALS AND METHODS

In vivo brain microdialysis

Male Sprague-Dawley rats (280–320 g) obtained from Iffa-Credo (Lyon, France) were kept in a 12-hour light-dark cycle and allowed free access to food and water. Animal work was conducted in compliance with the Spanish legislation regarding the protection of animals used for experimental and other scientific purposes, and in accordance with the directives of the European Union on this subject. Rats were subjected to cerebral microdialysis following the method of Adell and Artigas (1998), with modifications. The day before ischemia, the rats were anesthetized with 4% halothane (Fluothane; Zeneca) in a mixture of 70% N_2O and 30% O_2 through a face mask. They were placed on a stereotaxic frame (Kopf Instruments) and anesthesia was maintained with 1.5% to 2% halothane. After making a cranial midline skin incision, a microdialysis probe (MAB2; Microbiotech, Stockholm, Sweden) was implanted into the right striatum through a burr hole at the following co-ordinates: 1.2 mm anteroposterior, 2.5 mm lateral, and 6 mm ventral to bregma (Paxinos and Watson, 1986). The membrane on the probe was made of polyether sulphone and had an outer diameter of 0.6 mm and a length of 3 mm. The probe was fixed to the skull with two miniature screws and dental cement. The wound was sutured and the animal was allowed to recover for 24 hours. Thereafter, one-hour transient MCA occlusion was carried out in the hemisphere ipsilateral to probe implantation ($n = 7$), and reperfusion was allowed. Rats were allowed to recover from anesthesia for 30 minutes, placed in a plastic cage with a mounted liquid swivel system (Instech Laboratories, Plymouth Meeting, PA, U.S.A.) and microdialysis was initiated. In a group of control rats, microdialysis was initiated without any intervention, other than probe implantation the day before ($n = 7$). Microdialysis was carried out in the awake, freely moving rat by pumping artifical CSF containing 125 mmol/L NaCl, 2.5 mmol/L KCl, 1.18 mmol/L $MgCl_2$, and 1.26 mmol/L $CaCl_2$ at a constant rate (1 μL/min) and samples were collected as 10-minute fractions. In preliminary experiments ($n = 4$), perfusion and fraction collection was continuously carried out for about 10h, but this procedure led to continuous draining and did not allow for significant accumulation of MMPs in the dialysates. Before dialysate collection, an initial wash with artificial CSF (10 μL/min) was performed 30 minutes after 1-hour ischemia (i.e., 24 hours after probe implantation). Microdialysis was then carried out discontinuously for 40 minutes (as four 10-minute fractions) at 0.5, 5.5, 10.5, and 24 hours after the initial 10-minute wash. Thus, the first dialysate was taken after 1 hour of reperfusion. Thereafter, certain rats subjected to microdialysis and controls (rats not subjected to any surgical procedure) were anesthetized, killed, and the ipsilateral and contralateral cortex and striatum were removed. Tissues and microdialysis samples were immediately frozen in liquid nitrogen and kept at −80°C until further analysis.

Focal cerebral ischemia

Focal cerebral ischemia was produced by transient intraluminal occlusion of the MCA according to the method of Longa et al. (1989), with modifications as previously reported (Justicia et al., 2001). Briefly, rats were anesthetized with 4% halothane in a mixture of 70% N_2O and 30% O_2. After tracheal intubation for controlled ventilation, anesthesia was maintained with 1% to 1.5% halothane. The left femoral artery was cannulated to monitor blood pressure, and body temperature was maintained at 37.5°C with a heating pad controlled by a thermoregulatory system connected to a rectal probe. A 2.6-cm

length of 3–0 monofilament nylon suture heat-blunted at the tip was introduced into the external carotid artery through a puncture. In addition, both common carotid arteries were clamped to minimize collateral circulation, as reported elsewhere (Soriano et al., 1997). After 50 minutes of ischemia, the clip on the left common carotid artery was released and reperfusion was visually assessed. Ten minutes later the filament was gently removed and the clip on the right common carotid artery was released. Following surgery, rats were allowed to recover spontaneous breathing and were kept in their cages with free access to food and water.

Gel zymography

Gel zymography was carried out with dialysate samples (10 μL) or brain tissue samples previously homogenized and subjected to extraction of gelatinase activity following the method of Zhang and Gottschall (1997), with modifications (Planas et al., 2001). Gels containing 10% acrylamide and porcine gelatin (1 mg/mL) were prepared. Samples were loaded in zymography loading buffer containing 80 mmol/L Tris-HCl (pH 6.8), 4% sodium dodecyl sulphate (SDS), 10% glycerol, and 0.01% bromophenol blue. A known amount of MMP-9 and MMP-2 standard (CC073; Chemicon International) was loaded in one lane of each gel. SDS/PAGE was carried out at 25 mA at 4°C. Gels were briefly washed in distilled water and then three times for 15 minutes each using 150 mL 2.5% Triton ×100 at room temperature, before incubation in 250 mL buffer containing 50 mmol/L Tris-HCl (pH 7.5), 10 mmol/L $CaCl_2$, and 0.02% NaN_3 for 42 hours at 37°C. After the incubation period, gels were stained in 150 mL 0.1% amido black (naphthol blue black; Sigma) in a 1:3:6 mixture of acetic acid:methanol:distilled water for 1 hour at room temperature. Gels were then unstained in 150 mL 1:3:6 acetic acid:methanol:distilled water four times for 30 minutes each, and were then washed in distilled water for 20 minutes.

Western blot

The presence of MMP-9 protein in dialysates was studied by Western blot analysis. Dialysate samples (10 μL) were mixed with loading buffer (as for zymography) and were loaded in 10% polyacrylamide gels for electrophoresis. Proteins were then transferred to a membrane (Immobilon-P, Millipore) that was incubated overnight at 4°C with the primary antibody, mouse monoclonal antibody against MMP-9 Ab2 (MAB 13420; Chemicon) diluted 1:150. In brain tissue, myeloperoxidase (MPO) expression was studied by Western blot analysis in the same rats used for microdialysis. For this study we used an aliquot of crude tissue homogenates, as MPO is tightly bound to membranes. Protein content in these fractions was determined (Bradford assay; Bio-Rad). Samples were diluted with loading buffer containing DTT, heated at 100°C for 5 minutes, and loaded on a denaturing 10% polyacrylamide gel for electrophoresis. Proteins were transferred to a membrane incubated with mouse monoclonal antibody against MPO (Menarini Diagnostics) diluted 1:500. A rabbit polyclonal antibody against actin (Sigma) diluted 1:10,000 was used as a control for protein gel loading. Secondary antibodies were peroxidase-linked antimouse or antirabbit Ig (Amersham), diluted 1:2,000. The reaction was developed with a chemiluminescence reagent containing luminol.

Immunohistochemistry

At 48 hours after probe implantation (24 hours after MCA occlusion) rats were perfused with 4% paraformaldehyde and their brains were postfixed overnight with the same fixative, embedded in paraffin, and cut into 5-μm thick coronal sections using a microtome. Paraffin was removed, endogenous peroxidases were blocked with methanol-H_2O_2, and unspecific-binding sites were blocked with 10% normal goat serum for 2 hours. Sections were then incubated with a rabbit polyclonal antibody against MPO (diluted 1:800; A 0398; Dako) for 2 hours at room temperature, biotinylated goat antirabbit antibody (diluted 1:200; Vectastain; Vector) for 1 hour, and the avidin-biotin complex (diluted 1:100; ABC kit; Vector Laboratories) for 1 hour. The reaction was developed with 0.05% diaminobenzidine and 0.03% H_2O_2.

Data analysis

Gels were scanned with a Kodak camera (DC-120) and analyzed with appropriate software (Kds1D; Kodak). In order to

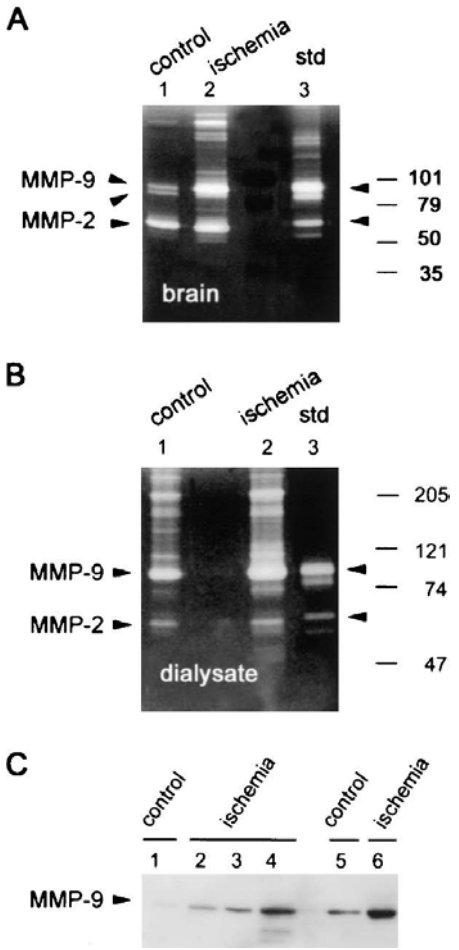

FIG. 1. Gel zymography **(A** and **B)** and Western blot analysis **(C)** show increased matrix metalloproteinase-9 (MMP-9) expression 24 hours after 1-hour middle cerebral artery occlusion followed by reperfusion. **(A)** Brain tissue from ischemic and control rats not subjected to dialysis. Two MMP-9 bands (95 and 88 kd) are detected. An increase in MMP-9 is seen at 24 hours. **(B)** Ischemia increases MMP-9 in dialysates, but the nonischemic rats subjected to microdialysis also show MMP-9. Dialysates from ischemic and control rats show 95-kd MMP-9 proform and dimers, and a cleaved form of approximately 70 kd, but the 88-kd form found in tissue is not detected. Std, MMP-9 and MMP-2 standards. Numbers in the right side indicate molecular weight markers. **(C)** The 95-kd MMP-9 protein is detected by Western blot analysis in the dialysates after ischemia (at 0.5 hours in lane 2, 10.5 hours in lane 3, and at 24 hours in lanes 4 and 6) and, to a lesser extent, in controls (at 24 hours, lanes 1 and 5).

compare data from different gels, raw band intensity values of the samples were normalized by calculating the ratio between their net band intensity and net band intensity of an MMP-9 standard in each gel. We then applied two-way ANOVA by treatment (ischemic or control) and time (of sample collection), followed by the Bonferroni *post hoc* test. Values are expressed as mean ± SEM of net band intensity measures. The MPO data from Western blot analyses were also measured (expressed as percent of mean control), and analyzed with one-way ANOVA and the Bonferroni test.

RESULTS

Matrix metalloproteinases in the tissue and dialysates 24 hours after middle cerebral artery occlusion/reperfusion

Zymography in gelatinolytic extracts from brain homogenates revealed that MMP-9 and MMP-2 are expressed in the control rat brain (Fig. 1A). This technique allowed us to detect several bands, mainly one MMP-9 proform band of 95 kd and one intermediate form of 88 kd, together with one form of MMP-2 that was approximately 65 kd and the most intense band in the gel. In addition, MMP-9 forms dimers found at 210 kd. Band intensity for MMP-9 increased at 24 hours after ischemia in extracts of brain homogenates (Fig. 1A). The *in vivo* microdialysis technique revealed several bands in the dialysates, even in control rats not subjected to ischemia (Fig. 1 B). Bands detected in the dialysate were 95-kd MMP-9 and dimeric MMP-9 forms, and, to a lesser extent, MMP-2, whereas the 88-kd form of MMP-9 found in tissue was not detected in the dialysate (Fig. 1B). At 24 hours after MCA occlusion/reperfusion, MMP-9 bands in the dialysate were more intense than in the corresponding timed controls (Fig. 1B). The presence of a 95-kd MMP-9 proform in the extracellular space was also evidenced by Western blot analysis of the dialysate samples (Fig. 1C).

In vivo brain microdialysis: time course

Zymographic analysis of dialysates showed bands corresponding to MMP-9 and MMP-2 proforms in ischemic (Fig. 2A) and control (Fig. 2B) rats. Matrix metalloproteinases were found in the dialysates of all ischemic rats (six), whereas no signal was detected in two out of six controls. These two control rats were not considered in the statistical analysis in order to find differences between controls and ischemic rats showing MMP-9. The intensity of the 95-kd MMP-9 band after ischemia was higher than in controls and accumulated at 24 hours, which was the longest time point studied here (Figs. 2A and 2B). A two-way ANOVA, by treatment (ischemic versus controls) and time, showed a significant difference after ischemia ($F_{1,28} = 5.68$, $P < 0.05$), and the Bonferroni post hoc test showed that ischemia increased 95-kd MMP-9 at 24 hours ($P < 0.05$) compared with controls. Western blot analysis also showed that the abundance of free MMP-9 protein increased from the beginning of microdialysis (Fig. 1C, lane 2: 0.5 hours, and lane 3: 10.5 hours) to 24 hours (Fig. 1C, lanes 4 and 6) after ischemia, and to a lesser extent in controls (Fig. 1C, lanes 1 and 5).

Source of matrix metalloproteinase-9

We investigated whether neutrophils had infiltrated the tissue by examining MPO expression at the end of

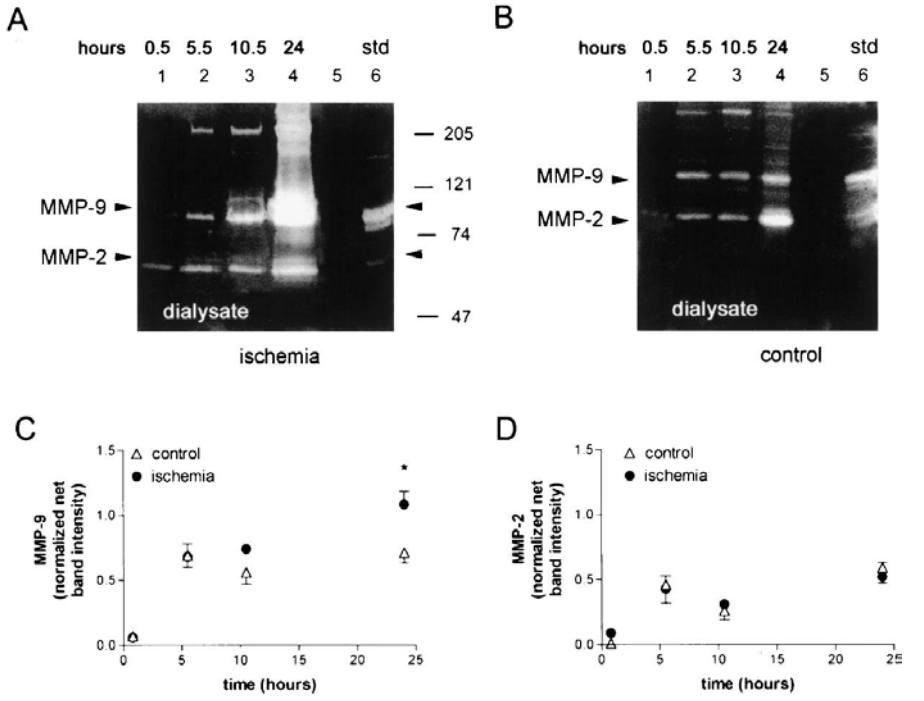

FIG. 2. **(A** and **B)** Gel zymography of dialysates of ischemic **(A)** and control **(B)** rats obtained at several time points after the beginning of microdialysis (0.5, 5.5, 10.5, and 24 hours, lanes 1 to 4), which correspond to 1, 6, 11, and 24 hours after middle cerebral artery occlusion. Matrix metalloproteinases (MMP) accumulate in the dialysate. **(C** and **D)** Densitometric measurements of 95-kd MMP-9 **(C)** and MMP-2 **(D)**. Ischemia causes release and accumulation of MMP-9 to the extracellular space at 24 hours compared with controls. Net band intensity data of samples is normalized by the intensity of the standard in each gel. $^*P < 0.05$ as tested with two-way ANOVA by treatment (ischemic vs. control) and time. Std, MMP-9 and MMP-2 standards. Numbers on the right side show molecular weight markers.

the study (i.e., 48 hours after probe implantation). Indeed, we found that nonischemic rats subjected to probe implantation and microdialysis showed MPO expression in homogenates of the ipsilateral, but not the contralateral, hemisphere, to an extent comparable with that seen in the corresponding ischemic rats (Fig. 3A). Measures of MPO net band intensity in Western blots followed by one-way ANOVA showed that, compared with the contralateral hemisphere, the ipsilateral hemisphere had a 7-fold and 10-fold increase in control ($P < 0.05$) and ischemic rats ($P < 0.01$), respectively.

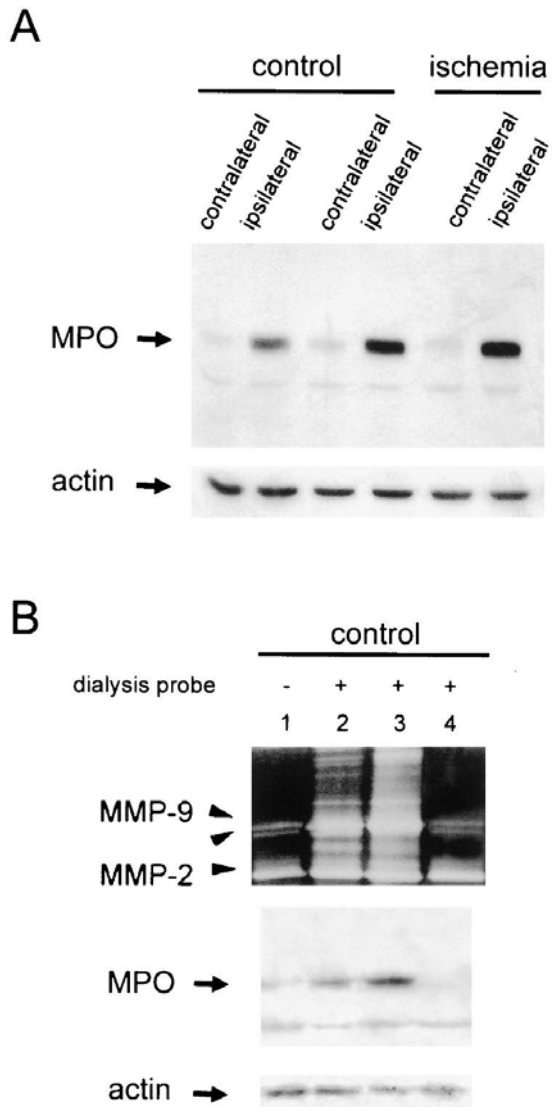

FIG. 3. (A) Western blot showing myeloperoxidase (MPO) expression in brain homogenates obtained from dialyzed rats. No MPO is detected in the contralateral hemisphere, whereas MPO expression is markedly increased in the hemisphere ipsilateral to microdialysis. MPO is found even in control dialyzed rats not subjected to ischemia. Actin is shown to illustrate the amount of loaded protein in each lane of the gel. **(B)** Zymographic analysis of brain tissue from controls showing that probe implantation caused increase of matrix metalloproteinase-9 (MMP-9) bands in certain rats. Brain MMP-9 increases were associated to expression of MPO in the parenchyma of the same brain tissues. Actin illustrates protein gel loading.

We examined MMPs in the brains of control (nonischemic) rats subjected to microdialysis and compared the dialyzed hemisphere with the nondialyzed hemisphere and with that of nonoperated controls. Microdialysis largely increased 95-kd MMP-9 proform and MMP-9 dimers in the brain (Fig. 3B), an effect that might be attributable to the mechanical injury caused by the intracerebral probe. This effect was concomitant with the appearance of MPO expression in brain tissue (Fig. 3B). We investigated whether brain MMP-9 had increased in the two control rats subjected to microdialysis that showed no MMP-9 in the dialysates. We found no MMP-9 increase in these brains and no MPO was detected (Fig. 3B), suggesting that those rats suffered little traumatic damage after probe implantation.

In rats showing MMP-9 in dialysates, immunohistochemistry against MPO showed the massive presence of neutrophils in the area surrounding the site of microdialysis probe implantation (Figs. 4A and 4B, control; Figs. 4C and 4D, ischemia). Infiltration of isolated neutrophils within the parenchyma was exclusively seen in rats subjected to ischemia (Figs. 4E and 4F).

Free and bound matrix metalloproteinase-9 forms

The 88-kd MMP-9 form detected in tissue homogenate was not observed in brain dialysates (Fig. 1). Before zymography, brain homogenates were subjected to extraction of gelatinolytic activity (see Materials and Methods), whereas brain dialysates were directly analyzed. A similar procedure was used for dialysate samples to rule out that the 95-kd form had been cleaved to the 88-kd form *in vitro* during extraction. However, the 88-kd MMP-9 form was not detected in the extracted dialysate (data not shown). Therefore, this form was not soluble in the extracellular fluid, and is likely associated with cells or bound to the matrix. In addition to the 95-kd MMP-9 proform, which was the major MMP-9 form in the dialysate, and the dimeric forms, a minor band of lower molecular weight (approximately 70 kd) was observed at 24 hours when the fraction corresponding to the proform was very high (Figs. 1B and 2).

DISCUSSION

Matrix metalloproteinases contribute to basement membrane degradation and blood–brain barrier breakdown, and play many other roles (Mun-Bryce and Rosenberg, 1998). Here we show, by *in vivo* microdialysis, that 95-kd MMP-9 progressively accumulated in brain dialysates from the striatum during reperfusion after focal ischemia. This finding suggests that MMP-9 is released and accumulates in the extracellular space after ischemia. Matrix metalloproteinase 9 was also detected

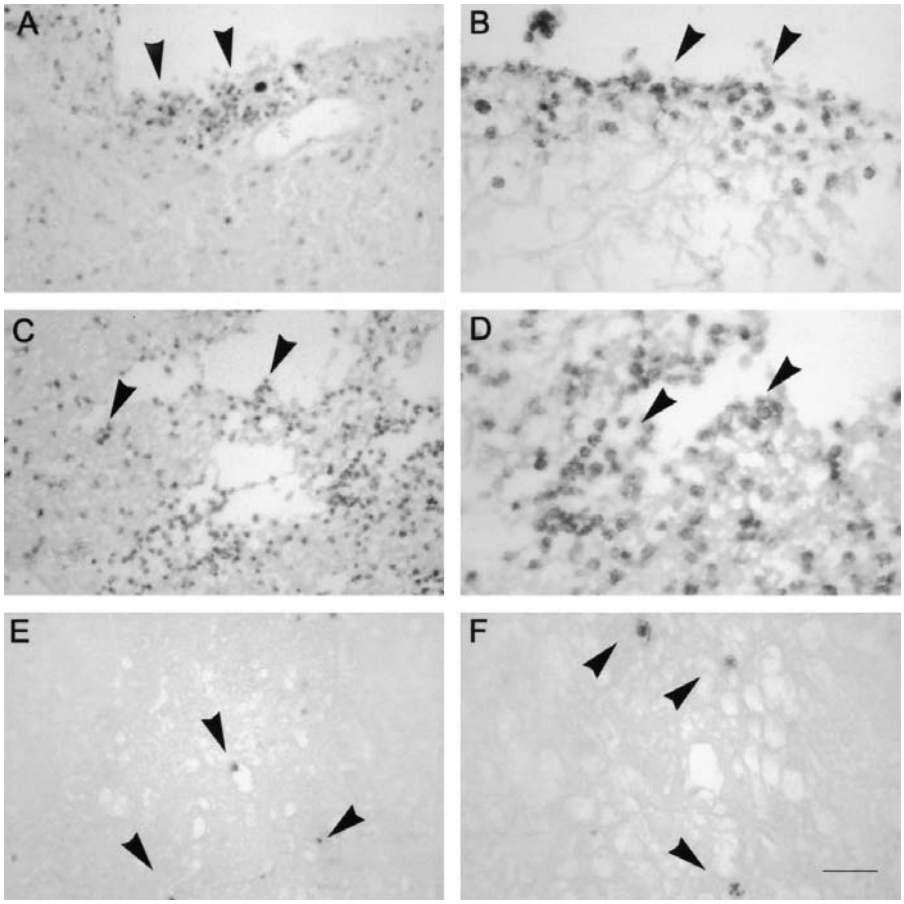

FIG. 4. Immunohistochemistry against myeloperoxidase (MPO; 48 hours after microdialysis probe implantation; i.e., 24 hours after ischemia) shows neutrophil accumulation (dark cells) in the area surrounding the site of probe implantation (arrows in **A–D**) in controls **(A** and **B)** and in rats subjected to ischemia **(C** and **D)**. In addition, infiltration of several isolated neutrophils (arrows) was observed within the parenchyma of ischemic rats **(E** and **F)**. Bar scale = 90 μm **(A, C, E)** and 45 μm **(B, D, F)**.

in the dialysates of some control brains, although this does not necessarily imply that MMP-9 is normally free in the extracellular space. Indeed, we have evidence suggesting that the mechanical lesion caused by microdialysis probe implantation is responsible, at least in part, for 95-kd MMP-9 accumulation in the dialysates from controls. First, the brain hemisphere subjected to microdialysis in controls showed increased intensity of MMP-9 zymographic bands compared with the nonoperated hemisphere and with rats not subjected to probe implantation. Second, we found the presence of MPO expression (Wright et al., 1987) in the control brains subjected to microdialysis at 48 hours after probe implantation, and MPO-stained neutrophils surrounded the site of probe implantation. Two out of six controls showed no MMP-9 in the dialysates, and no raise in MMP-9 levels was detected in the brains of those rats, which did not show MPO expression. These findings support the idea that vascular damage and neutrophil infiltration are involved in MMP-9 release to the extracellular space after brain injury. Indeed, injury caused by probe implantation disrupts the blood–brain barrier in the vicinity of the probe, which leads to vasogenic edema (Dykstra et al., 1992). This appears to be a transient alteration and the integrity of the blood–brain barrier may recover after 1 hour of probe implantation (Benveniste et al., 1984; Terasaki et al., 1992). However, the blood–brain barrier remains permeable to small molecules for a few days after probe implantation, although it recovers earlier for permeability to proteins (Morgan et al., 1996). *A priori*, we decided to carry out microdialysis 24 hours after inserting the probe as the barrier should be at least partially recovered. However, the initial lesion facilitated capillary damage and neutrophil recruitment.

It is likely that a mechanical lesion caused by the microdialysis probe induces MMP-9 accumulation in the extracellular space at the time ischemia was induced (24 hours after probe implantation). Then ischemia would progressively contribute to extracellular MMP-9 accumulation for the following 24 hours, as a significant increase of free MMP-9 was found in the dialysates of rats subjected to ischemia compared with control dialysates. Previous studies using reverse transcription polymerase chain reaction showed increased MMP-9 mRNA production after ischemia (Asahi et al., 2000), showing that ischemia triggers *de novo* synthesis of MMP-9 proform. Similarly to MMP-9 expression, infiltration of neutrophils peaks 24 to 48 hours after cerebral ischemia (Garcia et al., 1994) and traumatic brain injury (Royo et al, 1999). Neutrophils are rich in MMP-9 (Kjeldsen et al.,

1992), and MMP-9 labeling has been detected by immunohistochemistry in infiltrated neutrophils after ischemia (Romanic et al., 1998; Rosenberg et al., 2001). Furthermore, blockade of neutrophil infiltration reduces MMP-9 accumulation in the brain after ischemia (C. Justicia and A.M. Planas, unpublished data, 2002). Therefore, it is feasible that neutrophils themselves are a source of extra-MMP-9 expression and activity in the brain and contribute to the induction of MMP-9 expression in the tissue, as has been found in the myocardium following ischemia/reperfusion (Lindsey et al., 2001). However, the detection of infiltrating neutrophils in the tissue subjected to microdialysis does not fully rule out other sources of MMP-9.

Early increases in MMP-9 proform have been reported in brain tissue homogenates as soon as 2 to 4 hours after permanent MCA occlusion in mice (Asahi et al., 2000; Gasche et al., 1999). Likewise, MMP-9 is enhanced after 3 to 4 hours of reperfusion following 1-hour MCA occlusion in mice (Fujimura et al., 1999; Gasche et al., 2001) and rats (Planas et al., 2000). These early increases in MMP-9 are further enhanced at 10 to 15 hours and at 24 hours in permanent ischemia in rats (Romanic et al., 1998) and mice (Asahi et al., 2000), and after ischemia/reperfusion in rats (Planas et al., 2001; Rosenberg et al., 1998). We detected significant accumulation of MMP-9 only in the extracellular fluid from 12 to 24 hours after ischemia, but not earlier. However, we may have failed to detect low levels of MMP-9 for two reasons. First, microdialysis can induce neutrophil infiltration to the damaged striatum and MMP-9 release. Second, we probably obtained only a fraction of what is in the extracellular fluid in the dialysate, as we do not know the recovery of the technique. These constraints prevented us from determining the exact time at which ischemia-induced MMP-9 release was initiated. However, the finding of accumulation of MMP-9 in the extracellular space at 24 hours is robust and consistent with the results reported for tissue homogenates.

In addition to the increase in the 95-kd MMP-9 proform, a MMP-9 form of lower molecular weight (88 kd), which was taken as an active MMP-9 form (Zhang et al., 1998), has been described in brain tissue (Planas et al., 2000, 2001; Zhang and Gotshall, 1997; Zhang et al., 1998). In ischemia, the 88-kd form increases during the first hours of reperfusion in mice (Fujimura et al., 1999) and rats (Planas et al., 2000), and after permanent ischemia in mice (Gasche et al., 1999). However, the MMP forms that we found in the dialysates did not include the 88-kd form, thus implying that it is not soluble in the extracellular fluid. This form may be trapped in the extracellular matrix or it may bind to the cells, as there is evidence that certain MMP-9 forms are associated with cytoskeletal proteins or other structural proteins (Nelson and Siman, 1989).

In contrast to MMP-9, no major accumulation of MMP-2 due to ischemia was detected in the dialysate at 24 hours. Previous examinations of brain tissue homogenates in rats showed no major MMP-2 increases at 24 hours, but persistent activation was found at 4 to 5 days after focal ischemia/reperfusion (Planas et al., 2001; Rosenberg et al., 1998) and permanent focal ischemia (Romanic et al., 1998) associated with macrophagic cells.

In conclusion, ischemia induced progressive MMP-9 release into the extracellular space and accumulation by 24 hours. Mechanical injury caused by microdialysis triggered release of MMP-9 that was accompanied with the presence of neutrophils. The major form of MMP-9 in the dialysates was the 95-kd proform and dimeric forms, whereas the 88-kd form observed in the tissue was not found in dialysates. We propose that vascular alterations and neutrophil infiltration contribute to MMP-9 release and accumulation in the extracellular space of the brain after mechanical injury and focal ischemia.

REFERENCES

Adell A, Artigas F (1997) *In vivo* brain microdialysis: principles and applications. In: *Neuromethods: general techniques, in vivo*, vol 32 (Boulton AA, Baker GB, Bateson AN, eds), Totowa: Humana Press, pp 1–33

Adell A, Artigas F (1998) A microdialysis study of the *in vivo* release of 5-HT in the media raphe nucleus of the rat. *Br J Pharmacol* 125:1361–1367

Asahi M, Asahi K, Jung J-C, del Zoppo GJ, Fini ME, Lo EH (2000) Role of matrix metalloproteinase 9 after cerebral ischemia: effects of gene knockout and enzyme inhibition with BB-94. *J Cereb Blood Flow Metab* 20:1681–1689

Backstrom JR, Tökés ZA (1995) The 84-kDa form of human matrix metalloproteinase-9 degrades substance P and gelatin. *J Neurochem* 64:1312–1318

Benveniste H, Drejer J, Schousboe A, Diemer NH (1984) Elevation of the extracellular concentrations of glutamate and aspartate in rat hippocampus during transient cerebral ischemia monitored by intracerebral microdialysis. *J Neurochem* 43:1369–1374

Bovolenta P, Fernaud-Espinosa I (2000) Nervous system proteoglycans as modulators of neurite outgrowth. *Prog Neurobiol* 61:113–132

Bruno G, Todor R, Lewis I, Chayette D (1998) Vascular extracellular matrix remodeling in cerebral aneurysms. *J Neurosurg* 8:259–282

Celio MR, Spreafico R, De Biasi S, Vitellaro-Zuccarello L (1998) Perineuronal nets: past and present. *Trends Neurosci* 21:520–515

Clark AW, Krekoski CA, Bou SS, Chapman KR, Edwards DR (1997) Increased gelatinase A (MMP-2) and gelatinase B (MMP-9) activities in human brain after focal ischemia. *Neurosci Lett* 238:53–56

Dykstra KH, Hsiao JK, Morrison PF, Bungay PM, Mefford IN, Scully MM, Dedrick RL (1992) Quantitative examination of tissue concentration profiles associated with microdialysis. *J Neurochem* 58:931–940

Fujimura M, Gasche Y, Morita-Fujimura Y, Massengale J, Kawase M, Chan PH (1999) Early appearance of activated matrix metalloproteinase-9 and blood-brain barrier disruption in mice after focal cerebral ischemia and reperfusion. *Brain Res* 842:92–100

Garcia JH, Liu KF, Yoshida Y, Lian J, Chen S, del Zoppo GJ (1994) Influx of leukocytes and platelets in an evolving brain infarct (Wistar rat). *Am J Pathol* 144:188–199

Gasche Y, Copin J-C, Saguwara T, Fujimura M, Chan PH (2001) Matrix metalloproteinase inhibition prevents oxidative stress-associated blood-brain barrier disruption after transient focal cerebral ischemia. *J Cereb Blood Flow Metab* 21:1393–1400

Gasche Y, Fujimura M, Morita-Fujimura Y, Copin JC, Kawase M, Massengale J, Chan, PH (1999) Early appearance of activated matrix metalloproteinase-9 after focal cerebral ischemia in mice: a possible role in blood-brain barrier dysfunction. *J Cereb Blood Flow Metab* 19:1020–1028

Gijbels K, Proost P, Masure S, Carton H, Billiau A, Opdenakker G (1993) Gelatinase B is present in the cerebrospinal fluid during experimental autoimmune encephalomyelitis and cleaves myelin basic protein. *J Neurosci Res* 36:432–440

Hamann GF, Okada Y, Fitridge R, del Zoppo GJ (1995) Microvascular basal lamina antigens disappear during cerebral ischemia and reperfusion. *Stroke* 26:2120–2126

Heo JH, Lucero J, Abumiya T, Koziol JA, Copeland BR, del Zoppo GJ (1999) Matrix metalloproteinases increase very early during experimental focal cerebral ischemia. *J Cereb Blood Flow Metab* 19:624–633

Justicia C, Pérez-Asensio FJ, Burguete MC, Salom JB, Planas AM (2001) Administration of transforming growth factor-α reduces infarct volume after transient focal cerebral ischemia in the rat. *J Cereb Blood Flow Metab* 21:1097–1104

Kieseier BC, Seifert T, Giovannoni G, Hartung, HP (1999) Matrix metalloproteinases in inflammatory demyelination: targets for treatment. *Neurology* 53:20–25

Kjeldsen L, Bjerrum OW, Hovgaard D, Johnsen AH, Sehested M, Borregaard N (1992) Human neutrophil gelatinase: a marker for circulating blood neutrophils. Purification and quantitation by enzyme linked immunosorbent assay. *Eur J Haematol*, 49:180–191

Lapchak PA, Chapman DF, Zivin JA (2000) Metalloproteinase inhibition reduces thrombolytic (tissue plasminogen activator)-induced hemorrhage after thromboembolic stroke. *Stroke* 31:3034–3040

Lindsey M, Wedin K, Brown MD, Keller C, Evans AJ, Smolen J, Burns AR, Rossen RD, Michael L, Entman M (2001) Matrix-dependent mechanism of neutrophil-mediated release and activation of matrix metalloproteinase 9 in myocardial ischemia/reperfusion. *Circulation* 103:2181–2187

Longa EZ, Weinstein PR, Carlson S, Cummins R (1989) Reversible middle cerebral artery occlusion without craniotomy in rats. *Stroke* 20:84–91

Lukes A, Mun-Bryce S, Lukes M, Rosenberg GA (1999) Extracellular matrix degradation by metalloproteinases and central nervous system diseases. *Mol Neurobiol* 1999;19:267–284

Montaner J, Alvarez-Sabín J, Molina CA, Anglés A, Abilleira S, Arenillas J, and Monasterio J (2001) Matrix metalloproteinase expression is related to hemorrhagic transformation after cardioembolic stroke. *Stroke* 32:2762–2767

Morgan ME, Singhal D, Anderson BD (1996) Quantitative assessment of blood-brain barrier damage during microdialysis. *J Pharmacol Exp Ther* 277:1167–1176

Mun-Bryce S, Rosenberg GA (1998) Gelatinase B modulates selective opening of the blood-brain barrier during inflammation. *Am J Physiol* 274 (*Regul Integr Comp Physiol* 43):R1203-R1211

Nelson RB, Siman R (1989) Identification and characterization of calcium-dependent metalloproteases in rat brain. *J Neurochem* 53: 641–647

Paxinos G, Watson C (1986) *The rat brain in stereotaxic coordinates.* New York: Academic Press

Planas AM, Solé S, Justicia C, Rodríguez-Farré E (2000) Estimation of gelatinase content in rat brain: effect of focal ischemia. *Biochem Biophys Res Commun* 278:803–807

Planas AM, Solé S, Justicia C (2001) Expression, and activation of matrix metalloproteinase-2 and -9 in rat brain after transient focal cerebral ischemia. *Neurobiol Dis* 8:834–846

Romanic AM, White RF, Arleth AJ, Ohlstein EH, Barone FC (1998) Matrix metalloproteinase expression increases after cerebral focal ischemia in rats: inhibition of matrix metalloproteinase-9 reduces infarct size. *Stroke* 29:1020–1030

Rosenberg GA, Kornfeld M, Estrada E, Kelley RO, Liotta LA, Stetler-Stevenson WG (1992) TIMP-2 reduces proteolytic opening of the blood-brain barrier by type IV collagenase. *Brain Res* 576:203–207

Rosenberg GA, Dencoff JE, McGuire PG, Liotta LA, Stetler-Stevenson WG (1994) Injury-induced 92-kDa gelatinase and urokinase expression n rat brain. *Lab Invest* 71:417–422

Rosenberg GA, Navratil M. Barone FC, Feuerstein GZ (1996) Proteolytic cascade enzymes increase in focal cerebral ischemia in rat. *J Cereb Blood Flow Metab* 16:360–363

Rosenberg GA, Estrada, EY, Dencoff JE (1998) Matrix metalloproteinases and TIMPs are associated with blood-brain-barrier opening after reperfusion in rat brain. *Stroke* 29:2189–2195

Rosenberg GA, Estrada EY, Dencoff JE, Stetler-Stevenson WG (1995) Tumor necrosis factor-alpha-induced gelatinase B causes delayed opening of the blood-brain barrier: an expanded therapeutic window. *Brain Res* 703:151–155

Rosenberg GA, Cunningham LA, Wallace J, Alexander S, Estrada EY, Grossetete M, Razhagi A, Miller K, Gearing A (2001) Immunohistochemistry of matrix metalloproteinases in reperfusion injury to rat brain: activation of MMP-9 linked to stromelysin-1 and microglia in cell cultures. *Brain Res* 893:104–112

Royo NC, Wahl F, Stutzmann JM (1999) Kinetics of polymorphonuclear neutrophil infiltration after a traumatic brain injury in rat. *Neuroreport* 10:1363–1367

Soriano MA, Sanz O, Ferrer I, Planas AM (1997) Cortical infarct volume is dependent on the ischemic reduction of perifocal cerebral blood flow in a three-vessel intraluminal MCA occlusion/reperfusion model in the rat. *Brain Res* 747:273–278

Springman EB, Angleton EL, Birkedal-Hansen H, Van Wart HE (1990) Multiple modes of activation of latent human fibroblast collagenase: evidence for the role of a Cys^{73} active-site zinc complex in latency and a "cysteine switch" mechanism for activation. *Proc Natl Acad Sci U S A* 87:364–368

Terasaki T, Deguchi Y, Kasama Y, Pardridge WM, Tsuji A (1992) Determination of *in vivo* steady state unbound drug concentration in the brain interstitial fluid by microdialysis. *Int J Pharmacol* 81:143–152

Wright J, Yoshimoto S, Offner GD, Blanchard RA, Troxler R, Tauber AI (1987) Structural characterization of the isoenzymatic forms of human myeloperoxidase. *Biochim Biophys Acta* 915:68–76

Woessner JF Jr (1991) Matrix metalloproteinases and their inhibition in connective tissue remodeling. *FASEB J* 5:2145–2154

Yamaguchi Y (2000) Lecticans: organizers of the brain extracellular matrix. *Cell Mol Life Sci* 57:276–289

Yong VW, Power C, Forsyth PA, Edwards DR (2001) Metalloproteinases in biology and pathology of the nervous system. *Nat Neurosci* 2:502–511

Yurchenco PD, Schittny JC (1990) Molecular architecture of basement membranes. *FASEB J* 4:1577–1590

Zhang JW, Gottschall PE (1997) Zymographic measurement of gelatinase activity in brain tissue after detergent extraction and affinity-support purification. *J Neurosci Methods* 76:15–20

Zhang JW, Deb S, Gottschall PE (1998) Regional and differential expression of gelatinases in rat brain after systemic kainic acid or bicuculline administration. *Eur J Neurosci* 10:3358–3368

Article nº 4:

Neutrophil infiltration increases matrix metalloproteinase-9 in the ischemic brain after occlusion/reperfusion of the middle cerebral artery in rats.

Justicia C, Panés J, Solé S, Cervera A, Deulofeu R, Chamorro A and Planas AM

Departament de Farmacologia i Toxicologia de l' Institut d'Investigacions Biomèdiques de Barcelona, CSIC-IDIBAPS.
Servei de Neurologia de l'Hospital Clínic, IDIBAPS.

Publicat en la revista: *Journal of Cerebral Blood Flow and Metabolism* 23: 1430-1440. (2003).

Journal of Cerebral Blood Flow & Metabolism
23:1430–1440 © 2003 The International Society for Cerebral Blood Flow and Metabolism
Published by Lippincott Williams & Wilkins, Inc., Baltimore

Neutrophil Infiltration Increases Matrix Metalloproteinase-9 in the Ischemic Brain after Occlusion/Reperfusion of the Middle Cerebral Artery in Rats

*Carles Justicia, †Julián Panés, *Sònia Solé, †Álvaro Cervera, †Ramon Deulofeu, †Ángel Chamorro, and *Anna M. Planas

*From the *Departament de Farmacologia i Toxicologia, IIBB-CSIC; and the †Hospital Clínic, IDIBAPS, Barcelona, Spain.*

Summary: Matrix metalloproteinase-9 (MMP-9) activity increases in the brain during the first day after focal ischemia and might be involved in the pathogenesis of tissue damage. We previously showed MMP-9 in the extracellular space of brain parenchyma along with neutrophil recruitment after ischemia. In the present study, we tested whether neutrophils were a direct source of enhanced MMP-9 in the ischemic brain. Neutrophil infiltration was prevented either by injecting an antibody against ICAM-1, which abrogates neutrophil adhesion to the endothelial vessel wall, or by inducing neutropenia. One-hour intraluminal middle cerebral artery occlusion with reperfusion was induced, and studies were performed at 24 hours. Circulating neutrophils expressed 95-kDa MMP-9 and dimers, and infiltrated neutrophils stained positive for MMP-9. The expression of MMP-9 (mainly 95-kDa proform and dimers and, to a lesser extent, 88-kDa form) increased in brain after ischemia/reperfusion. Treatments preventing neutrophil infiltration failed to preclude the ischemia-induced increase in 88-kDa MMP-9 form and gelatinase activity in neurons and blood vessels. However, these treatments prevented the major increase in 95-kDa MMP-9 form and dimers. We conclude that neutrophil infiltration highly contributes to enhanced MMP-9 in the ischemic brain by releasing MMP-9 proform, which might participate in the tissular inflammatory reaction. **Key Words:** MMP-9—ICAM-1—Neutropenia—Gelatinase—Inflammation—Stroke.

Matrix metalloproteinases (MMPs) degrade the extracellular matrix and are involved in several brain diseases (Lukes et al., 1999; Mun-Bryce and Rosenberg, 1998; Yong et al., 1998). MMPs degrade components of the basal lamina, and several lines of evidence support their involvement in blood-brain barrier breakdown after ischemia (Asahi et al., 2000, 2001; Fujimura et al., 1999; Gasche et al., 1999; Heo et al., 1999; Rosenberg et al., 1998). MMP-9 becomes activated in brain tissue during the first day after cerebral ischemia/reperfusion (Asahi et al., 2000; Planas et al., 2000, 2001; Rosenberg et al., 1998, 2001) and also after permanent ischemia (Romanic et al., 1998). A correlation between MMP-9 activity and hemorrhagic transformation of the ischemic lesion has been reported (Heo et al., 1999; Lapchack et al., 2000; Sumii et al., 2002). Several strategies engineered to prevent activation of MMP-9 after ischemia, such as pharmacologic inhibition (Asahi et al., 2000; Romanic et al., 1998) or the availability of MMP-9 knockout animals (Asahi et al., 2000, 2001), are protective against brain infarct. The cellular source of MMP-9 is not fully known, as immunohistochemical studies have shown different results depending upon the specific antibodies used (Asahi et al., 2001; Planas et al., 2001, 2002; Romanic et al., 1998). Neutrophils express MMP-9 (Planas et al., 2002; Romanic et al., 1998), but whether the large increase of MMP-9 activity that is observed in brain after ischemia/reperfusion is caused by neutrophil recruitment remains to be proved. We previously showed that MMP-9 is released to the extracellular space of the ischemic brain concomitantly with neutrophil tissue recruitment (Planas et al., 2002). Neutrophil adhesion to the endothelial surface before infiltration into brain parenchyma is mediated by ICAM-1, among other adhesion molecules. In the present study, we tested whether neutrophils contribute to enhanced MMP-9 in focal ce-

Received May 21, 2003, final revision received July 22, 2003, accepted July 23, 2003.

Supported by grants from the European Commission (CE QLG1-CT-2000-00562), Fondo de Investigaciones Sanitaras (FIS 01/0099), and Ministerio de Ciencia y Tecnologia (SAF2002-01963).

Address correspondence to Anna M. Planas, Departament de Farmacologia i Toxicologia, IIBB-CSIC, IDIBAPS, Rosselló, 161, planta 6, 08036 - Barcelona, Spain; e-mail: ampfat@iibb.csic.es.

DOI: 10.1097/01.WCB.0000090680.07515.C8

rebral ischemia/reperfusion by either causing neutropenia (Batteur-Parmentier et al., 2000) or by blocking ICAM-1 with a mAb (1A29) (Chopp et al., 1996; Furuya et al., 2001; Zhang et al., 1994, 1995).

METHODS

Animals and surgery for middle cerebral artery occlusion

Focal ischemia was produced in male Sprague-Dawley rats (280 to 320 g body weight) (Iffa-Credo, Lyon, France) by 1-hour intraluminal occlusion of the middle cerebral artery (MCA) with reperfusion, as reported previously (Justicia et al., 2001; Soriano et al., 1997). Rats were anesthetized (halothane) and intubated through the trachea for controlled ventilation. Mean arterial blood pressure (MABP) was monitored, and body temperature was maintained at 37.5°C during MCA occlusion. At 24 hours, rats were anesthetized with halothane and killed to obtain brain samples. For biochemical studies, rats were perfused through the heart with saline to remove blood from the cerebral vessels, and the region corresponding to the territory of the MCA ipsilateral and contralateral to the occlusion was dissected out and frozen at −80°C. For immunohistochemistry, rats were perfused with 4% paraformaldehyde, fixed overnight with the same fixative, and either embedded in paraffin and cut in 5-μm sections or cut in 50-μm sections with a vibratome. For the study of cellular gelatinase activity by *in situ* zymography, the brain was immediately frozen in isopentane at −60°C and sliced in 20-μm sections in a cryostat. Animal work was conducted in compliance with the Spanish legislation and in accordance with the Directives of the European Union.

Drug treatments

A mouse IgG1 against rat ICAM-1 (1A29) and a control nonbinding murine IgG1 against human (Ma et al., 1994) but not rat (Panes et al., 1995; Sans et al., 1999) P-selectin (P-23) were scaled up and purified by protein A/G chromatography at Pharmacia Upjohn Laboratories (Kalamazoo, MI, U.S.A.). ICAM-1 (n = 12) or P-23 (n = 12) antibodies (2 mg/kg) were injected intraperitoneal (Sans et al., 1999) during MCA occlusion at 15 minutes before reperfusion. Nontreated rats subjected to ischemia (n = 9) and nonoperated controls (n = 9) were also studied. Another group of rats was intravenously given either saline (n = 11) or vinblastine (Sigma) (0.5 mg/kg body weight) (n = 14) at day 0 (Batteur-Parmentier et al., 2000), and 4 days

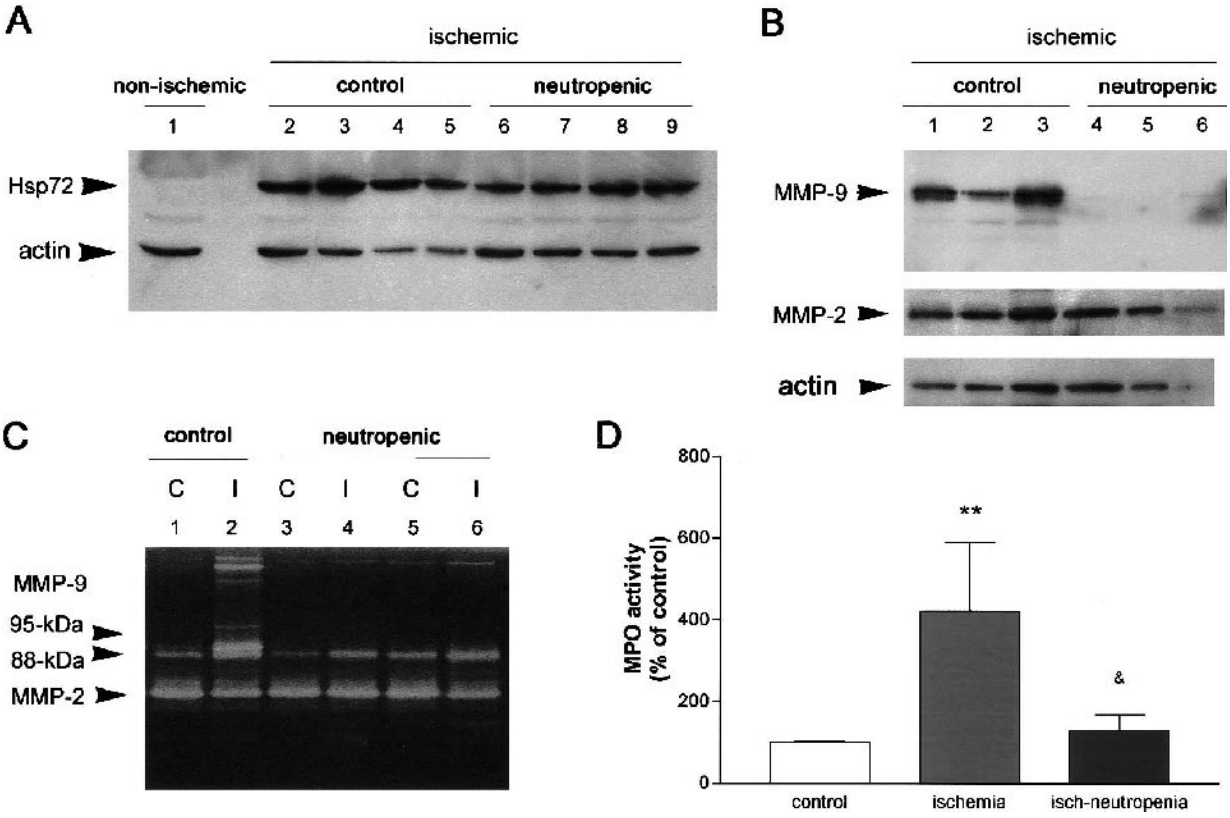

FIG. 1. Effects of neutropenia. **(A)** Ischemia induces the expression of Hsp72 in rats treated with saline (treatment controls) (lanes 2 to 5) and rats receiving vinblastine (neutropenic) (lanes 6 to 9), but Hsp72 is not found in the control nonischemic brain (lane 1). **(B)** Western blot showing that MMP-9 expression in brain is enhanced after ischemia in the ipsilateral cortex and striatum in rats receiving saline (lanes 1 to 3), but this effect is prevented by vinblastine (lanes 4 to 6). MMP-2 is not affected by the treatment. Actin illustrates protein loading in the different lanes of the same gel as for MMP-9 and MMP-2. **(C)** Zymogram showing enhanced MMP-9 gelatinase activity in the ipsilateral (i.e., ischemic) hemisphere, I, (lane 2), in relation to the contralateral, C, (lane 1) after saline (treatment control). The intensity of MMP-9 bands (two bands corresponding to 95- and 88-kDa, and high molecular weight dimers) is enhanced after ischemia (lane 2 versus lane 1). However, the raise in 95-kDa band in the ipsilateral, I, hemisphere is prevented in neutropenic rats subjected to ischemia (lanes 4 and 6) versus their corresponding contralateral, C, hemisphere (lanes 3 and 5). **(D)** MPO activity (mean ± SD: 0.046 ± 0.001 U/g of tissue weight in nonischemic control animals) increases at 24 hours after ischemia ($P < 0.01$), and this effect is prevented by neutropenia (isch/neutropenia) ($P < 0.05$). MMP-9, matrix metalloproteinase; MPO, myeloperoxidase.

later ischemia was induced. At day zero, rats (saline or vinblastine) received the following antibiotics to prevent infection: 150,000 U/kg benzathinebenzylpenicillin (Benzatizil, Antibiotics Farma S.A.) and 10 mg/kg gentamicin (B. Braun S.A.). At days 0 and 4 (before MCA occlusion), arterial blood samples were withdrawn to count neutrophils (Sysmex SE-9000). Comparison of neutrophil counts in vinblastine-treated rats with rats receiving saline, as well as body weight and physiologic parameters, was made with the Mann-Whitney U-test.

Gel zymography

Frozen tissue samples were subjected to detergent extraction, purification of gelatinolytic activity, and zymography, as previously reported (Planas et al., 2001; Zhang and Gottschall, 1997). Frozen tissue was homogenized with lysis buffer containing 50 mM Tris-HCl pH 7.6, 150 mM NaCl, 5 mM $CaCl_2$, 0.05% Brij-35, 0.02% NaN_3, and 1% Triton X-100. All reagents, unless otherwise stated, were from Sigma. After homogenization and centrifugation 12,500 rpm for 5 minutes at 4°C, the supernatants were used for extraction of gelatinolytic activity. Protein (15 mg) in 500 μL was incubated with 50 μL of gelatin-sepharose (Gelatin Sepharose 4B, Amersham Biosciences, Uppsala, Sweden) under constant shaking at 4°C for 1 hour and centrifuged at 2,500 rpm for 2 minutes at 4°C. The pellet with gelatin-sepharose, which retained the gelatinases, was washed with 500 μL of washing buffer (containing the same components as the previous buffer, with the exception of Triton X-100) and each time centrifuged at 2,500 rpm for 2 minutes at 4°C before the separation of gelatinases with 150 μL of elution buffer (washing buffer containing 10% DMSO) by incubation at 4°C under constant shaking for 30 minutes followed by centrifugation, as described above. Extracted brain samples (3 μL; corresponding to 300 μg of protein in the supernatant obtained after tissue homogenization) were loaded in the gels, and a mixture of MMP-9 and MMP-2 (CC073, Chemicon) was used as the gelatinase standard. After electrophoresis, gels were incubated to allow gelatinase activity to take place (Planas et al., 2001). After staining, the gels were analyzed to determine intensity of the bands (Kds1D software, Kodak). Statistical analysis was carried out with two-way ANOVA by treatment (anti-ICAM-1 Ab versus anti-P-23 control Ab) and by MMP-9 band (95-kDa and 88-kDa).

Zymographic assay of plasma and neutrophils: isolation of neutrophils

Blood (2 mL) (citrate) was mixed with 2% dextran (Amersham) in saline and kept for 25 minutes at room temperature (RT). The supernatant (1 mL) was added to (0.5 mL) Ficoll (Biochrom KG, L6113, SeroMed), centrifuged (3,800 rpm 25 minutes, RT), and the resulting pellet (containing granulocytes)

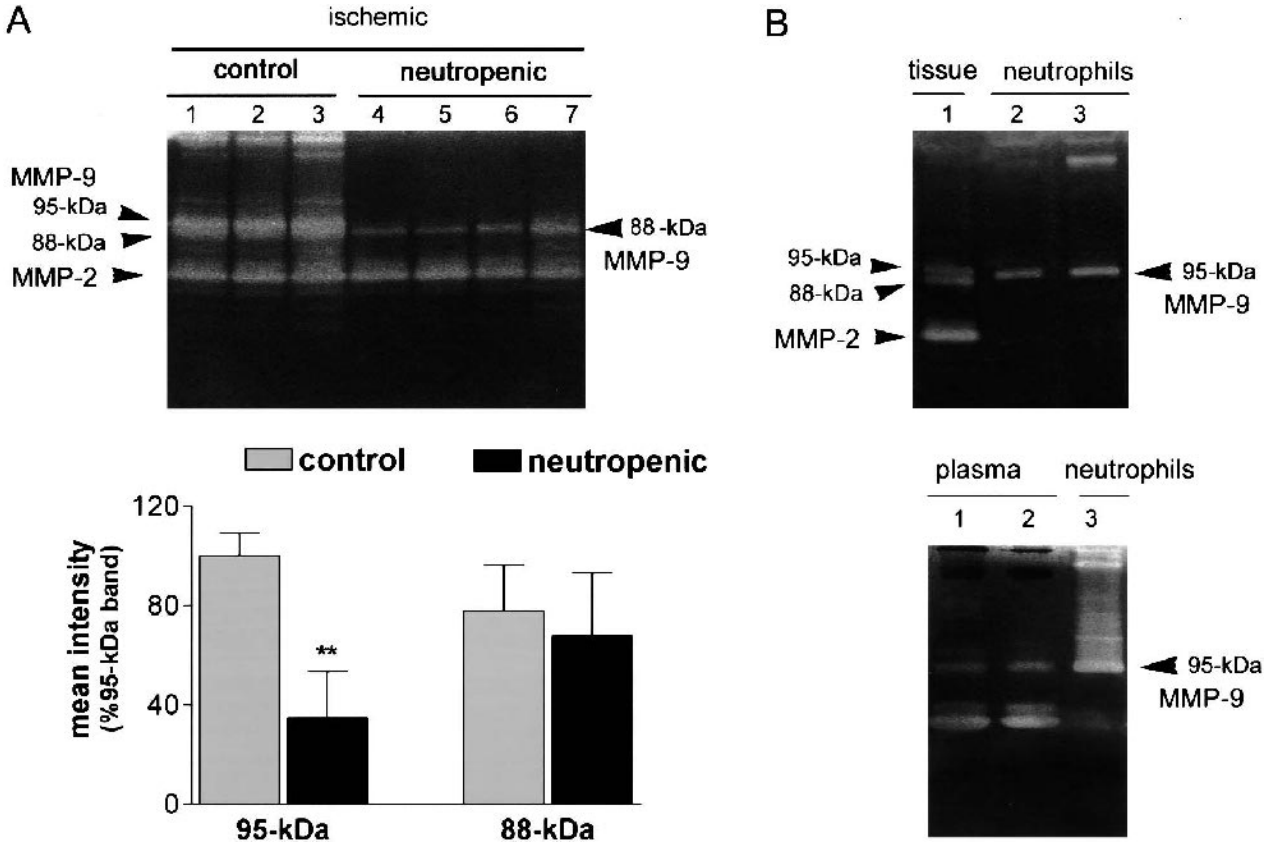

FIG. 2. Neutropenia prevents the ischemia-induced raise of MMP-9 in the brain. **(A)** Neutropenia (lanes 4 to 7) abrogates the ischemia-induced increase in 95-kDa MMP-9 form observed in treatment controls (lanes 1 to 3). Whereas a significant reduction of band intensity was detected for the 95-kDa form ($P < 0.01$ by two-way ANOVA), the raise in the lower MMP-9 band is not really affected by neutropenia, as detected after densitometric measures of gel bands. Values (mean ± SD) of band intensity are expressed as percent of the 95-kDa band in saline-treated ischemic rats. **(B)** Zymography of neutrophils showing a band at 95 kDa and dimeric forms of higher molecular weight (lanes 2 to 3), but the 88-kDa MMP-9 form seen in brain tissue (lane 1) is not detected. MMP-2 is expressed in tissue, but it is hardly detected in isolated neutrophils compared with MMP-9. In the bottom, zymography is shown to compare neutrophils (lane 3) with plasma (lanes 1 to 2). Plasma is richer in MMP-2 than in MMP-9, and comparatively MMP-9 dimers are scarce. MMP, matrix metalloproteinase.

was washed (2 mL phosphate-buffered saline) and centrifuged (3,800 rpm, 10 minutes, RT). Any contaminant erythrocytes in this fraction were lysed with 10 mL 0.15M ammonium chloride for 10 minutes at 37°C and removed by centrifugation (2,500 rpm, 7 minutes) with two PBS washes. The pellet was mixed with 50 μL lysis buffer (as for gelatinase extraction) and sonicated, and the protein content was determined (Bradford, Bio-Rad). Zymography was performed with these samples and with 0.5 μL of plasma. We incubated the gels in the presence or absence of 50 mM EDTA, which inhibits the activity of gelatinases. In addition, we used two specific inhibitors for MMP-9: MMP-9/MMP-13 Inhibitor I (10 μM) and MMP-2/MMP-9 Inhibitor II (30 μM) (Calbiochem, San Diego, CA, U.S.A.).

Protein expression

Of the extracted brain samples, 75 μL was concentrated with trichloroacetic acid protein precipitation (Planas et al., 2001). The pellet was dissolved in loading buffer, and samples were run in a denaturing 10% polyacrylamide gel. Prestained SDS-PAGE molecular weight standards (Bio-Rad, Madrid, Spain) were run in one lane of each gel. Western blotting was carried out for MMP-9 with a mouse monoclonal antibody (mAb) (MAB 13420, Chemicon, 1:150) and for MMP-2 with a rabbit polyclonal Ab (pAb) (AB 809, Chemicon, 1:2000), as described previously (Planas et al., 2000, 2001).

Myeloperoxidase (MPO) expression (Wright et al., 1987) was studied by western blot (mAb M 1464, Menarini Diagnostics, 1:500) using crude brain homogenates obtained from the same animals used for studying MMP-9. In addition, the expression of an inducible heat shock protein (Hsp72) was examined in brain tissue by Western blot (mAb, Oncogene, 1:500) to check that the rats went through an episode of cerebral ischemia after MCA occlusion (Planas et al., 1997). Correct protein charge was tested with a rabbit pAb against actin (1:10,000) (Sigma).

Presence of myeloperoxidase in brain

MPO activity was determined (Batteur-Parmentier et al., 2000; Bradley et al., 1982) in nonischemic rats (n = 4) and rats subjected to ischemia (saline n = 4, and vinblastine n = 3) at 24 hours. Rats were anesthetized and perfused through the heart with saline. Frozen tissue samples were weighed and homogenized (Polytron PT3100) in 3 mL of 50 mM Tris-HCl pH 7.4 (10,000 rpm, 30 seconds on ice), and then 1 mL was mixed with 5 mL of 5 mM phosphate buffer pH 6.0 and centrifuged (22,000 rpm, 30 minutes, 4°C). The pellet was dissolved in 1 mL of 50 mM phosphate buffer pH 6.0 containing 0.5% hexadecyltrimethylammonium bromide. The mixture was frozen, unfrozen at 37°C, and sonicated for 10 seconds, and this procedure was repeated three times. Samples were kept on ice for 20 minutes, centrifuged (14,000 rpm, 15 minutes), and the supernatant was mixed with o-dianisidine dihydrochloride (Sigma) (0.167 mg/mL final concentration). MPO activity was determined with a spectrophotometer at 460 nm (Ultrospec 3000, Pharmacia Biotech) 3 minutes after the addition of 0.0005% H_2O_2. A standard curve with human MPO (Sigma) was used for calibration. Values obtained for the various groups of rats were compared with one-way ANOVA.

Immunohistochemistry

Immunohistochemistry was performed in paraffin sections (Planas et al., 2001) from rat brains obtained at 24 hours after MCA occlusion in groups of rats receiving mAb against ICAM-1 (n = 3), P-23 control mAb (n = 3), and nontreated (n = 3). The primary mouse mAb against MMP-9 were as follows: MAB 13420 (Chemicon) or Ab-10 (Oncogene), both diluted 1:50. After biotinylated anti-mouse Ab and the avidin-biotin complex (Vector Laboratories), the reaction was developed with diaminobenzidine (DAB) (brown stain). Several sections were counterstained with hematoxylin, and others were used for further staining with a rabbit pAb against MPO (A 0398, Dako). Double immunohistochemistry was performed as previously reported (Planas et al., 2001). A positive reaction gives a dark blue precipitate that appears as fine granules.

In addition, we performed immunohistochemistry with the 1A29 monoclonal antibody against ICAM-1 diluted (1:200) in control (n = 2) and ischemic brains at 24 hours (n = 3). In this experiment, we perfused the rats with 4% paraformaldehyde, kept the brains in the fixing solution overnight, and then obtained 50-μm thick sections with a vibratome. Sections were processed free-floating for immunohistochemistry using DAB to reveal anti-ICAM-1 staining and were then counterstained with hematoxylin to visualize cell nuclei.

In situ zymography

Frozen cryostat brain sections from ischemic rats (control n = 3 and vinblastine n = 3) were brought to RT and incubated with FITC-labeled DQ-gelatin (Molecular Probes) overnight at 37°C in a humidified chamber. Then, sections were washed

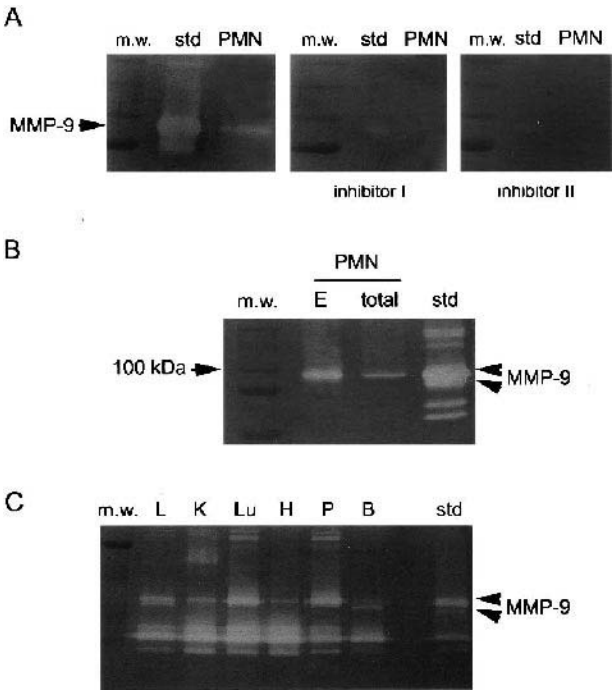

FIG. 3. MMP-9 inhibitors prevent the formation of gelatinolytic bands. Neutrophils show a major 95-kDa MMP-9 band, whereas the 88-kDa band was associated to certain rat tissues. **(A)** Degradation of gelatin by MMP-9 bands is prevented in the presence of MMP-9 inhibitors. Zymography gels were incubated in the absence or presence of MMP-9 inhibitors (see Methods): Inhibitor I (10 μM) inhibits MMP-9 and MMP-13, and Inhibitor II (30 μM) inhibits MMP-9 and MMP-2. **(B)** Neutrophils show a major 95-kDa band either after extracts (E) or prior (total) to gelatinolytic extraction. **(C)** Extraction of gelatynolitic activity from various rat tissues followed by gelatin zymography shows the presence of the 95-kDa MMP-9 band in all tissues, whereas the 88-kDa band is found in brain (B) and liver (L) but is not as apparent in kidney (K), lung (Lu), heart (H), or pancreas (P). PMN, neutrophils; std, zymography standards; m.w., molecular weight standards; MMP, matrix metalloproteinase.

with PBS and examined by fluorescence microscopy to reveal gelatinase activity at the cellular level. Some sections were also stained with a mAb against neuronal nuclei (NeuN, Chemicon, diluted 1:500) followed by a TRIC-labeled secondary Ab.

RESULTS

Several forms of MMP-9 increase in brain after ischemia: neutropenia prevents the ischemia-induced increase of the MMP-9 proform

Ischemia affected the cortex and striatum ipsilateral to MCA occlusion. Induction of 72-kDa heat shock protein (Hsp72) was used as an indicator of ischemia (Planas et al., 1997) (Fig. 1A). Hsp72 was hardly detected in nonoperated controls and in the contralateral hemisphere but was induced by ischemia (Fig. 1A). Ischemic rats showed MMP-9 in the ipsilateral cortex and striatum, as revealed by western blot (Fig. 1B). Zymographic analysis of these proteases revealed their activity on the gels with white bands where gelatin was degraded (Fig. 1C). The specific enzymes were identified by their molecular weight. Controls and the contralateral (C) hemisphere showed two faint bands of MMP-9, which were associated to molecular weights of 95 and 88 kDa and a major band corresponding to MMP-2 (Fig. 1C, lane 1). After ischemia, rats showed an increase of MMP-9 in the ischemic ipsilateral (I) cortex and striatum affecting both MMP-9 bands, particularly the 95-kDa band, whereas no main alteration in the MMP-2 was detected (Fig. 1C, lane 2).

The presence of neutrophils in blood was deeply reduced 4 days after vinblastine administration. Controls showed (mean ± SD neutrophils expressed as percent of total leukocyte counts) 14.28 ± 1.07% neutrophils, whereas vinblastine-treated showed 0.5 ± 0.36% neutrophils ($P < 0.001$) before ischemia. Body weight (mean ± SD) was 322.3 ± 18.9 g on day 1 and 329.3 ± 20.0 g on day 4 in saline-injected rats and 322.9 ± 14.1 on day 1 and 323.3 ± 13.6 on day 4 in vinblastine-treated rats. During surgery for MCA occlusion, mean ± SD rectal temperature was 36.88 ± 0.15°C in the saline and 36.95 ± 0.17°C in the vinblastine group. MABP was also monitored during surgery, and group means ± SD were as follows: 90.98 ± 3.65 mmHg and 93.11 ± 3.83 mmHg in the saline and vinblastine groups, respectively. No differences were found between groups for these physiologic variables. Neutrophil infiltration in the affected ischemic brain tissue was assessed by measurement of brain myeloperoxidase activity (MPO). Ischemia induced an increase ($P < 0.01$) in MPO activity in brain tissue as a result of neutrophil infiltration (Fig. 1D). Neutropenia significantly reduced ($P < 0.05$) the increase of MPO induced by ischemia (Fig. 1D). Likewise, the increase in the 95-kDa MMP-9 band that was induced by ischemia was completely prevented in neutropenic rats

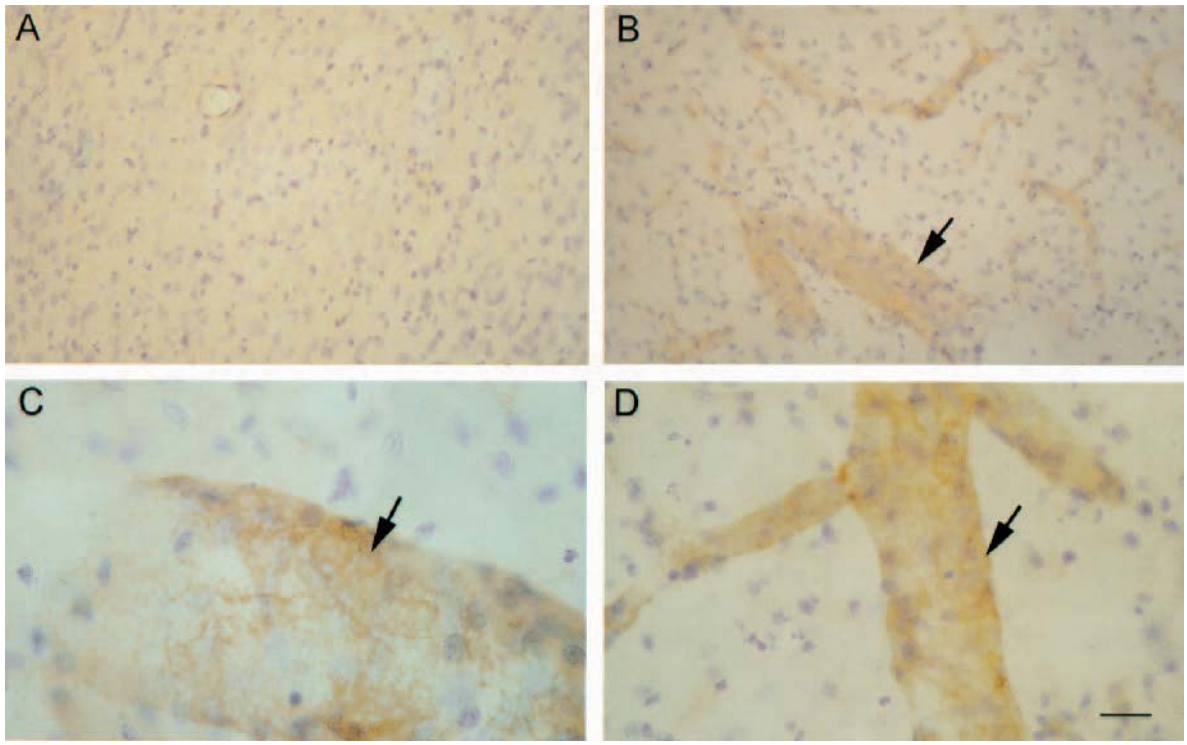

FIG. 4. Induction of ICAM-1 after ischemia. Immunohistochemistry with 1A29 monoclonal antibody against ICAM-1 showing induction of ICAM-1 (brown) in the endothelial vessel wall at 24 hours after ischemia **(B–D)** in relation to controls **(A)**. Sections are counterstained with hematoxylin (blue). Bar scale: **A–B** = 100 μm, **D** = 50 μm, **C** = 25 μm.

(Fig. 1C, lanes 4 and 6). Indeed, densitometric analysis of the gels showed a significant reduction in the intensity of the 95-kDa MMP-9 band ($P < 0.01$) (Fig. 2A). The effect of neutropenia was selective on the 95-kDa MMP-9 band, whereas ischemia-induced activation of the 88-kDa band was not abrogated by this treatment (Fig. 2A).

Neutrophils are rich in 95-kDa MMP-9 and dimers

Zymographic analysis of isolated blood granulocytes showed that these cells were rich in the 95-kDa MMP-9 proform and dimers (Figs. 2B and 3B). MMP-2 was less abundant than MMP-9 in neutrophils. In contrast, plasma was richer in MMP-2 than in MMP-9 (Fig. 2B). To verify that the 95-kDa band in the gel zymogram corresponded to gelatinase B (MMP-9), we incubated gels containing the same samples (MMP standard and neutrophils) in the presence or absence of EDTA to reveal gelatinase activity. This completely prevented band formation (not shown). In addition, we used two specific inhibitors for MMP-9: MMP-9/MMP-13 Inhibitor I and MMP-9/MMP-2 Inhibitor II. The band attributed to MMP-9 was no longer seen in the presence of inhibitors (Fig. 3A).

Neutrophils showed the 95-kDa band, whereas the 88-kDa MMP-9 band found in brain tissue was not detected in granulocytes. We demonstrated that the 88-kDa band was not produced as an artifact during the extraction procedure by comparing MMP-9 bands in total neutrophil homogenates before extraction (total) with bands in the neutrophil gelatinolytic extracts (E) (Fig. 3B). Thus the 88-kDa band was associated to brain tissue. We then performed gelatinolytic extracts of various tissues in the control rat to find out whether the 88-kDa band was present. This band was found in the brain and liver, but was not so apparent in the kidney, lung, heart, or pancreas, showing a tissue-selective expression of the 88-kDa MMP-9.

Effect of treatment with anti-ICAM-1 mAb: reduction of MPO and MMP-9

Ischemia caused the induction of ICAM-1 expression in the endothelial vessel wall at 24 hours, as revealed by immunohistochemical studies with the 1A29 antibody (Fig. 4). This antibody was then administered systemically *in vivo* to block ischemia-induced ICAM-1 to prevent neutrophil adhesion to the endothelium and subsequent infiltration into brain parenchyma. Mean ± SD rectal temperature was 37.40 ± 0.12°C and 37.27 ± 0.11°C in the groups treated with the control and the anti-ICAM-1 mAbs, respectively. MABP was 100.80 ± 7.43 mmHg and 93.51 ± 4.16 mmHg for controls and anti-ICAM-1 groups. No differences were found between groups.

Hsp72 expression was examined as a marker of ischemia-induced cellular stress. All ischemic rats included in this study showed Hsp72, regardless of the treatment they received (Fig. 5A).

We checked the effect of anti-ICAM-1 mAb treatment on neutrophil infiltration by determining the expression of MPO by western blot in the brain samples of the same animals as used for MMP-9 study. MPO was undetectable in the control brain (Fig. 5A, lanes 1 and 2) because rats were perfused with saline before brain extraction to wash out any remaining blood in the tissue. Ischemia/reperfusion increased MPO expression at 24 hours in the brains of nontreated rats and in rats receiving the control mAb (P-23), as expected because of neutrophil infiltration

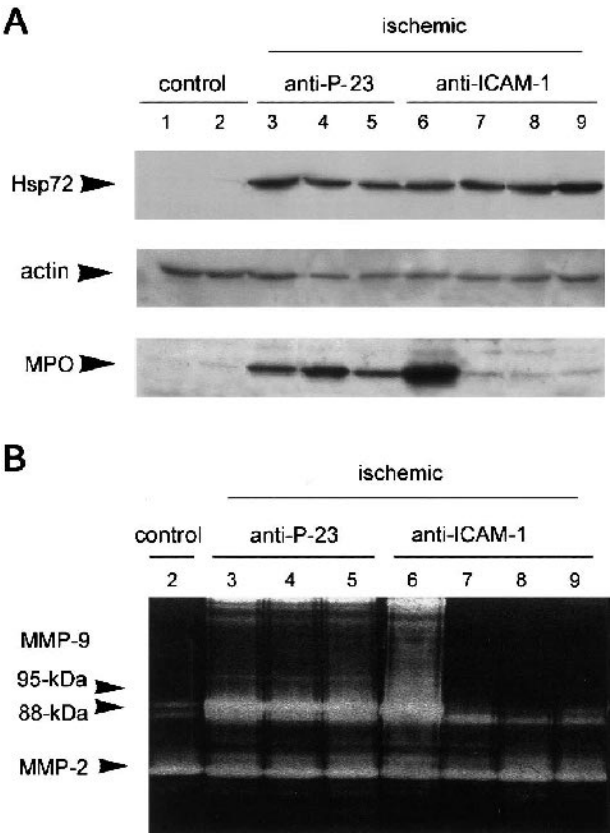

FIG. 5. Effects of anti-ICAM-1 mAb. **(A)** Western blot showing MPO expression in controls (lane 1: nonoperated rat; lane 2: contralateral hemisphere) and in the ipsilateral cortex and striatum of rats subjected to ischemia (lanes 3 to 9), which were treated with control (anti-P-23 Ab) (lanes 3 to 5) or anti-ICAM-1 antibodies (lanes 6 to 9). MPO is abrogated after anti-ICAM-1 treatment (lanes 7 to 9) in most but not all rats (lane 6). Hsp72 is shown to evidence ischemic cellular stress, and actin illustrates protein gel loading. **(B)** Zymography showing MMP-9 (95-kDa, 88-kDa, and dimers of around 210 kDa) and MMP-2 in a control (lane 2) and in ischemic rats (lanes 3 to 9) treated with either anti-P-23 Ab (lanes 3 to 5) or anti-ICAM-1 (lanes 6 to 9). Samples in each lane correspond to the same rats as in the lanes that are shown in **(A)**. Blocking ICAM-1 prevented induction of 95-kDa and dimeric forms of MMP-9 in most rats (lanes 7 to 9) but not in rats showing MPO (lane 6). No changes in MMP-2 were detected after ischemia and treatment. MMP, matrix metalloproteinase; MPO, myeloperoxidase.

(Fig. 5A, lanes 3 to 5). Anti-ICAM-1 mAb preventedMPO increase in the ischemic tissue in six out of nine rats (Fig. 5A, lanes 7 to 9). The remaining three rats showed MPO expression indicative of neutrophil infiltration (Fig. 5A, lane 6).

MMP-9 activity (95-kDa and 88-kDa forms and dimeric forms of high molecular weight, around 210 kDa) increased 24 hours after MCA occlusion in the ipsilateral brain tissue (Fig. 5B, lanes 3 to 5) in relation to controls (Fig. 5B, lane 2), as revealed by zymography. Anti-ICAM-1 mAb, in rats in which neutrophil infiltration was prevented, strongly reduced the ischemia-induced rise in 95-kDa MMP-9 band and dimers (Fig. 5B, lanes 7 to 9). However, the three rats also treated with anti-ICAM-1 mAb but showing high MPO expression showed an increase in MMP-9 (Fig. 5B, lane 6) that was thus correlated with the presence of neutrophils. Measuring raw band intensity showed significant ($P < 0.001$) reduction of the 95-kDa MMP-9 form after blocking ICAM-1 (Fig. 6A). However, comparatively, the intensity of the 88-kD band was not significantly affected by this treatment (Fig. 6A).

The effect of ICAM-1 blockade on MMP-9 was further examined in the same animals by protein precipitation of samples and western blot analysis with a mAb against MMP-9. The expression of MMP-9 was highly increased 24 hours after MCA occlusion, but MMP-9 protein expression was dramatically reduced in rats treated with anti-ICAM-1 mAb compared with rats administered with the control mAb (Fig. 6B, lanes 4 to 6). However, treatment did not cause changes in MMP-2, as revealed by zymography and western blot (Figs. 5B, 6A, and 6B).

Cellular MMP-9 distribution

Tissue distribution of MMP-9 was examined by immunohistochemistry using two different monoclonal antibodies, which gave similar results. Basal expression of MMP-9 was detected in neuronal fibers (Fig. 7A). At 24 hours after MCA occlusion/reperfusion, the most striking feature was that the filamentous appearance of brown stain seen in controls turned to a more granular appearance (Figs. 7B and 7C), and occasionally, staining appeared in discrete enlargements in fibers. In addition,

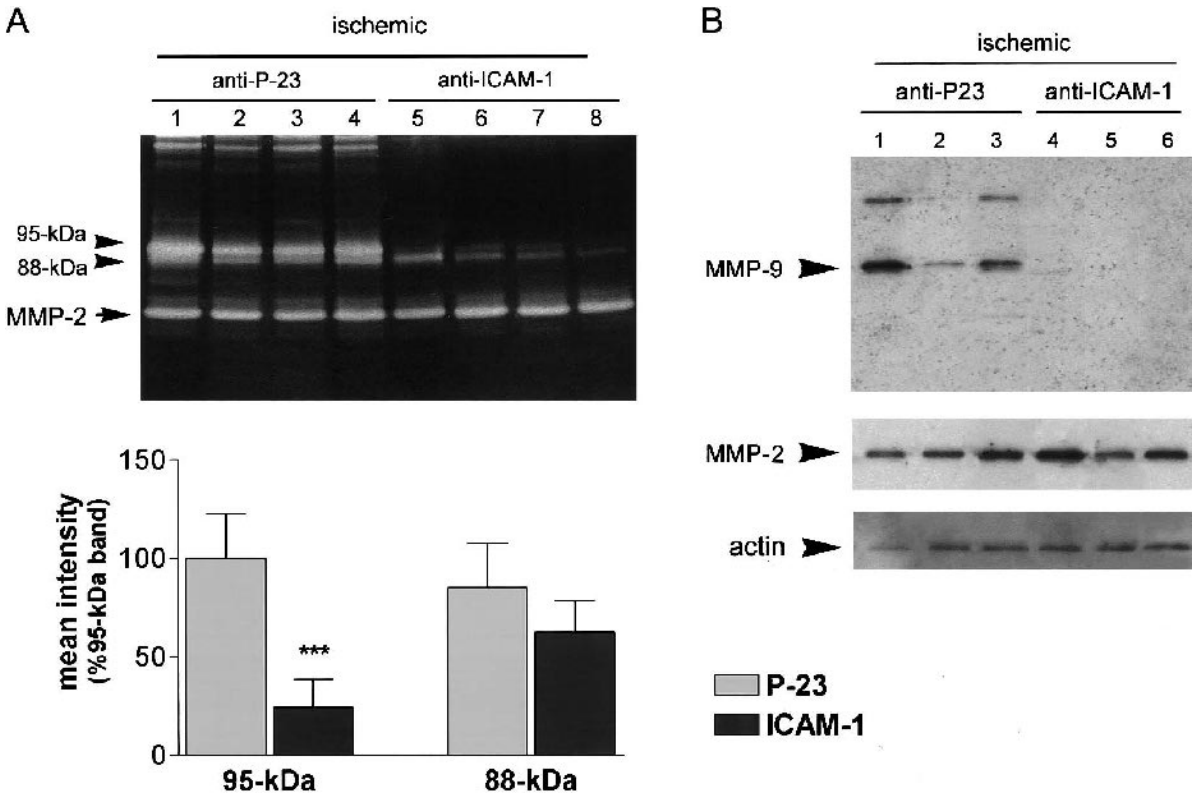

FIG. 6. Anti-ICAM-1 mAb prevents the ischemia-induced raise of MMP-9 in brain. **(A)** Zymography showing MMP-9 (95-kDa, 88-kDa, and dimers of high molecular weight). MMP-9 bands are strongly induced in ischemic rats (lanes 1 to 4). Anti-ICAM-1 Ab prevents ischemia-induced increase in 95-kDa MMP-9 and dimers (lanes 5 to 8). Densitometric analysis of band mean intensity showing that ICAM-1 significantly reduces intensity of 95-kDa-form ($P < 0.001$), with no significant change in 88-kDa-band intensity. Values (mean ± SD) of band intensity are expressed as percent of the 95-kDa band in anti-P-23-treated ischemic rats. **(B)** Western blot shows that ischemia-induced MMP-9 (95-kDa proform and 210-kDa dimmers) (upper band) is prevented by anti-ICAM-1 treatment. In contrast, no change of MMP-2 is seen. Actin illustrates protein gel loading. MMP, matrix metalloproteinase.

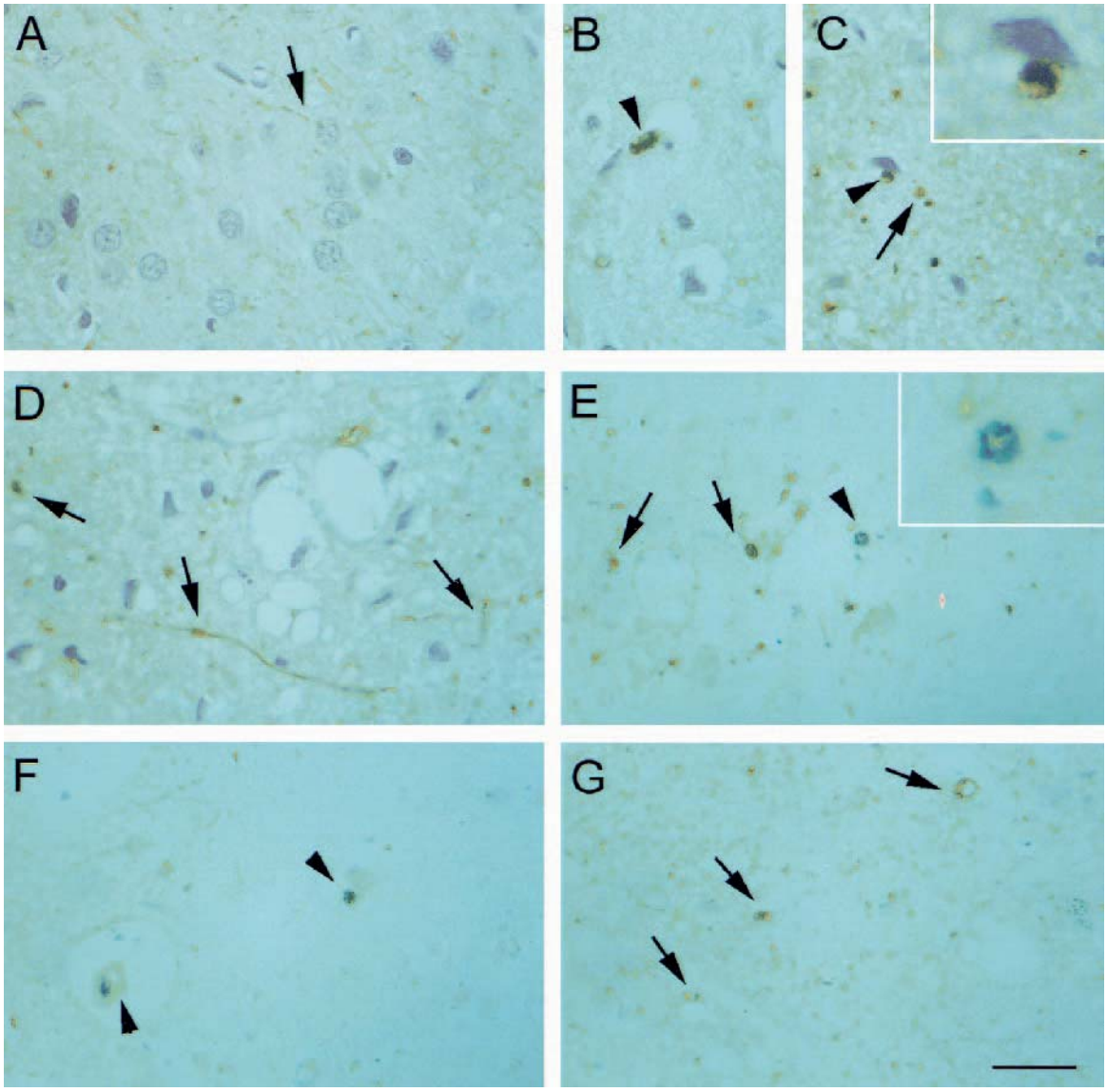

FIG. 7. Cellular localization of MMP-9. Immunohistochemistry for MMP-9 in the cortex of control **(A)** and ischemic rats **(B–G)** that were treated with either P-23 control Ab **(B, C, E, F)** or anti-ICAM-1 Ab **(D, G)**. Images in **A–D** show MMP-9 in brown and are counterstained with hematoxyin (blue) to evidence cell nuclei. Stained fibers are apparent in control cortex **(A)**, and axonal enlargements are seen after ischemia (arrows in **B–D**), regardless of treatment. Ischemia induces MMP-9 in small blood vessels, and again this induction is still apparent after blocking ICAM-1 (top arrow in **G**). Cells with the morphology of neutrophils (**B, C;** inset in **C**) are found in the anti-P-23 rats, whereas they are rare in rats treated with anti-ICAM-1 Ab **(D)**. Double-staining with antibodies against MMP-9 (brown) and against MPO (dark blue) shows neutrophils expressing MMP-9 after ischemia (arrowheads in **E** and **F**; inset in **E**) but not in rats receiving anti-ICAM-1 Ab **(G)**. Antibodies anti-MMP-9 show similar results (**A–D**: MAB 13420; **E–G**: Ab-10). Bar scale: 25 μm. Insets in **C** and **E** are magnified ×6. MMP, matrix metalloproteinase; MPO, myeloperoxidase.

brown stain was detected in cells showing a morphology that was compatible with neutrophils, including polymorphous nucleus (arrowheads in Figs. 7B and 7C; inset in Fig. 7C) and in endothelial walls of small vessels. These later features were more abundantly seen at the edges of the ischemic core (particularly in the endopiriform cortex and surrounding zones). Double labeling with antibodies against MMP-9 (brown) and MPO (dark blue) revealed MMP-9 positive neutrophils in ischemic rats receiving control mAb (arrowheads in Figs. 7E and 7F; inset Fig. 7E). Ischemic rats treated with anti-ICAM-1 mAb (Fig. 7G) still showed the MMP-9 staining in fibers (Fig. 7D) and endothelium (Fig. 7G, arrow on the right), but they did not show the cellular MMP-9 stain that was attributed to neutrophils.

Gelatinase activity increases in neural cells

The degradation of gelatin was increased in ischemic neurons located within the ischemic core in cortex and striatum at 24 hours after MCA occlusion/reperfusion

(Fig. 8). The raise in gelatinase activity was restricted to the MCA territory in the ipsilateral hemisphere but did not affect the contralateral hemisphere (Figs. 8A and 8B). Gelatinase activity was found mainly in neural cells and some blood vessels (Fig. 8C), and many cells were identified as neurons with the neuronal NeuN marker (Fig. 8D). This effect was seen even after neutropenia (Figs. 8E and 8F), suggesting that the neuronal raise in gelatinase activity was not dependent upon neutrophil infiltration.

DISCUSSION

Ischemia/reperfusion induces a large increase in cerebral MMP-9 activity, which might participate in the pathogenesis of ischemic damage (Asahi et al., 2000). This study was addressed to find out whether neutrophil infiltration contributed to the enhanced MMP-9 activity in ischemia. We addressed this query because our previous findings showed release of MMP-9 proform in the extracellular space of the ischemic brain that was concomitant with neutrophil recruitment (Planas et al., 2002). To answer this question, we used the strategies of either preventing neutrophil adhesion to the endothelial vessel wall by systemic treatment with a mAb against ICAM-1 or depleting circulating neutrophils. The mAb against ICAM-1 that we used in the present study was administered to rodents in previous studies of focal cerebral ischemia (Chopp et al., 1996; Furuya et al., 2001; Zhang et al., 1994, 1995). Overall, treatments were effective; they abrogated the MPO rise in the ischemic brain at 24 hours. Rats in which treatment successfully prevented neutrophil infiltration showed a strongly reduced rise in MMP-9. Neutrophils are known to contain and to degranulate gelatinase granules, together with other types of granules, such as those stained with lactoferrin and azurophil granules identified by MPO (Borregaard et al., 1997). Those gelatinase granules have been described to contain and release MMP-9 (Pugin et al., 1999). Furthermore, we showed that the proforms of

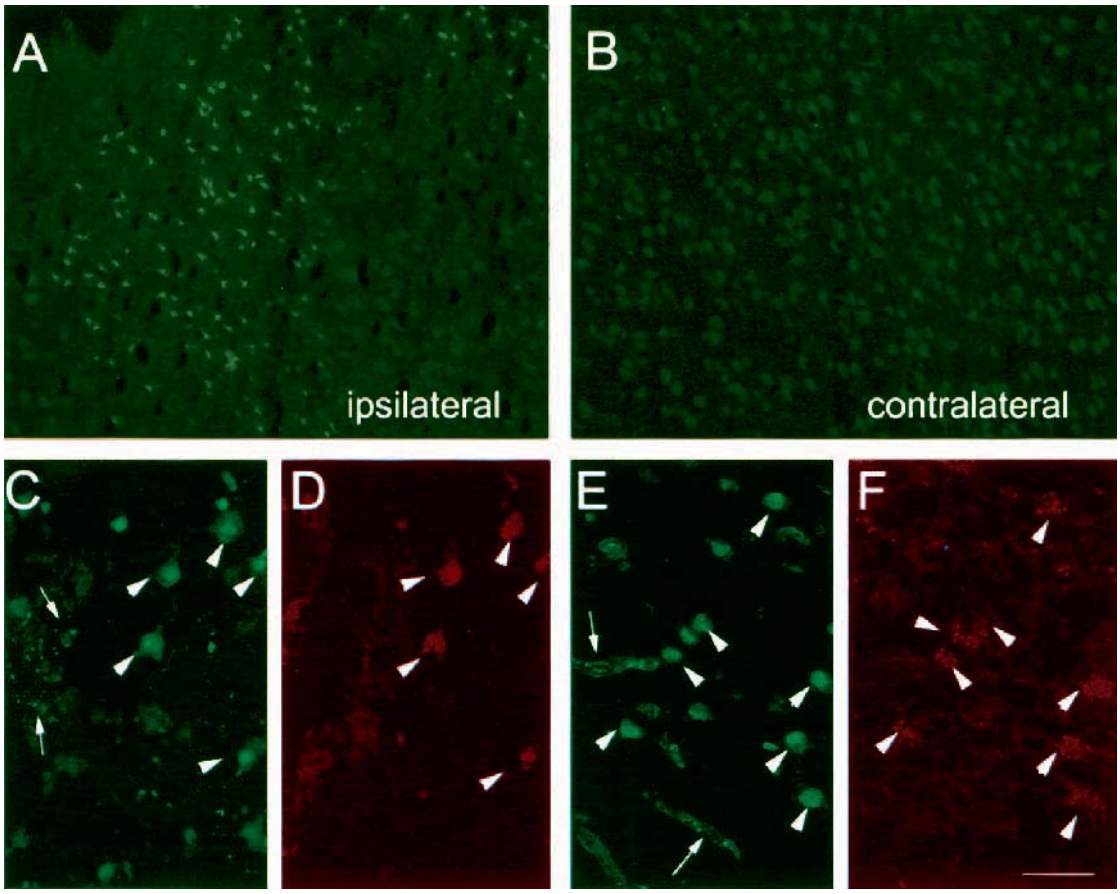

FIG. 8. Cellular gelatinase activity increases in neurons and blood vessels after ischemia, regardless of neutrophil infiltration. Gelatinase activity **(A–C, E)** was studied *in situ* in cryostat brain sections incubated with DQ-gelatin, an FITC-labeled product that becomes fluorescent after degradation. **(A)** An increase of labeled cells was detected at 24 hours in the ischemic brain tissue but not in the contralateral hemisphere **(B)**. **(C)** Many of the stained cells (arrowheads) correspond to neurons as revealed with NeuN staining (**D**, arrowheads). Most cellular increases in gelatinase activity are seen even when neutrophil infiltration is abolished in neutropenic rats **(E)**, and again many stained cells (arrowheads) are identified as neurons with NeuN (**F**, arrowheads). Stained vessels showing gelatinase activity are also apparent (arrows in **C** and **E**). Bar scale, **A–B**: 50 μm; **C–F**: 25μm.

MMP-9 were abundant in neutrophils, and, in agreement with other authors (Romanic et al., 1998; Rosenberg et al., 2001), we detected MMP-9 staining in neutrophils within the ischemic brain tissue by immunohistochemistry. These findings led us to conclude that neutrophil infiltration into the ischemic parenchyma was necessary for the enhanced MMP-9 expression and activity (95-kDa proform and dimers) that occurs in the brain after ischemia. Besides neutrophils, MMP-9 was also found in plasma, but compared with neutrophils, the former was richer in MMP-2. Despite the fact that neutrophils might produce MMP-2 (Warner et al., 2000), the amounts are negligible compared with the MMP-2 content in the brain and plasma. This thus indicates that plasma was not the major source of the increase in MMP-9 induced by ischemia at 24 hours because an even greater increase in plasma-borne MMP-2 would be expected, whereas no MMP-2 alterations became apparent at this time point.

Ischemia-induced 88-kDa MMP-9-increase was still found after neutropenia and ICAM-1 blockade, thus suggesting that the increase in this form of MMP-9 was not derived from neutrophils but was intrinsic to the ischemic tissue. Also, we found constitutive MMP-9 protein expression in neuronal fibers and a change in MMP-9 distribution along fibers after ischemia, probably reflecting dynamic alterations in axons, together with increased MMP-9 staining in blood vessels, which is in agreement with previous reports (Mun-Bryce et al., 2002). Preventing neutrophil infiltration did not attenuate this pattern of MMP-9 expression after ischemia. In addition, we detected an increase in neuronal gelatinase activity at 24 hours after ischemia, which is in agreement with a previous report (Gu et al., 2002). Whether this neuronal gelatinase corresponds to MMP-9 remains to be demonstrated, but the neuronal increase in gelatinase activity was still found after abrogating neutrophil infiltration, suggesting an intrinsic activation of gelatinase in brain after ischemia. However, it is likely that the activation of MMP-9 occurs locally in the parenchyma of the injured tissue by a finely regulated process. For this reason, we cannot discard the possibility that, once in the tissue, neutrophils contribute to further enhancing the intrinsic cerebral MMP-9 response, either with protease activity or by releasing cytokines that might further induce MMP-9 gene expression, as occurs in myocardial ischemia/reperfusion (Lindsey et al., 2001).

In summary, ischemia/reperfusion induced a strong increase in several MMP-9 forms in the ischemic tissue. Among the increases in MMP-9 forms, we report that the increase in MMP-9 proform was essentially derived from infiltrating neutrophils, whereas the results suggest that other forms of gelatinase are increased in neural cells of the ischemic brain regardless of neutrophil infiltration. From the present results, we conclude that neutrophil infiltration contributes to the MMP-9 increase in the ischemic brain by releasing MMP-9 proform.

Acknowledgment: We thank Mr. Josep Moreno for excellent technical assistance.

REFERENCES

Asahi M, Asahi K, Jung J-C, del Zoppo GJ, Fini ME, Lo EH (2000) Role of matrix metalloproteinase 9 after cerebral ischemia: effects of gene knockout and enzyme inhibition with BB-94. *J Cereb Blood Flow Metab* 20:1681–1689

Asahi M, Wang X, Mori T, Sumii T, Jung J-C, Moskowitz MA, Fini ME, Lo EH (2001) Effects of matrix metalloproteinase-9 gene knock-out on the proteolysis of blood-brain barrier and white matter components after cerebral ischemia. *J Neurosci* 21:7724–7732

Batteur-Parmentier S, Margaill I, Plotkine M (2000) Modulation by nitric oxide of cerebral neutrophil accumulation after transient focal ischemia in rats. *J Cereb Blood Flow Metab* 20:812–819

Borregaard N, Cowland JB (1997) Granules of the human neutrophilic polymorphonuclear leukocyte. *Blood* 89:3503–3521

Bradley PP, Priebat DA, Christensen RD, Rothstein G (1982) Measurement of cutaneous inflammation: estimation of neutrophil content with an enzyme marker. *J Invest Dermatol* 78:206–209

Chopp M, Li Y, Jiang N, Zhang RL, Prostak J (1996) Antibodies against adhesion molecules reduce apoptosis after transient middle cerebral artery occlusion in rat brain. *J Cereb Blood Flow Metab* 16:578–584

Fujimura M, Gasche Y, Morita-Fujimura Y, Massengale J, Kawase M, Chan PH (1999) Early appearance of activated matrix metalloproteinase-9 and blood-brain barrier disruption in mice after focal cerebral ischemia and reperfusion. *Brain Res* 842:92–100

Furuya K, Takeda H, Azhar S, McCarron RM, Chen Y, Ruetzler CA, Wolcott KM, DeGraba TJ, Rothlein R, Hugli TE, del Zoppo GJ, Hallenbeck JM (2001) Examination of several potential mechanisms for the negative outcome in a clinical stroke trial of Enlimomab, a murine anti-human intercellular adhesion molecule-1 antibody. *Stroke* 32:2665–2674

Gasche Y, Fujimura M, Morita-Fujimura Y, Copin JC, Kawase M, Massengale J, Chan PH (1999) Early appearance of activated matrix metalloproteinase-9 after focal cerebral ischemia in mice: a possible role in blood-brain barrier dysfunction. *Cereb Blood Flow Metab* 19:1020–1028

Gu Z, Kaul M, Yan B, Kridel SJ, Cui J, Strongin A, Smith JW, Liddington RC, Lipton SA (2002) S-nitrosylation of matrix metalloproteinases: signaling pathway to neuronal cell death. *Science* 297:1186–1190

Heo JH, Lucero J, Abumiya T, Koziol JA, Copeland BR, del Zoppo GJ (1999) Matrix metalloproteinases increase very early during experimental focal cerebral ischemia. *J Cereb Blood Flow Metab* 19:624–633

Justicia C, Pérez-Asensio FJ, Burguete MC, Salom JB, Planas AM (2001) Administration of transforming growth factor-α reduces infarct volume after transient focal cerebral ischemia in the rat. *J Cereb Blood Flow Metab* 21:1097–1104

Lapchak PA, Chapman DF, Zivin JA (2000) Metalloproteinase inhibition reduces thrombolytic (tissue plasminogen activator)-induced hemorrhage after thromboembolic stroke. *Stroke* 31:3034–3040

Lindsey M, Wedin K, Brown MD, Keller C, Evans AJ, Smolen J, Burns AR, Rossen RD, Michael L, Entman M (2001) Matrix-dependent mechanism of neutrophil-mediated release and activation of matrix metalloproteinase 9 in myocardial ischemia/reperfusion. *Circulation* 103:2181–2187

Lukes A, Mun-Bryce S, Lukes M, Rosenberg GA (1999) Extracellular matrix degradation by metalloproteinases and central nervous system diseases. *Mol Neurobiol* 19:267–284

Ma L, Raycroft L, Asa D, Anderson DC, Geng JG (1994) A sialoglycoprotein from human leukocytes functions as a ligand for P-selectin. *J Biol Chem* 269:27739–27746

Mun-Bryce S, Lukes A, Wallace J, Lukes-Marx M, Rosenberg G (2002) Stromelysin-1 and gelatinase A are upregulated before

TNF-α in LPS-stimulated neuroinflammation. *Brain Res* 933: 42–49

Mun-Bryce S, Rosenberg GA (1998) Matrix metalloproteinases in cerebrovascular disease. *J Cereb Blood Flow Metab* 18:1163–1172

Panes J, Perry MA, Anderson DC, Manning AA, Leone B, Cepinskas G, Rosenbloom CL, Miyasaka M, Kvietys PR, Granger DN (1995) Regional differences in constitutive and induced ICAM-1 expression *in vivo*. *Am J Physiol* 269: H1955–H1964

Planas AM, Justicia C, Solé S, Friguls B, Cervera A, Adell A, Chamorro A (2002) Certain forms of matrix metalloproteinase-9 accumulate in the extracelular space after microdialysis probe implantation and middle cerebral artery occlusion/reperfusion. *J Cereb Blood Flow Metab* 22:918–925

Planas AM, Solé S, Justicia C (2001) Expression and activation of matrix metalloproteinase-2 and –9 in rat brain after transient focal cerebral ischemia. *Neurobiol Dis* 8:834–846

Planas AM, Solé S, Justicia C, Rodríguez-Farre E (2000) Estimation of gelatinase content in rat brain: Effect of focal ischemia. *Biochem Biophys Res Commun* 278:803–807

Planas AM, Soriano MA, Estrada A, Sanz O, Martín F, Ferrer I (1997) The heat shock stress response after brain lesions: induction of 72 kDa heat shock protein (cell types involved, axonal transport, transcriptional regulation) and protein synthesis inhibition. *Prog Neurobiol* 51:607–636

Pugin J, Widmer M-C, Kossodo S, Liang C-M, Preas II HL, Suffredini AF (1999) Human neutrophils secrete gelatinase B *in vitro* and *in vivo* in response to endotoxin and proinflammatory mediators. *Am J Respir Cell Mol Biol* 20:458–464

Romanic AM, White RF, Arleth AJ, Ohlstein EH, Barone FC (1998) Matrix metalloproteinase expression increases after cerebral focal ischemia in rats. Inhibition of matrix metalloproteinase-9 reduces infarct size. *Stroke* 29:1020–1030

Rosenberg GA, Cunningham LA, Wallace J, Alexander S, Estrada EY, Grossetete M, Razhagi A, Miller K, Gearing A (2001) Immunohistochemistry of matrix metalloproteinases in reperfusion injury to rat brain: activation of MMP-9 linked to stromelysin-1 and microglia in cell cultures. *Brain Res* 893:104–112

Rosenberg GA, Estrada EY, Dencoff JE (1998) Matrix metalloproteinases and TIMPs are associated with blood-brain-barrier opening after reperfusion in rat brain. *Stroke* 29:2189–2195

Sans M, Panes J, Ardite E, Elizalde JI, Arce Y, Elena M, Palacin A, Fernandez-Checa JC, Anderson DC, Lobb R, Pique JM (1999) VCAM-1 and ICAM-1 mediate leukocyte-endothelial cell adhesion in rat experimental colitis. *Gastroenterology* 116:874–883

Soriano MA, Sanz O, Ferrer I, Planas AM (1997) Cortical infarct volume is dependent on the ischemic reduction of perifocal cerebral blood flow in a three-vessel intraluminal MCA occlusion/reperfusion model in the rat. *Brain Res* 747:273–278

Sumii T, Lo EH (2002) Involvement of matrix metalloproteinase in thrombolysis-associated hemorrhagic transformation after embolic focal ischemia in rats. *Stroke* 33:831–836

Warner RL, Bless NM, Lewis CS, Younkin E, Beltran L, Guo R, Johnson KJ, Varani J (2000) *Free Radic Biol Med* 29:8–16

Wright J, Yoshimoto S, Offner GD, Blanchard RA, Troxler R, Tauber AI (1987) Structural characterization of the isoenzymatic forms of human myeloperoxidase. *Biochim Biophys Acta* 915:68–76

Yong VW, Kerkoski CA, Forsyth PA, Bell R, Edwards DR (1998) Matrix metalloproteinases and diseases of the CNS. *Trends Neurosci* 21:75–80

Zhang RL, Chopp M, Jiang N, Tang WX, Prostak J, Manning AM, Anderson DC (1995) Anti-intercellular adhesion molecule-1 antibody reduces ischemic cell damage after transient but not permanent middle cerebral artery occlusion in the Wistar rat. *Stroke* 26:1438–1443

Zhang RL, Chopp M, Li Y, Zaloga C, Jiang N, Jones ML, Miyasaka M, Ward PA (1994) Anti-ICAM-1 antibody reduces ischemic cell damage after transient middle cerebral artery occlusion in the rat. *Neurology* 44:1747–1751

Zhang JW, Gottschall PE (1997) Zymographic measurement of gelatinase activity in brain tissue after detergent extraction and affinity-support purification. *J Neurosci Meth* 76:15–20

Article nº 5:

Activation of matrix metalloproteinase-3 and agrin cleavage in cerebral ischaemia / reperfusion.

Solé S, Petegnief V, Gorina R, Chamorro A, Planas AM.

Departament de Farmacologia i Toxicologia de l' Institut d'Investigacions Biomèdiques de Barcelona, CSIC-IDIBAPS.
Institut de Malalties del Sistema Nerviós (IMSN), Hospital Clínic, Institut d'Investigacions Biomèdiques August Pi i Sunyer (IDIBAPS).

Publicat en la revista: *Journal of Neuropathology and Experimental Neurology.* (2004).

Journal of Neuropathology and Experimental Neurology

Vol. 63, No. 4
April, 2004
pp. 338–349

Activation of Matrix Metalloproteinase-3 and Agrin Cleavage in Cerebral Ischemia/Reperfusion

SÒNIA SOLÉ, VALÉRIE PETEGNIEF, ROSER GORINA, ÁNGEL CHAMORRO, AND ANNA M. PLANAS

Abstract. Matrix metalloproteinase-3 (MMP-3) degrades components of the extracellular matrix and may participate in the pathogenesis of stroke. Here we examine the expression, activation, and cellular location of MMP-3 and the cleavage of agrin, an MMP-3 substrate, following transient middle cerebral artery occlusion in the rat. MMP-3 was activated by ischemia/reperfusion, which was revealed by the appearance of a cleaved form and increased degradation of a substrate. MMP-3 was observed in ischemic neurons, oligodendrocytes, microvasculature, and reactive microglia/macrophages. In cell cultures, MMP-3 expression was observed in neurons and, to a lesser extent, in mature oligodendrocytes, but not in oligodendrocyte progenitors, astrocytes, or microglia. Casein zymography revealed MMP-3 in cultured neurons. Agrin was expressed in cultured neurons and cultured astrocytes. In brain tissue, agrin was detected in neurons, and following ischemia it was also detected in reactive astrocytes. Addition of MMP-3 to protein extracts from control brain caused neuronal agrin degradation. Following ischemia/reperfusion, agrin disappeared from the tissue membrane fraction and a cleaved agrin fragment was found in tissue protein extracts. The present results show MMP-3 activation and neuronal transmembrane agrin cleavage after ischemia/reperfusion. In addition, the finding that MMP-3 cleaves brain agrin strongly suggests that ischemia-induced MMP-3 activation causes agrin cleavage.

Key Words: Agrin; Ischemia/Reperfusion; Matrix metalloproteinase.

INTRODUCTION

Matrix metalloproteinase-3 (MMP-3), also named stromelysin-1, degrades a wide range of components of the extracellular matrix (1) and is involved in pathologies of the nervous system. In glial tumors, it is responsible for the invasive properties of astrocytoma cells (2). MMP-3 is upregulated prior to the onset of demyelinating diseases (3), it is associated with white matter damage in vascular dementia (4) and it seems to be involved in ischemic neuronal death (5). MMP-3 is expressed as a 57/59 kDa prozymogen; activation of the MMP family of proenzymes occurs following the cleavage of a coordination bond between a zinc ion at the active center and an unpaired cysteine in the aminoterminal propeptide, which can occur following a proteolytic or a chemical bond rupture (6). However, for MMP-3, disruption of the cysteine-75 and zinc ion coordination is not sufficient to activate the precursor protein, as conformational changes in pro-MMP-3 accompanied by the proteolytic cleavage of the cysteine-containing propeptide domain are necessary for the expression of proteolytic activity (7). This proteolytic cleavage, which seems to be essential for MMP-3 activation, results in the conversion of the pro-form to lower molecular weight active forms (45, 28, and 21 kDa).

Matrix substrates for MMP-3 include fibronectin, laminin, elastin, collagen IV, proteoglycans (8, 9), the glycoprotein osteopontin (10), and the cellular matrix protein SPARC (11). In addition to cleaving matrix proteins, MMP-3 degrades other substrates and has been reported to degrade myelin basic protein (12), to cleave intact IgG to produce a single chain Fc-like fragment (13), and to activate MMP-9 in human breast carcinoma cells (14). In addition to the devastating action of MMP-3 on a large spectrum of substrates, it might also have a beneficial anti-inflammatory role due to its ability to cleave all monocyte chemoattractant protein chemokines, generating CC chemokine receptor antagonists (15). MMP-3 also degrades agrin (16), a heparan sulfate proteoglycan (17), which is a component of the synaptic basal lamina at the neuromuscular junction (18). Following release by motoneurons, agrin has the ability to induce clustering of acetylcholine receptors on cultured myotubules (19). A shorter agrin isoform is expressed in the brain, where it remains bound to various types of neuronal cells (20), and is not restricted to cholinergic regions (21). A distinct promoter drives the expression of the neuronal form of agrin (22). Agrin is tightly associated, but not covalently bound (23), with axonal and synaptic membranes of neurons (23–25). Agrin derived from central nervous system basal lamina is functionally different from the agrin isoforms at the neuromuscular junction, as the former does not induce acetylcholine receptor aggregation on cultured myotubes (23). Although brain agrin function is not fully understood (26), several lines of evidence suggest that it can mediate transynaptic signaling (27) and that it regulates neuronal responses to excitatory neurotransmitters, as mice and cultured cortical neurons deficient in agrin are resistant to excitotoxic insults (28).

Ischemia causes early disturbances to the white matter and axons resulting in impaired synaptic transmission (29). As brain agrin has been attributed a putative function at the CNS synaptic cleft, agrin degradation might

From Departament de Farmacologia i Toxicologia (SS, RG, AMP), IIBB-CSIC, and Institut de Malalties del Sistema Nerviós (AC), Hospital Clínic, Institut d'Investigacions Biomèdiques August Pi i Sunyer (IDIBAPS), Barcelona, Spain.

Correspondence to: Dr. Anna M. Planas, Departament de Farmacologia i Toxicologia, IIBB-CSIC, IDIBAPS, Rosselló, 161, planta 6, 08036, Barcelona, Spain. E-mail: ampfat@iibb.csic.es

This study was supported by a grant from the Spanish Ministry of Science and Technology (MCYT, SAF2002-01963).

contribute to functional alterations following cerebral ischemia. A recent genomic study of the ischemic rat brain showed reduced expression of agrin mRNA (30), but whether agrin protein is modified after ischemia has not been explored. Active MMP-3 is a candidate to cause agrin cleavage in ischemia. MMP-3 expression has been shown in the ischemic brain (5), but MMP-3 activation following ischemia has not been demonstrated. Here we address the question of whether MMP-3 is activated in the rat brain following ischemia/reperfusion, and whether agrin is subsequently degraded.

MATERIALS AND METHODS

Animals and Surgery

Adult male Sprague-Dawley rats (275–325 g body weight; n = 50) obtained from Iffa-Credo (Lyon, France) were kept under a 12-hour light-dark cycle and allowed free access to food and water. Animal work was conducted in compliance with the Spanish legislation on "Protection of Animals used for Experimenting or other Scientific Purposes" and in accordance with the Directives of the European Community. Rats were initially anesthetized with 4% halothane in a mixture of 70% N_2O and 30% O_2, and after tracheal intubation for controlled ventilation, anesthesia was maintained with 1% to 1.5% halothane. The left femoral artery was cannulated for monitoring blood pressure and body temperature was maintained at 36.5 to 37.5°C with a heating blanket connected to a rectal probe. Transient focal cerebral ischemia was induced by middle cerebral artery (MCA) occlusion using an intraluminal technique, as reported previously (31). Briefly, the right MCA was occluded by introducing a 26-mm-long, 3/0 nylon monofilament, blunted at the tip, through the internal carotid artery to the level where the MCA branches out. Both common carotid arteries were clamped to minimize collateral circulation (32). After 50 min, the clip on the left common carotid artery was removed and 10 min later the filament was withdrawn and the clip on the right common carotid artery was also removed. Following surgery, rats were allowed to recover spontaneous breathing. Finally, rats were killed under halothane anesthesia at 4 hours, 1, 4, 7, and 14 days after the onset of reperfusion. For control purposes the left ipsilateral hemisphere of all the rats subjected to ischemia/reperfusion was used, and in addition, the brains of nonoperated rats (n = 6) were also studied. Note: these rats were anesthetized before killing according to the ethical procedures of our institution.

Primary Cell Culture Preparation

Neuron-enriched cultures were prepared from embryonic day 18 (E18) Sprague-Dawley rats (Iffa-Credo) as previously described (33), with modifications. Reagents, unless otherwise stated, were from Invitrogen (Paisley, Scotland, UK). Cells were resuspended in modified Eagle's medium (MEM) (Sigma-Aldrich, Alcobendas, Spain) supplemented with 10% fetal calf serum and 100 μg ml^{-1} gentamycin and seeded at a density of 3,680 cells/mm^2. Six μM cytosine arabinose was added after 4 days in vitro. At 7 and 10 days in vitro, part of the medium was replaced with MEM containing B27 supplements with 3 μM cytosine arabinose to prevent proliferation of non-neuronal cells.

Glial cell cultures enriched in astrocytes were prepared from the cerebral cortex of P1-P2 postnatal Sprague-Dawley rats as previously described (34), with slight modifications. Cells were plated and maintained in Dulbecco's modified Eagle medium (DMEM, Gibco-BRL, Invitrogen, Paisley, UK) supplemented with 20% fetal bovine serum (FBS) (Gibco-BRL). The culture medium was changed twice per week. After 1 week, the flasks were shaken at 200 rpm for 2 hours to dislodge microglia. The medium was removed and replaced with fresh medium containing 10% FBS. Subsequently, until the cells reached confluence, 7% FBS was used in the medium.

Microglial cultures were prepared from cultures of rat primary mixed glia at 7 to 8 days in vitro by shaking the cells for 2 hours at 200 rpm, as reported elsewhere (35). Floating cells were collected and sub-cultured at 5×10^4 cells ml^{-1} and maintained with the tissue medium as above, containing 7% FBS.

Oligodendrocyte cultures from rat brain were provided by Dr. Eduardo Molina-Holgado and were prepared as described elsewhere (36). Oligodendrocyte progenitors were grown in culture for 3 days in serum-free medium containing 2.5 ng ml^{-1} basic fibroblast growth factor and human recombinant platelet-derived growth factor-α (PreproTech Inc., Rocky Hill, NJ), which expanded the number of cells while preventing differentiation by maintaining the cells as a population of homogeneous bipolar cells. Mature oligodendrocytes were obtained by further culturing the cells for up to 10 days in the same medium as above, supplemented with 3% calf serum (Gibco-BRL). These cells acquired a complex morphology with ramified processes.

Protein Expression by Western Blotting

Cell culture and tissue samples were homogenized in radioimmunoprecipitation assay lysis buffer with a protease inhibitor cocktail (Boehringer Mannheim, Mannheim, Germany), as reported previously (34). Samples were sonicated and then centrifuged at 12,000 × *g* for 15 min at 4°C, and the supernatants were used as the protein fraction. The protein content was determined with the Bradford assay (Bio-Rad, Hercules, CA). A different set of frozen tissue samples from control and ischemic brains was used to obtain the cytosolic membrane protein fraction using a sucrose gradient method, as previously reported (37). Each sample (controls, n = 3; ischemic, n = 3) was obtained by pooling frozen brain tissue from 2 rats. Briefly, tissue was homogenized with a loose Dounce homogeniser in buffer (1:3 w/v) containing 1 mM $NaHCO_3$ and 0.5 mM $CaCl_2$, pH 7.5. The homogenate was filtered and centrifuged at 1,000 × *g* for 20 min. The pellet was resuspended in the same buffer and centrifuged at 1,500 × *g* twice for 15 min each, then resuspended and centrifuged at 1,550 × *g*. The pellet was then resuspended in 80% sucrose to a final volume of 10 ml and homogenized with a tight Dounce homogenizer. Then, a sucrose gradient (solutions were made in 5 mM tris-HCl buffer, pH 7.5) was prepared by sequentially adding 8 ml 80% sucrose, 8 ml 48% sucrose, 8 ml 47% sucrose, and 6 ml 41% sucrose, which was subjected to ultracentrifugation at 90,000 × *g* for 2 hours. The membrane enriched fraction (found between 47%–41% sucrose) was centrifuged at 100,000 × *g* for 30 min in 10 mM Tris-HCl buffer pH 7.4 containing 3 mM EGTA. Finally, the

pellet was resuspended in the last buffer and the protein content was determined as above.

Protein samples were run alongside prestained molecular weight markers (Bio-Rad) in denaturing 6% to 8% polyacrylamide gels and were transferred to a membrane (Immobilon-P, Millipore, Bedford, MA), as reported previously (34). Membranes were incubated overnight at 4°C with one of the following primary antibodies: mouse monoclonal antibodies against rat Agrin (Agr-520, StressGen, Victoria, Canada) diluted 1:250, β-tubulin (Boehringer Mannheim) diluted 1:5,000, synaptophysin (clone SY 38, Dako, Glostrup, Denmark) diluted 1:7,000, ED1 (MCA341, Serotec, Kidlington, Oxford, UK) diluted 1:300; and rabbit polyclonal antibodies against the MMP-3 hinge region (M4802, Sigma) diluted 1:1,000, actin (Sigma) diluted 1:5,000, MMP-2 (AB809, Chemicon, Temecula, CA) diluted 1:2,000, glial fibrillary acidic protein (GFAP, Dako) diluted 1:1,000. The secondary antibodies (Amersham, Piscataway, NJ) were peroxidase-linked anti-mouse Ig or anti-rabbit Ig diluted 1:2,000. The reaction was developed with a chemiluminescence reagent containing luminol. Densitometric analysis of band intensity in the blots was carried out with a Kodak camera (DC-120) and Kds1D Digital Science System software.

Enzymatic Assay of MMP-3 Activity

MMP-3 activity was assessed by incubation of control and ischemic brain samples with a fluorogenic substrate (MMP-3 Substrate II, Calbiochem, San Diego, CA), which is degraded by MMP-3 (38). Frozen tissue was homogenized in lysis buffer containing 50 mM Tris-HCl pH 7.6, 150 mM NaCl, 5 mM $CaCl_2$, 0.05% Brij-35, 0.02% NaN_3, and 1% Triton X-100, and centrifuged at 12,000 × *g* for 5 min at 4°C. The supernatants, containing 200 μg of protein (in a volume of 50 μl), were mixed with assay buffer (50 mM Tris-HCl pH 7.6, 200 mM NaCl, 5 mM $CaCl_2$, 20 μM $ZnSO_4$ and 0.05% Brij-35) to a final volume of 200 μl, and different concentrations of the fluorogenic MMP-3 substrate (1, 2.5, 5, 10, and 30 μM) were added. The samples were incubated for 10 min at 37°C and fluorescence was measured on a fluorimeter (Spectra Max GeminiXS, Molecular Device Corporation, Sunnyvale, CA) (λ_{exc} = 328 nm and λ_{em} = 393 nm). A mixture of lysis buffer with assay buffer in the absence of tissue samples was incubated as above as a reaction blank. Data was analyzed by nonlinear regression and fitted to one-phase exponential association curves. The rate constant and the Y_{max} values were calculated and statistical comparisons between rat groups were performed with the unpaired *t*-test.

Immunohistochemistry and Histochemical Reactions

Rats were perfused with 4% paraformaldehyde and brains were postfixed overnight with the same fixative and then embedded in paraffin. Five-μm-thick coronal sections were obtained with a microtome. Studies were performed 1, 4, 7, and 14 days after ischemia and in controls (n = 3 per group). Paraffin was removed and sections were boiled in 10 mM citrate buffer, pH 6, for 20 min for antigen retrieval. Immunohistochemistry was carried out as previously reported (37). Endogenous peroxidases were blocked with methanol-H_2O_2, and *non*-specific-binding sites with 3% normal horse or goat serum for 2 hours. Sections were then incubated overnight in a humidified chamber at 4°C with either the mouse monoclonal antibody against CNS agrin (agr-520) diluted 1:25, a mouse monoclonal antibody against GFAP (Boehringer Mannheim) diluted 1:500, or a rabbit polyclonal antibody against MMP-3 (Sigma) diluted 1:200. Sections were incubated with biotinylated horse anti-mouse or goat anti-rabbit IgG (Vectastain, Vector, Burlingame, CA) diluted 1:200 for 1 hour and then avidin-biotin-peroxidase (ABC kit, Vector) (1:100) for 1 hour. The reaction was developed with 0.05% diaminobenzidine and 0.03% H_2O_2. Immunoreaction controls included omission of the primary antibody. Several sections were counterstained with hematoxylin. Double immunohistochemistry (37) was performed after the first immunoreactions. Sections previously reacted with the first primary antibody were incubated overnight with the second primary antibody, followed by a biotinylated secondary antibody. Then the sections were incubated with the avidin-biotin complex, washed with 0.01 M sodium phosphate buffer, pH 6, and preincubated for 10 min with 0.01% benzidine dihydrochloride and 0.025% sodium nitroferricyanide in 0.01 M sodium phosphate buffer, pH 6. The reaction was developed in this solution with 0.005% H_2O_2.

Lectin histochemistry to label microglia/macrophages was carried out by incubating the section with biotinylated lectin from Lycopersicon esculentum (Sigma), as reported previously (37), following incubation with the primary antibody. For control purposes, we carried out the same double histochemistry procedures in the absence of either the first primary antibody or the lectin.

For Luxol fast blue (Klüver-Barrera) staining, sections were immersed in 95% ethanol and were stained in a Luxol fast blue solution (0.1% in 95% ethanol) for 2 hours at 60°C, and the excess stain was rinsed with 95% ethanol. The sections were rinsed with distilled water and differentiated the staining by immersion in a 0.05% lithium carbonate solution for 30 seconds. We continued differentiation in the 70% ethyl alcohol and when differentiation was completed (i.e. grey and white matter was visually distinguished), we washed in distilled water, dehydrated the sections, and mounted the preparations.

Casein Zymography in Cultured Cells

Zymography was performed in 8% polyacrylamide gels containing casein (1 mg ml^{-1}). The casein solution (from bovine milk, Sigma) (10 mg ml^{-1}) was prepared by mixing with 1.5 M Tris-HCl pH 8.8 for 2 hours under vortex shaking. Ten μg of protein was loaded in the gel and SDS-PAGE was performed at 100 V. The gels were incubated in 250 ml of buffer containing 50 mM Tris-HCl pH 7.5, 10 mM $CaCl_2$ and 0.02% NaN_3 for 42 hours at 37°C. Incubation in the presence of 20 mM EDTA was carried out as a control for the specificity of the caseinolytic reaction. After incubation, gels were stained in 0.1% amido black (napthol blue black, Sigma) in acetic acid: methanol:water (1:3:6) for 30 min and washed in the solvent 4 times for 15 min each, followed by a final wash in distilled water.

Agrin Degradation by MMP-3

The tissue homogenates (as used for Western blot, described above) containing 300 μg of protein in approximately 30 μl were mixed to a final volume of 200 μl with incubation buffer

containing 50 mM Tris-HCl pH 7.5, 10 mM $CaCl_2$, and 0.02% NaN_3, and in the presence or absence of 500 U of human recombinant MMP-3 (catalytic domain, from Calbiochem) (1.6 U/μg of protein). Incubation was carried out for 18 hours at room temperature under constant shaking. Forty μg of protein was denatured and loaded on a 6% polyacrylamide gel for Western blot analysis of agrin.

RESULTS

Expression of MMP-3

Basal expression of MMP-3 pro-form in control brain tissue was detected by Western blot analysis as a band of ~57 kDa (Fig. 1A). A faint band of ~120 kDa, which might correspond to MMP-3 dimers, was detected in the blots, but no changes were seen in the intensity of this band after ischemia/reperfusion (Fig. 1A). However, ischemia/reperfusion caused the appearance of an additional band of lower molecular weight (45 kDa, n = 12), which corresponds to an active form of MMP-3 at 1, 4, and 7 days post-ischemia, but not at 4 hours (Fig. 1A). Quantification of the intensity of this band by densitometric analysis showed a significant ($p < 0.001$) increase at 1, 4, and 7 days after ischemia/reperfusion (Fig. 1B).

MMP-3 Activity in Brain Tissue after Ischemia

We determined the extent to which brain tissue samples were able to degrade a specific MMP-3 fluorogenic substrate, which becomes fluorescent following cleavage. We measured the fluorescence (excitation = 368 nm, emission = 459 nm) after addition of various substrate concentrations ranging from 0 to 30 μM. Data for each group of rats (4–6 rats per group) was obtained after 10-min incubation and fitted to a curve by means of *non*linear regression (1 phase exponential association) (Fig. 1B). The control group fitted with $R^2 = 0.998$, the 1-day post-ischemia experiment group fitted $R^2 = 0.996$, and the 4-day group fitted $R^2 = 0.997$. Mean ± SEM values for the rate constant (K) were 0.121 ± 0.011 for controls, while the corresponding values for 1 day and 4 days post-ischemia were 0.206 ± 0.039 and 0.1817 ± 0.020, respectively. The higher K value (Fig. 1C) after ischemia ($p < 0.05$) is compatible with an increase in the activity of MMP-3. Y_{max} values were 1,298 ± 63 for controls and 1,189 ± 105 and 1,843 ± 92 for 1 and 4 days post-ischemia, respectively. The Y_{max} value can be taken as the capacity of the enzyme to bind substrate, suggesting an increased MMP-3 protein expression by 4 days post-ischemia ($p < 0.001$) (Fig. 1C). At this time point, expression of MMP-3 was found in reactive microglia/macrophages (Fig. 2S), indicating that there was more enzyme present in the tissue for binding its substrate.

Cellular Localization of MMP-3

We detected expression of MMP-3 in the control brain (Fig. 2A, I, N), mainly localized in neurons as evidenced in Figure 2N by double immunostaining with NeuN, which is a marker of neuronal nuclei. Neurons showed faintly stained cytoplasm and processes, and a discrete granular staining in their nucleus. In addition, MMP-3-stained oligodendrocytes were detected in the control white matter as shown in Figure 2E (light brown) and Figure 2G (dark brown). Double immunohistochemistry with GFAP revealed no stained astrocytes (Fig. 2A, E). Likewise, no MMP-3 staining was detected in resting microglia, or the microvasculature (Fig. 2A, arrowhead).

At 24 hours of reperfusion after 1-hour MCA occlusion, increased MMP-3 staining was detected in neurons located in the periphery of the ischemic core (Fig. 2B). Within the ischemic core there were many MMP-3-stained neurons showing a typical morphology of ischemic neurons with a triangular shape and a very shrunken nucleus that was immunoreactive to MMP-3 (Fig. 2C, J, L). In this area, stained processes were no longer seen and, besides the stained neurons, the overall immunoreactivity was reduced compared with that in the contralateral hemisphere (Fig. 2C). At this time, MMP-3 staining was prominent in oligodendrocytes located in the ipsilateral white matter (Fig. 2F). MMP-3 staining in oligodendrocytes of the white matter was very intense by 4 days post-ischemia (Fig. 2H). At this time, disrupted myelin fibers were detected in the ipsilateral corpus callosum after Luxol fast blue staining (bright blue patch in Fig. 2H). Also, by 4 to 7 days post-ischemia, lectin-positive (Fig. 2Q) reactive microglia/macrophages within the infarcted core were immunoreactive to MMP-3 (Fig. 2S), and again no MMP-3 was detected in reactive astrocytes (not shown). At 14 days, the intense staining of oligodendrocytes and microglia/macrophages in the ipsilateral hemisphere was maintained and certain neurons in the periphery of the infarcted core showed intense staining, which became apparent even in the nucleus (not shown). In addition, we observed an increased MMP-3 staining in the microvasculature at 1 day (Fig. 2D, F) and 4 days (Fig. 2S) post-ischemia.

As MMP-3 was reported in astrocytes under certain conditions (39), we decided to separately culture different neural cell types to study MMP-3 expression. We studied primary cultures of rat astrocytes, neurons, microglia, and oligodendrocytes. Markers of the different cell types were used to illustrate the enrichment of each culture in each particular cell type (Fig. 1E). In agreement with data obtained from brain tissue, the results in cultured cells (Fig. 1E) revealed expression of MMP-3 in neurons (Fig. 1E, lanes 1 and 2) and mature oligodendrocytes (Fig. 1E, lane 8), but not in oligodendrocyte precursors (Fig. 1E, lane 7), astrocytes (Fig. 1E, lanes 5 and 6), or microglial cells (Fig. 1E, lanes 3 and 4). Casein zymography in extracts of the different cell types showed MMP-3 activity in neurons (Fig. 1F). The intensity of the neuronal zymography

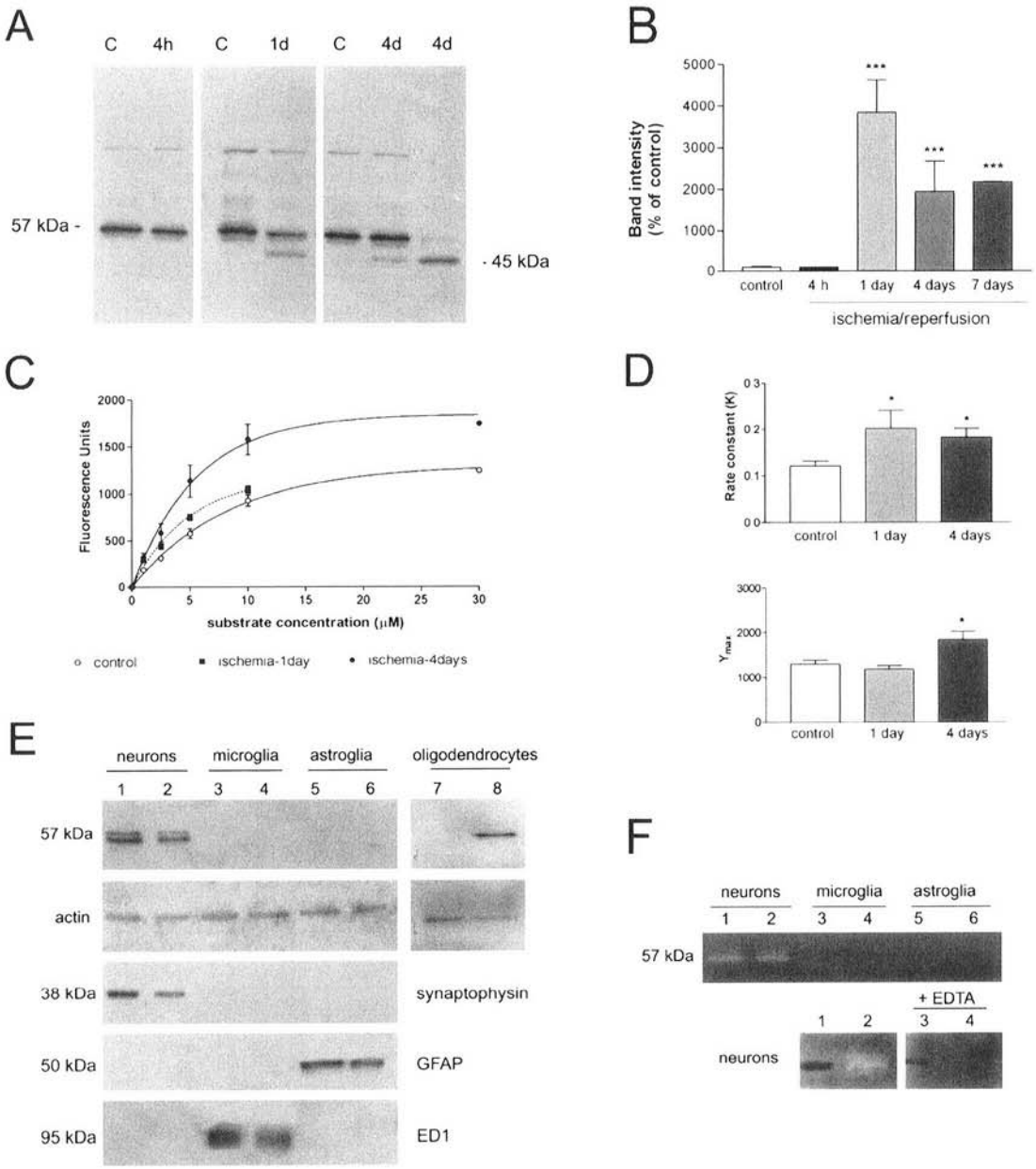

Fig. 1. MMP-3 is activated in the rat brain following MCA occlusion/reperfusion and is expressed in neurons and mature oligodendrocytes in cell cultures, but not in astroglia or microglia. **A:** A 57-kDa precursor form of MMP-3 is expressed in the control brain (from rats not subjected to ischemia and in the contralateral hemisphere of ischemic rats). At 1 and 4 days after the onset of ischemia, but not at 4 hours, a 45-kDa band corresponding to an active form of MMP-3 is found. This is accompanied with some loss of the prozymogen, which is more apparent at 4 days. **B:** Densitometric analysis of the intensity of the 45-kDa band shows a significant (*** indicates $p < 0.001$, *t*-test) increase at 1 day ($n = 7$), 4 days ($n = 3$), and 7 days ($n = 2$) following MCA occlusion in relation to controls ($n = 10$). Values are expressed as the percentage of control. **C:** Homogenates of brain tissue ($n = 4$ to 6 rats in each group: controls, 1 day and 4 days ischemia) were incubated in vitro for 10 min with an MMP-3 substrate that emits fluorescence once it has been cleaved by the enzyme (see Materials and Methods). We measured the fluorescence (excitation = 368 nm, emission = 459 nm) that was produced using several substrate concentrations ranging from 0 to 30 μM. Points were fitted to 1-phase exponential association curves using *non*linear regression analysis and the rate constant and Y_{max} parameters were estimated. **D:** The rate constant was higher in both ischemic groups than in the control, indicating a higher activity of the enzyme, whereas the Y_{max} value was higher only at 4 days post-ischemia, compatible with a higher binding capacity in this group (* indicates $p < 0.05$ using the unpaired *t*-test assay). **E:** In cell cultures, the precursor form of MMP-3 was found in cultured neurons (lanes 1, 2) and mature oligodendrocytes (lane 8), but not in precursor oligodendrocytes (lane 7), microglia (lanes 3, 4), or astroglia (lanes 5, 6). Actin is shown as a control for protein loading. Synaptophysin, GFAP, and ED1 blots are shown to identify neurons, astrocytes, and microglia, respectively. **F:** Casein zymography revealed the presence of a band in neurons (lanes 1, 2) but not in microglia (lanes 3, 4) or astroglia (lanes 5, 6). In the bottom part of the figure, casein zymographies

band was attenuated when incubation for casein degradation was performed in the presence of 20 mM EDTA, which inhibits Ca^{2+}-dependent MMP-3 activity (Fig. 1F, bottom gels).

MMP-3 Degrades Brain Agrin and Agrin Is Degraded following Ischemia/Reperfusion

We incubated extracts of control brain in the presence or absence of MMP-3 for 18 hours at room temperature. MMP-3 caused agrin degradation of the full transmembrane agrin form of 220 kDa, as revealed by Western blot (Fig. 3A). Likewise, ischemia/reperfusion caused transmembrane agrin cleavage, as a reduction of the 220-kDa band was detected in membrane extracts (Fig. 3B). In whole brain protein homogenates, attenuation of the intensity of the 220-kDa band after ischemia/reperfusion (at 1, 4, and 7 days) was accompanied by the formation of a lower molecular weight band (135 kDa) (Fig. 3C). The low molecular weight band seen in the total protein extracts of the ischemic brains was not detected in the membrane extracts of ischemic brains (Fig. 3B), demonstrating that the cleaved form of agrin did not remain attached to the membrane. The cleaved fragment of agrin that we detected here contains the C-terminal domain, as the antibody used recognized an epitope located close to the C-terminus of agrin forms containing inserts at splicing site Z; expression of these forms is restricted to the brain.

Cellular Localization of Agrin

We studied agrin expression in primary cultures of neurons, astrocytes, microglia, and oligodendrocytes. Agrin was detected in cultured neurons, and to a lesser extent cultured astrocytes, but not in oligodendrocytes or microglia (Fig. 3D).

Low agrin expression was found in the control rat brain tissue by immunohistochemistry and staining was located in neurons (Fig. 4A). Staining was localized in neuronal processes and around the cell bodies, which is compatible with the presence of agrin in the cell membrane. At 24 hours post-ischemia, agrin staining faded away within the ischemic core (Fig. 4C). However, in the vicinity of the ischemic core, in a penumbra-like area surrounding the core, the intensity of staining was increased around the cell bodies of scattered neurons (Fig. 4B). Here the pattern of agrin staining in neuronal fibers changed, as some parts of neuronal processes showed a higher intensity of staining (Fig. 4B), which might reflect disturbances in agrin trafficking from cell bodies to the synaptic terminals. By 4 to 7 days after MCA occlusion, agrin staining was found in reactive astrocytes forming the glial scar around the infarcted core (Fig. 4D, E) and in extracellular deposits in the vicinity of blood vessels (Fig. 4H). Within the infarcted core, strong staining was observed in granulated deposits inside reactive microglia/macrophages (Fig. 4F). Formation of the agrin-positive granules progressed with time, as they became more intensely stained and showed a more compacted appearance by 14 days post-ischemia (Fig. 4I).

DISCUSSION

MMP-3 in Neurons of the Ischemic Brain

We demonstrated activation of MMP-3 in cerebral ischemia/reperfusion by the appearance of an active band of 45 kDa that was not present in the control brain. MMP-3 expression after ischemia has previously been shown in ischemic neurons and microglial cells at 24 hours following transient MCA occlusion in rats (5). In agreement with this study, we found strong expression of MMP-3 in ischemic neurons in the core showing a typical triangular morphology, which is compatible with a process of ischemic cell death (39). Thus, besides its extracellular role in degrading matrix components, it is likely that neuronal MMP-3 becomes active inside the cells and acts as a proteolytic enzyme degrading cellular components during ischemic cell death. This does not necessarily imply that MMP-3 is involved in causing cell death, as it might simply be a consequence of the cell death process.

MMP-3 Cleaves Transmembrane Neuronal Agrin

We have shown that MMP-3 degrades brain agrin, which is located in neurons, and we observed the disappearance of neuronal agrin from cell membranes after ischemia. Concomitantly, we found an agrin fragment of lower molecular weight that did not remain associated with the membranes, suggesting the release of cleaved agrin to the parenchyma. Agrin removal from the synaptic basal lamina by MMP-3 has been shown at the neuromuscular junction (16) for this agrin isoform, named LN form, but it has not been previously described for the brain agrin isoform, named SN form (20). Although these 2 agrin isoforms are derived from the same gene, they correspond to proteins with different NH_2 termini that differ in their subcellular location, tissue distribution, and function (20). Both isoforms are externalized from cells, but whereas LN agrin assembles into the basal lamina,

←

are shown for aliquots of the same neuronal culture (lanes 2 and 4). Lanes 1 and 3 show a prestained molecular weight marker (50 kDa). The gel on the left side was incubated in the absence of EDTA, whereas the gel on the right side was incubated in the presence of 20 mM EDTA, which inhibits MMP-3.

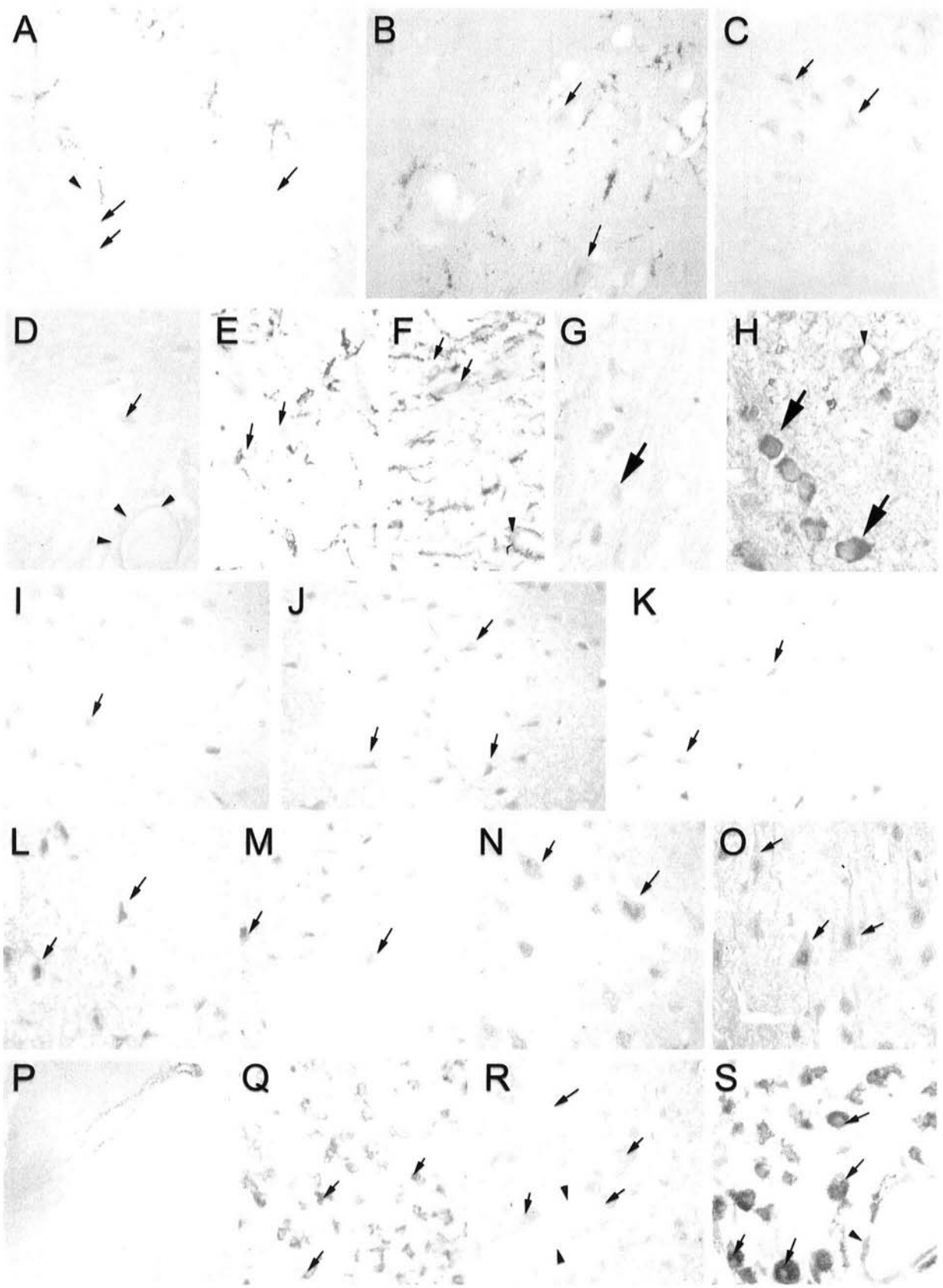

Fig. 2. MMP-3 is expressed in control neurons and, after ischemia/reperfusion, MMP-3 expression increases in ischemic neurons, oligodendrocytes, microvasculature, and reactive microglia, but it is not detected in astrocytes. The regions shown are in cortex (**A–C, I–S**), striatum (**D**), and corpus callosum (**E–H**) of control (**A, E, G, I, N, P**) and at 1 day (**B–D, F, J–M, O**)

SN-agrin is cell-associated since it is a type-II transmembrane protein with an intracellular N-terminus and an extracellular C-terminus (22). The N-terminus can externalize cytosolic proteins and might serve as an association domain (27). The antibody that we used in the present study against rat agrin recognizes an epitope located close to the C-terminus of agrin forms containing the 8aa, 11aa, or 19aa insert at splicing site Z; these forms are restricted to the CNS (44). Here we show that C-terminal fragments of cleaved agrin after ischemia do not remain associated with the membrane. Whether this has a functional implication other than loss of neuronal membrane agrin remains to be seen. Proteolytic cleavage through ectodomain shedding, resulting from the action of MMP-3, might represent a regulatory control of agrin function in the CNS (27). The fact that agrin is a transmembrane protein in the CNS suggests that it acts as a receptor that mediates the translocation of signals from the extracellular space to the cytoplasm (22). In CNS neurons, agrin signals through synaptic receptors (42) that have been identified as integrins (27). Agrin regulates synapse differentiation in hippocampal neurons (43, 44) and a role in regulating activity-dependent changes in synaptic efficacy has been proposed (45). A decrease in the number of differentiated synapses and defective synaptic transmission has been found in the superior cervical ganglion deficient in agrin (46). Furthermore, agrin-deficient neurons and mice are resistant to excitotoxic injury, thus suggesting that agrin is involved in glutamatergic transmission and in neuronal Ca^{2+} homeostasis (28). Therefore, loss of agrin from cell membranes in ischemia might contribute to impaired synaptic transmission, but it might confer resistance to excitotoxicity. Nevertheless, the fate and function of the cleaved C-terminal fragments remain unknown. C-terminal brain agrin fragments are able to induce CREB phosphorylation and c-*fos* expression, and several lines of evidence suggest that they bind to a discrete neuronal receptor at the synapses (26). According to this view, C-terminal agrin fragments that are released to the extracellular space in ischemia might stimulate neuronal Ca^{2+} influx and exacerbate the excitotoxic cascade.

MMP-3 Is Not Present in Resting Brain Astrocytes, but Agrin Is Found in Reactive Astrocytes following Ischemia/Reperfusion

Agrin was not found in resident astrocytes of the control brain. However, by the time that the glial scar was formed at 4 days post-ischemia, we observed that the reactive astrocytes showed some immunoreactivity to agrin. It is likely that this new agrin location results from agrin synthesized de novo by reactive astrocytes, and it was found surrounding the cell body and processes, suggesting that it was the transmembrane form of agrin. Agrin expression was also detected in cultured astrocytes, which were studied at the time they reached confluence. These cultured astrocytes showed basal expression of 27-kDa heat-shock protein (34), which is not normally found in resident astrocytes of the control brain (47), suggesting that they have some degree of reactivity. It is conceivable that agrin in reactive astrocytes might contribute to astrocytic connection and communication and might be involved in the formation of a *non*permissive environment to axon growth, as the C-terminal fragment of agrin inhibits axon elongation (48). Agrin in reactive astrocytes would remain protected from proteolytic cleavage because these cells are devoid of MMP-3, offering an explanation of why it remained in the glial scar for several days.

MMP-3, but not Agrin, Is Expressed in Mature Oligodendrocytes and MMP-3 Expression Is Increased in Oligodendrocytes following Ischemia/Reperfusion

In contrast to astrocytes, oligodendrocytes were immunoreactive to MMP-3 in the corpus callossum of control brains. Following ischemia, the intensity of MMP-3

←

and 4 days (**H, Q–S**) post-ischemia. **A–F:** MMP-3 staining in brown does not colocalize with GFAP staining in dark blue. **A:** Low MMP-3 (brown) staining in control neurons (arrows), but not astrocytes (black) and vessels (arrowhead). **B, D:** In the zone surrounding the ischemic core the intensity of staining increases in neurons (arrows) and microvasculature (**D,** arrowheads). **C:** Neurons within the ischemic core show MMP-3 staining concentrated in their nuclei (arrows). **E:** MMP-3 stains oligodendrocytes (arrows) in the control corpus callosum, and (**F**) the intensity of staining increases following ischemia in these cells (arrows) and in vessels (arrowhead). **G, H:** MMP-3-stained oligodendrocytes are shown in brown and myelinated fibers are stained bright blue with Luxol fast blue; oligodendrocytes show a strong increase in MMP-3 staining 4 days post-ischemia (**H,** arrows) relative to controls (**G,** arrows). Blue staining patches in (**H**) indicate disrupted myelin fibers. **I–M:** Hematoxylin counterstained sections in the presence (**I, J, L**) or absence (**K, M**) of the primary antibody against MMP-3 in a section from a control rat (**I**) and in sections from ischemic rats (**J–M**). **N, O:** Double immunohistochemistry against MMP-3 (brown) and the NeuN neuronal marker (black) in control (**N**) and ischemic (**O**) cortex. Ischemic, shrunken neurons showing triangular morphology are apparent in (**J–M**) and (**O,** arrows). **P–S**: Staining of MMP-3 (brown) and lectin (dark blue), a marker of microglia/macrophages, shows colocalization (**S**) at 4 days post-ischemia. **P:** No cellular staining is detected in the control cortex, but MMP-3-labeled reactive microglia/macrophages (**S**, arrows) are apparent 4 days post-ischemia. Immunoreaction controls include (**Q**) omission of the primary antibody against MMP-3 (revealing reactive microglia/macrophages stained in black, arrows), and (**R**) omission of lectin (evidencing MMP-3 stained cells with the morphology of reactive microglia/macrophages, arrows). Bar scale: G–H = 15 μm; A–F, L–S = 25 μm; I–K = 50 μm.

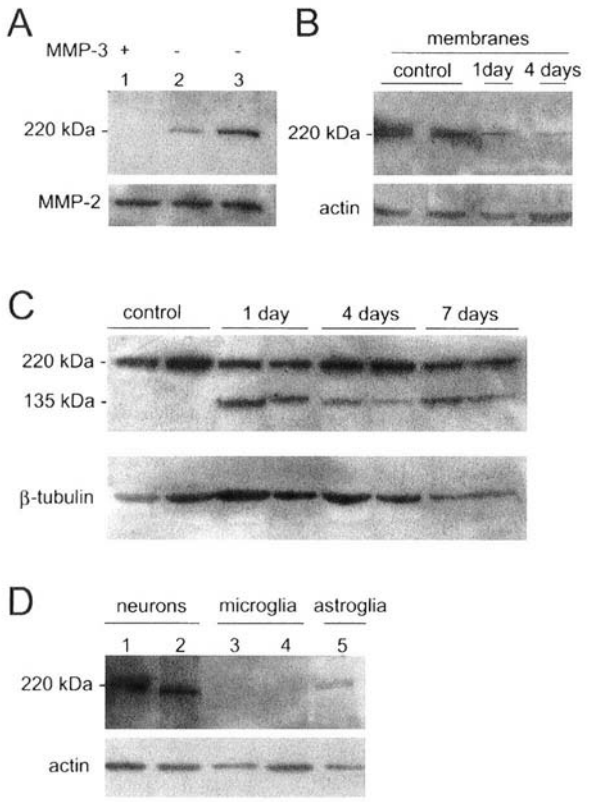

Fig. 3. MMP-3 degrades transmembrane neuronal agrin, which becomes cleaved following ischemia, concomitant with MMP-3 activation. **A:** Homogenates of control brain tissue (from rats not subjected to ischemia) were incubated in the presence (lane 1) or absence (lanes 2, 3) of 1.6 U of human recombinant MMP-3 per μg of tissue protein. Samples in lanes 1 and 2 were incubated at 37°C in MMP-3 buffer (see Materials and Methods) for 18 hours, whereas the sample in lane 3 was directly loaded on the gel without prior incubation. MMP-2 expression in the same gel is shown to illustrate equal protein loading in each lane. MMP-3 has the ability to degrade brain agrin. **B:** Isolated membrane preparations from brain tissue of controls or brains obtained at 1 and 4 days post-ischemia show reduced transmembrane agrin expression following ischemia. Actin is shown at the bottom as a protein loading control. **C:** In homogenates of brain tissue from controls and at 1, 4, and 7 days post-ischemia the reduction of 220-kDa transmembrane agrin is accompanied by the formation of a 135-kDa agrin-cleaved fragment containing the C-terminal region, where the recognition epitope for the antibody used is located. β-tubulin is shown as a control for protein loading in the different lanes. **D:** In cultured cells, transmembrane agrin is detected in neurons and to a much lesser extent in astrocytes, but not in microglia. Actin is shown as a protein loading control.

staining was markedly increased in oligodendrocytes located in the ischemic area, including those in the ipsilateral corpus callossum and also in the cortex and striatum in the vicinity of, and within, the glial scar. In the injured CNS, oligodendrocytes become reactive; they show signs of hypertrophy, they divide, and then differentiate to provide new oligodendrocytes for re-myelination (49). MMP-3 expression correlates with the invasive properties of human astrocytoma cell lines due to the proteolytic effects of MMP-3 on extracellular matrix macromolecules (2). Although oligodendrocytes might use MMP-3 to migrate within the parenchyma, we did not find MMP-3 in precursor oligodendrocytes. Lack of MMP-3 in oligodendrocyte precursors implies that these cells would be unable to degrade agrin, which might underlie the observation that astrocytes at the glial scar inhibit the migration of oligodendrocyte precursors (50). No expression of agrin was detected in oligodendrocytes in the tissue or in cultured cells.

Reactive Microglia/Macrophages Express MMP-3 and Contain Agrin Deposits

In addition to neurons and oligodendrocytes, some expression of MMP-3 was also detected in reactive microglia/macrophages following ischemia/reperfusion, in agreement with a previous report (5). These latter cells are located within the core of the infarction, where discrete deposits that were immunoreactive to agrin were observed surrounding blood vessels and within the infarcted parenchyma. Thus, these macrophage cells might remove matrix agrin accumulations within the infarcted regions. Accumulation of Luxol fast blue reactive material was also observed in reactive microglia/macrophages, which is compatible with myelin degradation. Myelin is also a substrate for MMP-3 (12), so it is likely that macrophage-associated MMP-3 contributes to agrin and myelin degradation by these cells.

Agrin and MMP-3 in the Microvasculature

Agrin is a component of the basal lamina (51–53), which is a specialized extracellular matrix structure that gives structural support to the microvasculature and in the brain has an essential role in maintaining the integrity of the blood-brain barrier (BBB). Following ischemia, the BBB breaks down and there is extravasation of plasma proteins to the parenchyma, with a maximum leakage by 1 to 2 days. In agreement with a previous report (5), we detected MMP-3 surrounding blood vessels after ischemia, which again might be responsible for agrin degradation at this location and thus contribute to increased BBB permeability. However, we did not observe agrin staining in the cerebral microvasculature since our antibody was specific to the neuronal form of agrin, whereas the form of agrin surrounding the microvasculature lacks the inserts at splicing site Z (54). Nevertheless, by 4 to 7 days after ischemia we detected strong agrin-immunoreactive deposits surrounding the blood vessels within the infarct, suggesting that certain neuronal agrin fragments formed after ischemia accumulated at this site.

In summary, this study shows 1) the activation of MMP-3 in ischemia/reperfusion, where it was found in

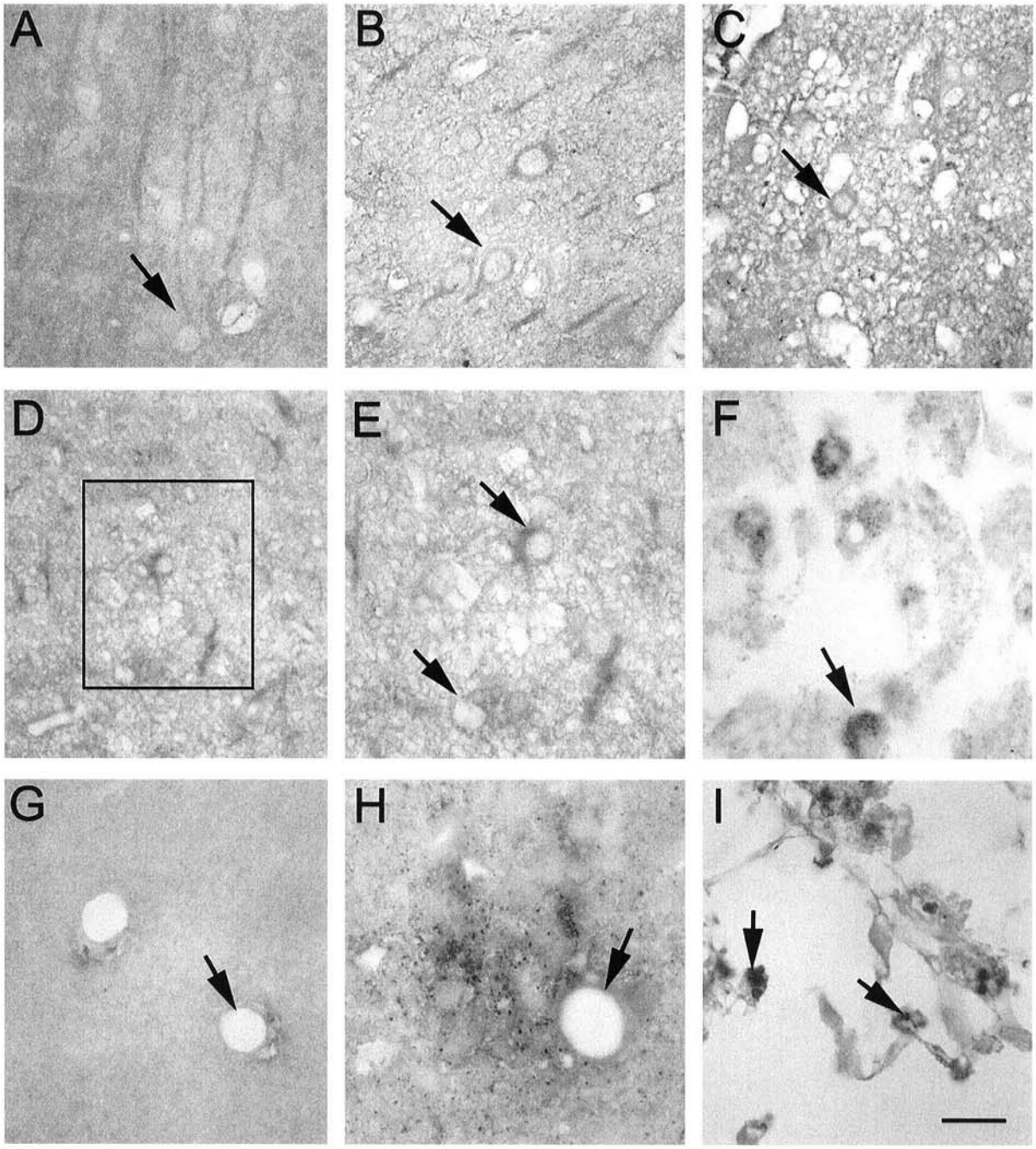

Fig. 4. Ischemia induces loss of neuronal transmembrane agrin, expression of transmembrane agrin in reactive astrocytes, and agrin deposits in microglia/macrophages and surrounding microvessels. **A:** Transmembrane agrin is detected in neurons (arrow) of the control cortex surrounding the cell bodies and cell processes, in rats not subjected to ischemia, and in the contralateral hemisphere of ischemic rats. **B:** At 24 hours following ischemia/reperfusion, cortical neurons in the vicinity of the ischemic core show stronger staining around the cell body (arrow) and discontinuous staining in neuronal processes, suggesting disturbances in axonal transport. **C:** Within the ischemic core, neuronal agrin staining is lost and only scattered immunoreactive neurons (arrow) are seen. **D:** Reactive astrocytes in the glial scar become immunoreactive to agrin. The area marked in the square is magnified in (**E**). **E:** Agrin staining in reactive astrocytes (arrows) is seen surrounding the cell body and processes at 4 days after the onset of ischemia. **F:** At 4 days, reactive microglia/macrophages in the infarcted area show agrin deposits, which become more marked at 14 days (**I**). **G:** Brain agrin is not found in the microvasculature (arrow) of control brains, but agrin deposits surrounding blood vessels (arrow) become apparent from 4 days post-ischemia (**H**). Control brain = **A, D, G**; 1-day post-ischemia = **B, C**; 4-day post-ischemia = **F–H**; 14-day post-ischemia = **D, E, I**. Bar scale: A–D = 20 μm, E–I = 12 μm.

neurons, oligodendrocytes, and reactive microglia/macrophages; 2) the ability of MMP-3 to cleave neuronal brain agrin; 3) the disappearance of neuronal membrane agrin following ischemia, with the generation of cleaved agrin fragments that did not remain associated with cell membranes; and 4) agrin expression by reactive astrocytes. These results support the view that ischemia/reperfusion causes MMP-3 activation, resulting in the cleavage of certain proteins such as agrin and myelin. This study also suggests that transmembrane neuronal agrin cleavage might impair synaptic neurotransmission and enhance excitotoxicity through the action of released C-terminal agrin fragments, and that agrin expression by reactive astrocytes might contribute to the generation of a *non*permissive environment for axon growth.

ACKNOWLEDGMENTS

We thank Dr. Eduardo Molina-Holgado for providing cultured oligodendrocytes. S. Solé and R. Gorina were recipients of fellowships from IDIBAPS, and Dr. V. Petegnief was supported by the MCYT. We wish to thank Mr. Robin Ryeroft for editorial assistance.

REFERENCES

1. Nagase H, Woessner JF Jr. Matrix metalloproteinases. J Biol Chem 1999;274:21491–94
2. Mercapide J, Lopez de Cicco R, Castresana JS, Klein-Szanto AJ. Stromelysin-1/matrix metalloproteinase-3 (MMP-3) expression accounts for invasive properties of human astrocytoma cell lines. Int J Cancer 2003;106:676–82
3. D'Souza CA, Mak B, Moscarello MA. The up-regulation of stromelysin-1 (MMP-3) in a spontaneously demyelinating transgenic mouse precedes onset of disease. J Biol Chem 2002;277:13589–96
4. Rosenberg GA, Sullivan N, Esiri MM. White matter damage is associated with matrix metalloproteinases in vascular dementia. Stroke 2001;32:1162–68
5. Rosenberg GA, Cunningham LA, Wallace J, et al. Immunohistochemistry of matrix metalloproteinases in reperfusion injury to rat brain: Activation of MMP-9 linked to stromelysin-1 and microglia in cell cultures. Brain Res 2001;893:104–12
6. Springman EB, Angleton EL, Birkedal-Hansen H, Van Wart HE. Multiple modes of activation of latent human fibroblast collagenase: Evidence for the role of a Cys73 active-site zinc complex in latency and a "cysteine switch" mechanism for activation. Proc Natl Acad Sci U S A 1990;87:364–68
7. Chen LC, Noelken ME, Nagase H. Disruption of the cysteine-75 and zinc ion coordination is not sufficient to activate the precursor of human matrix metalloproteinase 3 (stromelysin 1). Biochemistry 1993;32:10289–95
8. Murphy G, Cockett MI, Ward RV, Docherty AJ. Matrix metalloproteinase degradation of elastin, type IV collagen and proteoglycan. A quantitative comparison of the activities of 95 kDa and 72 kDa gelatinases, stromelysins-1 and -2 and punctuated metalloproteinase (PUMP). Biochem J 1991;277:277–79
9. Fosang AJ, Neame PJ, Hardingham TE, Murphy G, Hamilton JA. Cleavage of cartilage proteoglycan between G1 and G2 domains by stromelysins. J Biol Chem 1991;266:15579–82
10. Agnihotri R, Crawford HC, Haro H, Matrisian LM, Barda MC, Liaw L. Osteopontin, a novel substrate for matriz metalloproteinase-3 (Stromelysin-1) and matrix metalloproteinase-7 (Matrilysin). J Biol Chem 2001;276:28261–67
11. Sage EH, Reed M, Funk SE, et al. Cleavage of the matricellular protein SPARC by matrix metalloproteinase 3 produces polypeptides that influence angiogenesis. J Biol Chem 2003;278:37849–57
12. Chandler S, Coates R, Gearing A, Lury J, Wells G, Bone E. Matrix metalloproteinases degrade myelin basic protein. Neurosci Lett 1995;201:223–6
13. Gearing AJH, Thorpe SJ, Miller K, et al. Selective cleavage of human IgG by the matrix metalloproteinases, matrylisin and stromelysin. Immunol Lett 2002;81:41–48
14. Ramos-DeSimone N, Hahn-Dantonav E, Sipley J, Nagase H, French DL, Quigley JP. Activation of matrix metalloproteinase-9 (MMP-9) via a converging plasmin/stromelysin-1 cascade enhances tumor cell invasion. J Biol Chem 1999;274:13066–76
15. McQuibban GA, Gong J-H, Wong JP, Wallace JL, Clark-Lewis I, Overall CM. Matriz metalloproteinase processing of monocyte chemoattractant proteins generates CC chemokine receptor antagonists with anti-inflammatory properties in vivo. Blood 2002;100:1160–67
16. VanSaun M, Werle MJ. Matrix metalloproteinase-3 removes agrin from synaptic basal lamina. J Neurobiol 2000;43:140–49
17. Tsen G, Halfter W, Kroger S, Cole GJ. Agrin is a heparan sulfate proteoglycan. J Biol Chem 1995;270:3392–99
18. Reist NE, Magill C, McMahan UJ. Agrin-like molecules at synaptic sites in normal, denervated, and damaged skeletal muscles. J Cell Biol 1987;105:2457–69
19. Reist NE, Werle MJ, McMahan UJ. Agrin released by motor neurons induces the aggregation of acetylcholine receptors at neuromuscular junctions. Neuron 1992;8:865–68
20. Burgess RW, Skarnes WC, Sanes JR. Agrin isoforms with distinct amino termini: Differential expression, localization and function. J Cell Biol 2000;151:41–52
21. O'Connor LT, Lauterborn JC, Gall CM, Smith MA. Localization and alternative splicing of agrin mRNA in adult rat brain: Transcripts encoding isoforms that aggregate acetylcholine receptors are not restricted to cholinergic regions. J Neurosci 1994;14:1141–52
22. Neumann FR, Bittcher G, Annies M, Schumacher B, Kröger S, Ruegg MA. An alternative amino-terminus expressed in the central nervous system converts agrin to a type II transmembrane protein. Mol Cell Neurosci 2001;17:208–25
23. Kroger S, Mann S. Biochemical and functional characterization of basal lamina-bound agrin in the chick central nervous system. Eur J Neurosci 1996;8:500–509
24. Halfter W, Schurer B, Yip J, Yip L, Tsen G, Lee JA, Cole GJ. Distribution and substrate properties of agrin, a heparan sulfate proteoglycan of developing axonal pathways. J Comp Neurol 1997; 383:1–17
25. Koulen P, Honig LS, Fletcher EL, Kroger S. Expression, distribution and ultrastructural localization of the synapse-organizing molecule agrin in the mature avian retina. Eur J Neurosci 1999;11: 4188–96
26. Smith MA, Hilgenberg LGW. Agrin in the CNS: A protein in search of a function? NeuroReport 2002;13:485–95
27. Burgess RW, Dickman DK, Nunez L, Glass DJ, Sanes JR. Mapping sites responsible for interactions of agrin with neurons. J Neurochem 2002;83:271–84
28. Hilgenberg LGW, Ho KD, Lee D, O'Dowd DK, Smith MA. Agrin regulates neuronal responses to excitatory neurotransmitters in vitro and in vivo. Mol Cell Neurosci 2002;19:97–110
29. Witte OW, Bidmon HJ, Schiene K, Redecker C, Hagemann G. Functional differentiation of multiple perilesional zones after focal cerebral ischemia. J Cereb Blood Flow Metab 2000;20:1149–65
30. Lu A, Tang Y, Ran R, Clark JF, Aronow BJ, Sharp FR. Genomics of the periinfarction cortex after focal cerebral ischemia. J Cereb Blood Flow Metab 2003;23:786–810
31. Justicia C, Pérez-Asensio FJ, Burguete MC, Salom JB, Planas AM. Administration of transforming growth factor-α reduces infarct volume after transient focal cerebral ischemia in the rat. J Cereb Blood Flow Metab 2001;21:1097–1104

32. Soriano MA, Sanz O, Ferrer I, Planas AM. Cortical infarct volume is dependent on the ischemic reduction of perifocal cerebral blood flow in a three-vessel intraluminal MCA occlusion/reperfusion model in the rat. Brain Res 1997;747:273–78
33. Petegnief V, Friguls B, Sanfeliu C, Suñol C, Planas AM. Transforming growth factor-α attenuates NMDA toxicity in cortical cultures by preventing protein synthesis inhibition through an Erk1/2-dependent mechanism. J Biol Chem 2003;278:29552–59
34. Fauconneau B, Petegnief V, Sanfeliu C, Piriou A, Planas AM. Induction of heat shock proteins (HSPs) by sodium arsenite in cultured astrocytes and reduction of hydrogen peroxide-induced cell death. J Neurochem 2002;83:1338–48
35. Saura J, Petegnief V, Wu X, Liang Y, Paul SM. Microglial apolipoprotein E and astroglial apolipoprotein J expression *in vitro*: Opposite effects of lipopolysaccharide. J Neurochem 2003;85:1455–67
36. Molina-Holgado E, Khorchid A, Liu H-N, Almazan G. Regulation of muscarinic receptor function in developing oligodendrocytes by agonist exposure. Br J Pharmacology 2003;138:47–56
37. Planas AM, Justicia C, Soriano MA, Ferrer I. Epidermal growth factor receptor in proliferating reactive glia following transient focal ischemia in the rat brain. Glia 1998;23:120–29
38. Bickett DM, Green MD, Wagner C, Roth JT, Berman J, McGeehan GM. A high throughput fluorogenic substrate for stromelysin (MMP-3). Ann N Y Acad Sci 1994;732:351–55
39. Deb S, Gottschall PE. Increased production of matrix metalloproteinases in enriched astrocyte and mixed hippocampal cultures treated with beta-amyloid peptides. J Neurochem 1996;66:1641–47
40. Garcia JH, Yoshida Y, Chen H, Li Y, Zhang ZG, Lian J, Chen S, Chopp M. Progression from ischemic injury to infarct following middle cerebral artery occlusion in the rat. Am J Pathol 1993;142:623–35
41. Hoch W, Campanelli JT, Harrison S, Scheller RH. Structural domains of agrin required for clustering of nicotinic acetylcholine receptors. EMBO J 1994;13:2814–21
42. Hoover CL, Hilgenberg LGW, Smith MA. The COOH-terminal domain of agrin signals via a synaptic receptor in central nervous system neurons. J Cell Biol 2003;161:923–32
43. Böse CM, Qiu D, Bergamaschi A, et al. Agrin controls synaptic differentiation in hippocampal neurons. J Neurosci 2000;20:9086–95
44. Ferreira A. Abnormal synapse formation in agrin-depleted hippocampal neurons. J Cell Sci 1999;112:4729–38
45. Lesuisse C, Qiu D, Böse CM, Nakaso K, Rupp F. Regulation of agrin expression in hippocampal neurons by cell contact and electrical activity. Mol Brain Res 2000;81:92–100
46. Gingras J, Rassadi S, Cooper E, Ferns M. Agrin plays an organazing role in the formation of sympathetic synapses. J Cell Biol 2002;158:1109–18
47. Kato H, Araki T, Itoyama Y, Kogure K, Kato K. An immunohistochemical study of heat shock protein-27 in the hippocampus in a gerbil model of cerebral ischemia and ischemic tolerance. Neuroscience 1995;68:65–71
48. Mantych KB, Ferreira A. Agrin differentially regulates the rates of axonal and dendritic elongation in cultured hippocampal neurons. J Neurosci 2001;21:6802–9
49. Levine JM, Reynolds R, Fawcett JW. The oligodendrocyte precursor cell in health and disease. Trends in Neurosci 2001;24:39–47
50. Fawcett JW, Asher RA. The glial scar and the central nervous system. Brain Res Bull 1999;49:277–91
51. Rupp F, Payan DG, Magill-Solc C, Cowan DM, Scheller RH. Structure and expression of a rat agrin. Neuron 1991;6:811–23
52. Magill-Solc C, McMahan UJ. Motor neurons contain agrin-like molecules. J Cell Biol 1988;107:1825–33
53. Godfrey EW. Comparison of agrin-like proteins from the extracellular matrix of chicken kidney and muscle with neural agrin, a synapse organizing protein. Exp Cell Res 1991;195:99–109
54. Stone D, Nikolics K. Tissue- and age-specific expression patterns of alternatively spliced agrin mRNA transcripts in embryonic rat suggest novel developmental roles. J Neurosci 1995;15:6767–78

Received August 12, 2003
Revision received January 5, 2004
Accepted January 7, 2004

Article nº 6:

Matrix Metalloproteinase-9 in mitotic human neuroblastoma SH-SY5Y cells.

Solé S, Sanfeliu C, Chamorro A, Planas AM (2004)

Departament de Farmacologia i Toxicologia de l' Institut d'Investigacions Biomèdiques de Barcelona, CSIC-IDIBAPS.
Institut de Malalties del Sistema Nerviós (IMSN), Hospital Clínic, Institut d'Investigacions Biomèdiques August Pi i Sunyer (IDIBAPS).

Article en preparació

A protein resembling matrix metalloproteinase-9 is specifically and dynamically expressed during mitosis

Sònia Solé[1], Coral Sanfeliu[1], Ángel Chamorro[2], and Anna M. Planas[1]

[1] Departament de Farmacologia i Toxicologia, Institut d'Investigacions Biomèdiques de Barcelona, CSIC, IDIBAPS, Barcelona, Spain; and [2] IMSN, Hospital Clínic, IDIBAPS, Barcelona, Spain.

Matrix metalloproteinases (MMPs) degrade the extracellular matrix and carry out key functions in development, injury, and cancer. Besides its action on the extracellular matrix, here we present evidence supporting an intracellular function of a MMP-9-like protein during cell division, as follows: 1) Immunostaining with monoclonal antibodies against MMP-9 showed increased immunoreactivity in cells undergoing mitosis; 2) confocal microscopy evidenced a precise, dynamic and well-orchestrated expression of this protein at the different stages of cell division; 3) in situ zymography revealed a higher gelatinase activity in dividing cells; 4) MMP-9 inhibitors prevented cells from entering mitosis, as revealed by flow cytometry, and reduced cell culture growth; and 5) stimulation of cell growth with transforming growth factor-ζ was mediated through cellular MMP-9 activation. Taken altogether these results suggest that MMP-9, or a protein with features of MMP-9, participates in cell division and might be involved in cellular content reorganization and chromatid segmentation.

INTRODUCTION

Matrix metalloproteinases (MMPs) are zinc-dependent endopeptidases that degrade several components of the extracellular matrix. MMPs are normally found as latent zymogens that become active through proteolytic cleavage (Springman et al., 1990), by mechanisms ensuring sensitive and complex regulation of MMP activity *in vivo* (Woessner, 1991). The matrix suffers intense remodeling during development, neoplasia, inflammation, and tissue injury and recovery, which often involve enhanced release of certain proteases. MMPs are thought to have key functions in various pathologies, such as diseases of the central nervous system (Yong et al., 1998) and cancer (Stetler-Stevenson, 1990). Indeed, invasiveness requires that tumoral cells degrade the basement membrane, an event associated with liberation of MMPs (Stetler-Stevenson, 1990). In accordance, MMP inhibitors attenuate tumor cell growth and/or invasive capacity (Tonn et al., 1999; Rabbani et al., 2000). For instance, MMP inhibitors with broad inhibitory spectrum including prevention of MMP-9 activation, suppress cervical lymph node metastasis (Yamashita et al., 2003). Furthermore, increased MMP-9 expression is associated with enhanced proliferative capacity in mouse aortic smooth muscle cells (Moon et al., 2003), and mice injected with lymphoma cells constitutively expressing MMP-9 develop thymic lymphoma more rapidly than mice injected with control lymphoma cells (Aoudjit et al., 1999).

Growth factors up-regulate certain MMPs, such as gelatinases MMP-2 and MMP-9, in gliomas (Rooprai et al., 2000). MMPs are downstream targets of the epidermal growth factor receptor (EGFR) signaling pathway (Miettinen et al., 1999). Indeed, exposure of breast or carcinoma cells to EGFR ligands increases cell proliferation and induction of MMP-9 (Kondapaka et al., 1997; Visscher et al., 1997, O-charoenrat et al., 2000), which is mediated by mitogen-activated protein kinases (Reddy et al., 1999). Also, EGFR signaling pathway is associated with the proteolytic and invasive phenotype in head and neck squamous cell carcinomas (O-charoenrat et al., 1999).

Transforming growth factor-ζ (TGF-ζ) is also a ligand for EGFR with mitogenic activity for epithelial and mesenchimal cells (Massague, 1983; Derynck, 1988). TGF-ζ enhances MMP-9 in cervical-carcinoma SKG-IIIb cells (Ueda et al., 1997).

Although MMPs exert multiple functions in the extracellular space, MMPs could also play functions inside the cells. To test this hypothesis we first studied the intracellular expression and activation of MMP-9 in the SH-SY5Y neuroblastoma cell line. The first results indicated MMP-9 activation during mitosis, and we then accordingly progressed in the study to obtain evidences of any MMP effects on cell culture growth. Altogether the results that we present here suggest that MMP-9, or a protein with several features of MMP-9 (i.e., cross immunoreactivity with two different monoclonal antibodies against MMP-9, gelatinase activity, and response to MMP-9 pharmacological inhibition and activation), is involved in certain steps of cell division.

MATERIALS AND METHODS

Cell cultures and drug treatments

Human neuroblastoma SH-SY5Y cells (ECACC, European Collection of Cell Cultures, Salisbury, Wiltshire, U.K.) were grown in Ham's F12 and Eagle's MEM (1:1) containing 15% fetal calf serum, 1% non-essential amino acids, 2 mM glutamine and 20 σg/ml

gentamicin at 37 ºC, 5 % CO_2, in a humidified atmosphere. All culture media and reagents were from GibcoBRL. Cells were seeded at the density of 3-4 x 10^3 cells/cm^2 and drug treatment was initiated on the next day. Stock solutions of two MMP-9 inhibitors, inhibitor A (MMP-2/MMP-9 Inhibitor II #444249, Calbiochem, Darmstadt, Germany) and inhibitor B (MMP-9/MMP-13 Inhibitor I #444252, Calbiochem) were prepared in dimethylsulfoxide (DMSO) (0.5 % in the final concentration) and concentration-response curves were studied. In each experiment, control cells (0 σM inhibitor) were exposed to the vehicle for the same time. Human recombinant TGF-ζ (Calbiochem) was dissolved in 10 mM acetic acid and then phosphate-buffered saline (PBS) to yield a neutral pH. The day after seeding cells were exposed to TGF-ζ (10 ng/ml) and studies were performed at different time points ranging from 1 to 6 days. In some experiments the tyrosine kinase activity of EGFR was inhibited with 10 σM 4,5-dianilinophthalimide (DAPH) (RBI, Köln, Germany).

Immunocytochemistry

For studies of immunocytochemistry, cells were cultured in 8-well plastic chamber slides (Nunc, Denmark). Cells were fixed with cold methanol for 10 min, washed three times with PBS, and incubated for 1 h with the blocking solution containing 15% normal goat or donkey serum. The primary antibodies were mouse monoclonal antibodies against MMP-9 (MAB 13421 from Chemicon International, Inc., Pacisa-Giralt, Barcelona, Spain; or AB-10 from Oncogene) diluted 1:50, and against η-tubulin (Boehringer Mannheim, Germany) diluted 1:50. Incubation was carried out overnight at 4 °C in the presence of 1% normal goat or donkey serum, followed by either a red fluorescent cyanine ($Cy3^{TM}$)-labeled anti-mouse secondary antibody made in donkey (Jackson Immunoresearch, Pennsylvania, USA) diluted 1:200, or a green fluorescent FITC-labeled secondary anti-mouse antibody made in goat (Molecular Probes, Leiden, The Netherlands) diluted 1:1000, or a red fluorescent TRIC-labeled secondary anti-rabbit antibody made in goat (Sigma, Alcobendas, Madrid, Spain) diluted 1:200. The secondary antibody was incubated for 1-hour at room temperature in the presence of 1% normal donkey or goat serum. After this, cells were washed with PBS, mounted with a mounting media (Mowiol, Calbiochem), and fluorescence was examined under a 40x objective in an optical microscope (Eclipse E1000M/E1000, Nikon, IZASA, Barcelona, Spain) equipped with a super high pressure mercury lamp power supply (HB-10103AF, Nikon). Red fluorescence from $Cy3^{TM}$ fluorochrome (550 nm excitation and 570 nm emission) and green FITC-fluorescence (495 nm excitation and 519 nm emission) were observed using the corresponding filter cubes G-2A and B-2A (Nikon), respectively. Double staining was examined at the confocal microscope (TCS-NT, Leica, Wetzlar, Germany) under a 63x objective (PL APO 63x/1.40 oil). The confocal microscope was equipped with an argon-krypton laser and was used at 568 nm (DD488/568) excitation with a LP590 emission filter for red light, and at 510 nm (RSP510) excitation with a BP530/30 emission filter for green light. To visualize DNA, cells were counterstained with 5 σg/mL bisbenzimide (Hoechst 33258 dye, Sigma) in PBS for 20 min, which binds DNA and produces UV light. Hoechst 33258 (359 nm excitation and 461 nm emission) staining was examined under the fluorescence microscope (Eclipse E1000M/E1000, Nikon) with the corresponding filter cube (UV-2A) using the 20x and 40x objectives. Triple color staining ($Cy3^{TM}$, FITC, and UV) was examined with a 63x magnification objective (HCX PL APO 63x/1.32 oil PH3 CS) in a confocal microscope (SP2, Leica) equipped with UV-excitation (Argon laser-UV 351/364-nm), and the lasers used for green and red lights were: Argon 488-nm and Helium-Neon 543-nm, respectively. Images were acquired with the corresponding Leica Confocal Software. Figures composed of several images were prepared with Adobe Photoshop software and are presented in RGB color format. In a few experiments we tested MMP-9 immunoreactivity in cultured mouse fibroblasts that were kindly provided by Dr. Joan Serratosa.

Flow Cytometry analyses

The cell cycle was studied by measuring DNA cell content after incubating fresh cells with 0.1% Triton X-100, 0.2 mg/mL RNAse and 25 σg/mL propidium iodide (PI) for 30 min. Flow cytometry was carried out using an Epics XL flow cytometer (Coulter Corporation, Hialeah, Florida). The instrument was set up with the standard configuration: excitation of the sample was done using a standard 488nm air-cooled argon-ion laser at 15mW power. Forward scatter (FSC), side scatter (SSC), red (620 nm) fluorescence for PI was acquired. Red fluorescence was collected with a 645 dichroic long filter and a 675-band pass filter. Optical alignment was based on optimized signal from 10 nm fluorescent beads (Immunocheck, Epics Division, Aberystwyth, Wales, UK). Time was used as a control of the stability of the instrument. Red fluorescence was projected on a 1024 monoparametrical histogram and DNA analysis (Ploidy analysis) was done using Multicycle software (Phoenix Flow Systems, San Diego, CA). Aggregates were excluded gating single cells by their area vs. peak fluorescence signal.

MMP-9 content along the cell cycle was analyzed by antibody staining. Cells were harvested by mild trypsinization (0.01% trypsin in PBS with 0.02% EDTA), washed with PBS and resuspended in 0.5 ml of PBS. Methanol at –20ºC was added drop to drop up to a volume of 5 ml. After 4h of fixation, cells were permeabilized with 2.5% Triton X-100 for 5 min, preincubated with 1% BSA in PBS, and incubated overnight at 4ºC with a mouse monoclonal antibody against MMP-9 (MAB 13421, Chemicon International, Inc., diluted 1:50) in a roller shaking in the presence of 1% BSA. Cells were washed twice with PBS and incubated with the secondary antibody FITC conjugated (1: 100) for 1 h. Cells were counterstained with PI as

detailed above, and flow cytometry was carried out. Green (525 nM) fluorescence for FITC conjugated antibody was collected with a 550 dichroic long filter and a 525-band pas filter. Quantification of MMP-9 stain (FITC) intensity at distinct phases of the cell cycle (PI staining) was done simultaneously on FITC/IP dotplots.

Assays of cell growth and cytotoxicity

Changes in cell growth were determined by the reduction of the tetrazolium salt 3-(4,5-dimethylthiazol-2-yl)-2,5-diphenyl tetrazolium bromide (MTT) (Sigma) to the coloured product formazan, a general measure of cellular oxidative capacity (Hansel et al., 1989). MTT was dissolved at a concentration of 5 mg/ml in PBS, sterilized by filtration and stored for up to 1 month at 4ºC, protected from light, and tightly capped. This was added to the 96-well cell culture plates at a final concentration of 0.5 mg/ml and the plates were returned to an incubator. Two hours later, incubation was terminated by adding extraction solution (100 σl per well) containing 20% sodium dodecyl sulphate (SDS) in N,N-dimethyl formamide/water (1:1), pH 4.7. The plates were tightly wrapped with Parafilm to avoid evaporation and incubated overnight at 37ºC. Optical density (OD) was measured at 570 nm (reference wavelength 630 nm), using the extraction buffer solution as a blank, in a plate reader (iEMS MF, Labsystems, Helsinki, Findland).

Cell number counting was determined in parallel experiments using the trypan blue dye exclusion assay to check the viability of the cells. Cultures in 12-well plates were washed with PBS and mildly trypsinized in the presence of 0.02% EDTA. The reaction was stopped by adding 5% FBS and the cells were washed and resuspended in 0.5 ml of PBS. Half ml of 0.4% Trypan Blue solution (w/v) was added to each sample, mixed, and allowed to stand for 5 to 15 min. Viable (non-stained) and non-viable (stained) cells were counted in a hemocytometer.

The presence of mitosis was studied in 24-well plates after nuclear staining with Hoechst 33258 (Sigma). Staining was observed under an inverted microscope (IX50/IX70, Olympus) equipped with an inverted reflected light fluorescence observation attachment (IX-FLA) containing a mercury lamp and appropriate filter cube (U-MWU, BP 330-385 nm excitation) and barrier filter (BA420) for UV-light. Mitotic figures were counted and they were related to the number of cells in each microscopic field using the 20x objective.

PI staining was used to identify the presence of dead cells in fresh (non-fixed) cultures. PI enters cells with damaged membrane and greatly increases its fluorescence by binding to nucleic acids. PI was added to the cultures at a final concentration of 15 σg/mL and was incubated for 30 min, then media with PI was washed with warm PBS and the cultures were immediately observed under the inverted microscope (IX50/IX70, Olympus), as above, using an appropriate filter cube (U-MNG, BP 530-550 nm excitation) and barrier filter (BA590).

Gelatinase extraction and gel zymography

Culture medium was separated from the cells, which were trypsinized and washed with PBS, and the cellular pellets were subjected to detergent extraction, and purification of gelatinolytic activity following the method described by Zhang and Gottschall (1997), with modifications as reported (Planas et al. 2000, 2001, 2002). Briefly, samples were homogenized in lysis buffer (250 σl per 2-4 100-mm dishes) containing detergents (Brij-35 and 1% triton X-100). All reagents, unless otherwise stated, were from Sigma. Homogenates were centrifuged at 12,000-x *g* for 5 min, and an aliquot of the supernatant was taken as the protein fraction for Western blot analysis. The rest of the supernatant was incubated with gelatin-Sepharose 4B (Pharmacia) (25 σl) for 1 h at 4°C. After washing, MMPs were separated from the sepharose-pellet by incubating with 30 σl of elution buffer containing 10 % DMSO for 30 min at 4 °C. Gel zymography was carried out with samples of extracted cells (equivalent to 50 σg of protein in the supernatant after homogenization). Gels containing 10% acrylamide and porcine gelatin (1 mg/ml) were prepared and electrophoresis followed by gel staining were carried out, as reported (Planas et al., 2000). A mixture of MMP-9 and MMP-2 containing gelatinase (CC073, Chemicon International, Inc.) was used as a standard.

Western blotting

Samples from the protein fraction were subjected to Western blot analysis as reported (Planas et al., 2000) with a mouse monoclonal antibody against MMP-9 (MAB 13420, Chemicon International, Inc.) diluted 1:150. A mouse monoclonal antibody against η-tubulin (Boehringer Mannheim) diluted 1:5000, was used to control protein gel loading. Secondary antibody was peroxidase-linked anti-mouse Ig, (Amersham, Madrid, Spain) diluted 1:2000. The reaction was developed with a chemiluminescence method. Gels were scanned with a Kodak camera (DC-120) and analyzed with appropriate software to determine band intensity (Kds1D, Kodak).

In situ gelatin zymography

Cells were cultured in 8-well plastic slides and incubated with 10 σg/mL FITC-labeled DQ-gelatin (Molecular Probes) for 1 h at RT in a humidified chamber. Then sections were washed with PBS and counterstained with Hoechst 33258 dye. Green FITC fluorescence indicative of gelatinase activity was observed under a 20x objective of the fluorescence microscope (Eclipse E1000M/E1000, Nikon) with the corresponding filter cube (B-2A), as stated above for immunostaining. The same fields were observed under the UV-light to visualize DNA staining with Hoechst 33258 using the appropriate filter cube (UV-2A, Nikon).

RESULTS

MMP-9 in mitotic cells

We studied the cellular distribution of MMP-9 in SH-SY5Y cells (Fig. 1A) by means of immunocytochemistry. Faint MMP-9-like staining was found in the cytoplasm and cell extensions (Fig. 1B), and unexpectedly we detected very intense staining in cells undergoing mitosis (arrows in Fig. 1). This was confirmed with double staining with bisbenzimide (Hoechst 33258 dye), which binds DNA and produces UV light showing brighter staining in the condensed DNA of dividing cells (arrows in Fig. 1C). In mitotic cells (Fig. 1 D-I), MMP-9-like staining was distributed within the cell, excluding the area of the chromosomes. The specificity of the immunoreaction was tested by using two different monoclonal antibodies against MMP-9 (see Methods), by using two different fluorescent secondary anti-mouse antibodies (one labeled in green with FITC-fluorochrome –Fig. 1B-,

and the other labeled in red with Cy3^{TM}-fluorochrome –Fig. 1D, G-), and by omitting the primary antibody but not the secondary fluorescent antibody, which gave no signal.

In addition, we performed MMP-9 immunostaining with a mouse monoclonal antibody against MMP-9 followed by a FITC-labeled anti-mouse secondary antibody, combined with propidium iodide staining, and analyzed the cells by flow cytometry. FITC-immuno-fluorescence of cells at S/G2/M phases was 5.11±0.05 fluorescence units, a value that was higher (t-test $p<0.0005$, $n=4$) than that of cells at G1 phases (3.82±0.18 fluorescence units). Thus indicating that MMP-9-like staining was enhanced in cells that undergo division.

In situ gelatin zymography using fluorescein-labeleld gelatin showed some low gelatinase activity in the cells and a notably stronger activity in mitotic cells (Fig. 1J), as revealed with double staining with Hoechst 33258 dye (Fig. 1K). Gelatinase activity in mitotic cells was detected within the cell body excluding the chromosomal area (Fig. 1J,K).

Dynamic distribution of MMP-9-like staining in relation to microtubules during mitosis

MMP-9-like staining was very strong at prophase (Fig. 2A). In order to examine the cellular distribution of MMP-9-like immunoreactivity in relation to that of microtubules, we carried out double staining against MMP-9 and η-tubulin (Fig. 2). MMP-9-like immunoreactivity was detected surrounding the mitotic spindle at the different stages of mitosis. At prometaphase the nuclear envelope fenestrates allowing the microtubules entering the nucleus and forming the mitotic spindle (see spring-like lattice structure labeled in green in the cell at the top of Fig. 2C). A thick wall of MMP-9-like staining was distributed beyond the spindle though prometaphase and metaphase (Fig. 2C). At early anaphase, when partition of the two sister chromatids is initiated, and before the two centrioles also begin to separate towards opposite sides of the cell, the confocal microscopy projection image (Fig. 2D) showed MMP-9 mainly distributed in between the two poles of the mitotic spindle. More detailed examination of different 0.5 σm sections of the cell with confocal microscopy (Fig. E-I) showed MMP-9-like staining in a central location between the two poles of the spindle. During cytokinesis (Fig. 2J), by which segmentation takes place, a ring of MMP-9 surrounded two clearly separated zones containing one centriole each, which were interconnected through the microtubules of the spindle. At this period the segmentation sulk (arrow in Fig. 2J) is formed allowing cytoplasm division and further separation of the two daughter cells. Omission of the primary antibody against MMP-9, but in the presence of the secondary Cy3^{TM} -labeled antibody, followed by reaction with the primary anti-η-tubulin antibody and then the FITC-labeled secondary antibody showed no red reaction, as only green staining evidencing η-tubulin immunoreactivity became apparent (Fig. 2B). In addition, we examined whether this particular distribution of MMP-9 detected in SH-SY5Y cells was also observed in a different cell type. We performed MMP-9 immunocytochemistry in mouse fibroblasts and we also observed higher intensity of staining in mitotic cells (Fig. 2L). These results indicate that MMP-9, or a protein resembling MMP-9, might be involved in the rearrangement of the nuclear matrix, cell structures, and/or cytoplasm to allow cell division once DNA was duplicated.

The MMP-9-like protein might contribute to chromatide separation

Cells expressed MMP-9-like protein surrounding the cell during the early phases of mitosis from prophase to metaphase, before the two sister chromatids begin to separate (Fig.3, A,B, and Fig. 4A, B). Yet, MMP-9-like immunoreactivity became apparent in the center of the cell at the time that the two chromatids began to separate at anaphase (Fig. 3C, Fig. 4C, D). At telophase, when the two sets of chromosomes reach the poles of the spindle and become completely partitioned (Fig. 3D), MMP-9-like immunoreactivity was located within the segmentation sulk surrounding the contractile microtubule ring. At cytokinesis, immunoreactivity surrounded the daughter cells (Fig. 3E).

MMP-9 inhibitors caused cell cycle alterations

The cell cycle was examined by flow cytometry using propidium iodide staining after incubating the cells for 1 or 3 days in the presence or absence of MMP-9 inhibitors. Cells were incubated with two different MMP inhibitors. Inhibitor A is specific for MMP-9 and MMP-2, whereas inhibitor B was designed to target MMP-9 and MMP-13. Overall the inhibitors increased de percentage of cells in S phase, whereas they reduced the percentage of cells in G1 phase (Fig.

5) (n=4-9 samples from at least two independent experiments). For inhibitor A (Fig. 5A), the most marked effects were detected at 1 day when, according to the one-way ANOVA, S phase increases related to

controls were of 19% ($p<0.05$) and 38% ($p<0.001$) at the doses of 15 and 20 σM, respectively. Significant reductions in the percentage of cells in G1 phase were detected related to controls, -10% ($p<0.05$) and -17% ($p<0.001$) at the doses of 15 and 20 σM, respectively. For inhibitor B (Fig. 5B), the most marked effects were seen at 3 days when an increase of around 20% ($p<0.001$) in the percentage of cells in S phase was detected at the doses of 10 and 15 σM, together with an increase of about 16% ($p<0.05$ at the dose of 10 σM) in the percentage of cells at G2 phase. This inhibitor significantly reduced the percentage of cells in G1 phase by around -5 % ($p<0.001$). Examples of cycle analysis data are shown in Fig. 5C for a control and in Fig. 5D for MMP inhibitor A. These results indicate that the MMP inhibitors reduced the ability of cells to divide after DNA was synthesized during S phase, and cell proliferation was subsequently impaired.

MMP inhibitors reduce cell growth

We seeded the cells, let them grow for two days and then we incubated the cultures (time 0) in the presence or absence of different inhibitor concentrations (5-30 σM inhibitor A, and 1-35 σM inhibitor B). Gel zymography with cellular extracts showed the presence of intrinsic gelatinases in SH-SY5Y cells (Fig. 6A). In control cells gelatinase activity was essentially due to MMP-2, as the band corresponding to MMP-9 was comparatively fainter. MPP inhibitor A targeting MMP-9 and MMP-2 was found to reduced both gelatinase bands, whereas inhibitor B, mainly affected MMP-9 (Fig. 6B). Gelatinase bands were no longer seen when zymography gels were exposed to EDTA in the incubation buffer, as they require Ca^{2+} (not shown).

Three days after incubation in the presence or absence of the inhibitors we carried out the cell growth and viability MTT assay. MTT values were expressed as percentage of control (vehicle-treated in the absence of inhibitors). The inhibitors significantly prevented cell growth in a concentration-dependent manner as the MTT values were progressively reduced in relation to the control in a concentration-dependent manner (Fig. 6C, D). Data were fit to sigmoid concentration-response curves with variable slope (GraphPad Prism software). The goodness of the fit was indicated by R^2, which was 0.87 for inhibitor A and 0.91 for inhibitor B.

Reduction of cell growth by MPP inhibitors was not dependent on cell death

We performed the MTT assay at time 0 and at 3 days following incubation in the presence or absence of the inhibitors and referred the MTT values at 3 days as the percent increase in relation to MTT at time 0 (basal), in order to test whether inhibitors reduced MTT to values

no signs of increased cell death were observed (not shown).

Action of a growth factor and effect of MMP inhibitors

Treatment with 10 ng/ml TGF-ζ for 6 days (Fig. 9 A, B) increased cell growth and proliferation as revealed by the MTT assay (Fig. 9C) and by cell counting (Fig. 9D), and more mitotic figures were seen after DNA staining with Hoechst 33258 dye (2.0±0.08 % mitotic cells) compared with controls at the same time point (1.4±0.10 % mitotic cells). TGF-ζ-induced cell growth was dependent on the activity of the EGFR, as inhibition of the receptor tyrosine kinase activity with 10 σM DAPH reduced cell growth ($p<0.001$) and returned growth rate to control values (Fig. 9E). Exposure of cultures treated with TGF-ζ to MMP-9 inhibitors for 2 days significantly reduced MTT values in a dose dependent manner (Fig. 9F, G), suggesting that MMP-9 activity supports culture cell growth under a variety of conditions bearing different cell growth rates.

Expression of MMP-9 in the cells: effect of TGF-ζ

Western blotting showed the prozymogen form of MMP-9 as a 94-kDa band (Fig. 9A). TGF-ζ enhanced the expression of a lower molecular weight form of around 88-kDa, which was likely originated from proteolytic cleavage of the proform (Fig. 9H). Zymography assays of cellular gelatinase extracts (Fig. 9I) revealed that TGF-ζ enhanced gelatin degradation at a band of about 88-kDa, thus corresponding to an active MMP-9 form. These results suggest that MMP-9 is further activated in cells with a higher growth rate after TGF-ζ-treatment.

DISCUSSION

The results of this study strongly evidenced that MMP-9, or a protein resembling MMP-9, plays some function during cell division. First, we detected intense MMP-9-like staining in cells undergoing mitosis and MMP-9-like staining was distributed around the chromosomes in a dynamic and well orchestrated fashion at the different mitotic stages; second, MMP-9 inhibitors disturbed the cell cycle preventing that, once DNA is duplicated, cells at S/G2 enter cell division, and subsequently the inhibitors reduced cell culture growth; and third, stimulation of cell proliferation with a growth factor, TGF-ζ, was associated with MMP-9 activation. Because of the intracellular precise and dynamic distribution of MMP-9-like immunoreactivity during mitosis, the present results suggest that this metalloproteinase, or a likely protein, might participate in several steps of cell division in a highly controlled manner. It is therefore tempting to hypothesize that an MMP-9-like protein was involved in certain mitotic processes, such as rearrangement of the cellular matrix, breaking down the nuclear envelope, and/or cytoplasm segmentation.

The highest MMP-9 expression was found at the early phases of mitosis. As cell division progressed and the mitotic spindle was formed, it became apparent that MMP-9 was located surrounding the microtubules. In the pro-metaphase the nuclear membrane desintegrates, possibly through the tension generated by cytoplasmic dynein anchored on the outside of the nucleus (Gonczy, 2002). From the present observations, the possibility that an MMP-9-like activity might contribute to nuclear membrane breakdown and/or nuclear matrix re-organization deserves to be further explored. The nuclear matrix does not only maintain nuclear architecture but it is also an important cell cycle regulator (Loidl and Eberharter, 1995). It is composed of the nuclear lamina, which is located between the inner nuclear membrane and the peripheral chromatin and it is made of the lamins, the nucleolus and nuclear matrix proteins arranged in a fibrillogranular network (Bosman, 1999). Several lines of evidence now suggest that nuclear lamins are also present within the nucleoplasm and could form part of the nuclear matrix (Neri et al., 1999), and that proteins of the nuclear lamina specifically interact with the chromatin (Goldberg et al., 1999; Gotzmann and Foisner, 1999; Gruenbaum et al., 2000). The nuclear lamina is disassembled during mitosis, a process that is dependent on the phosphorylation of lamins (Ottaviano and Gerace, 1985). Interestingly, the nuclear matrix structure is deeply altered by malignancy, which leads to disturbances on protein folding, on the fidelity of genome replication, and on gene expression (Nickerson, 1998).

During the progression from metaphase to anaphase, when spindle length increases, MMP-9 appeared in between the two chromatids as they progressively separate from each other towards the opposite poles of the mitotic spindle. This location indicates that an MMP-9-like activity might participate in cellular matrix re-arrangement to facilitate separation of the sister chromatids, which hold together through the cohesin complex (Biggins and Murray, 1998; Orr-Weaver, 1999). Sister chromatid cohesion and separation at the metaphase to anaphase transition is essential to allow precise chromosome segregation, but the mechanism that controls this process is not yet fully understood (Biggins and Murray, 1998). Certain proteins, such as securin, maintain the cohesion between sister chromatids, whilst proteolytic proteins such as the endopeptidase separase remain inhibited until metaphase by affinity binding to securin and by specific inhibitory phosphorylation. Progression from metaphase to anaphase requires at various steps promoting loss of sister chromatid cohesion by the action of ubiquitin-dependent proteolysis (Yanagida, 1995). Proteolytic cleavage of the cohesin complex is necessary for sister separation to opposite poles of the cell during anaphase (Nasmyth, 1999; Uhlmann et al., 1999; Nasmyth et al., 2002). Separases become activated as their inhibitory proteins suffer proteolysis mediated by the anaphase-promoting complex (Nasmyth, 1999). Yet, at anaphase separase itself suffers proteolytic cleavage at three adjacent sites concomitant with separase activation (Zou et al., 2002). At the metaphase to anaphase transition both adequate sister chromatid separation and anaphase-promoting complex activation are necessary for spindle elongation and stability in budding yeast, but although this involves securin-dependent targets it seems to be independent of the separase Esp1 (Severin et al., 2001). These findings evidence the complexity of this highly coordinated process and the fact that certain proteases that remain unidentified participate in sister chromatid separation and ensure spindle stability.

Treatment with TGF-ζ, a mitogenic growth factor acting at the EGFR (Massague, 1983, Reynols et al., 1983; Derynck, 1988), increased cell growth and proliferation though an EGFR-dependent signaling pathway, and caused MMP-9 activation, in agreement with previous results showing that EGFR up-regulates MMP-9 (Kondapaka et al., 1997, Visscher et al., 1997; Reddy et al., 1999; O-charoenrat et al., 2000). MMP-9 inhibitors reduce tumor cell growth (Price et al., 1999; Rabbani et al., 2000; Tonn et al., 1999). Here, TGF-ζ-induced culture cell growth was also sensitive to the action of MMP-9 inhibitors, thus suggesting that MMP-9 activation was involved in this process. This is in consonance with the evidence that the EGFR signaling pathway is a target for the treatment of certain types of cancer (Humphreys and Hennighausen, 2000).

Taken altogether, the present results suggest that, in addition to their role in the extracellular space, MMP-9, or a likely protein, is expressed in the cellular compartment at precise locations, and that it might be involved in certain steps of cell division.

ACKNOWLEDGEMENTS

This study was supported by a grant from the Spanish Ministry of Science and Technology (MCYT, SAF2002-01963). S. Sole was recipient of a fellowship from IDIBAPS. We thank M. Martín for technical assistance in cell culturing. We are grateful to J. Comas, R. Garcia, and A. Bosch from the 'Serveis Científico-Tècnics' of the University of Barcelona at the 'Campus Diagonal' (J.C. and R.G.) and at the 'Campus Casanova' (A.B.) for excellent technical support with the flow cytometer (J.C.) and the confocal microscopes (R.G. and A.B.). We are indebted to Dr. Joan Serratosa from our Institution for kindly providing cultures of mouse fibroblasts.

REFERENCES

Aoudjit, F., S. Masure, G. Opdenakker, E. Potworowski, and Y. St-Pierre. 1999. Gelatianse B (MMP-9), but not its inhibitor (TIMP-1), dictates the growth rate of experimental thymic lymphoma. *Int. J. Cancer* 82:743-747.

Biggins, S., and A.W. Murray. 1998. Sister chromatid cohesion in mitosis. *Curr. Opin. Cell Biol*. 10:769-775.

Bosman, F.T. 1999. The nuclear matrix in pathology. *Virchows Arch*. 435:391-399.

Derynck, R. 1988. Transforming growth factor-ζ. *Cell* 54:593-595.

Goldberg, M., A. Harel, and Y. Gruenbaum. 1999. The nuclear lamina: molecular organization and interaction with chromatin. *Crit. Rev. Eukaryot. Gene Expr*. 9:285-293.

Gonczy P. 2002. Nuclear envelope: torn apart at mitosis. *Curr. Biol.* 12:R242-244.

Gotzmann, J., and R. Foisner. 1999. Lamins and lamin-binding proteins in functional chromatin organization. *Crit. Rev. Eukaryot. Gene Expr.* 9:257-265.

Gruenbaum, Y., K.L. Wilson, A. Harel, M. Goldberg, and M. Cohen. 2000. Review: nuclear lamins--structural proteins with fundamental functions. *J. Struct. Biol.* 12:9313-9323.

Humphreys, R.C., and L. Hennighausen. 2000. Transforming growth factor alpha and mouse models of human breast cancer. *Oncogene* 19:1085-1091.

Kondapaka, S. B., R. Fridman, and K.B. Reddy. 1997. Epidermal growth factor and amphiregulin up-regulate matrix metalloproteinase-9 (MMP-9) in human breast cancer cells. *Int. J. Cancer* 70:722-726.

Loidl, P., and A. Eberharter. 1995. Nuclear matrix and the cell cycle. *Int. Rev. Cytol*. 162B:377-403.

Massague, J. 1983. Epidermal growth factor-like transforming growth factor. II Interaction with epidermal growth factor receptors in human placenta membranes and A431 cells. *J. Biol. Chem.* 258:13614-13620.

Miettinen, P.J., J.R. Chin, L. Shum, H.C. Slavkin, C.F. Shuler, R. Derynck, and Z. Werb. 1999. Epidermal growth factor receptor function is necessary for normal craniofacial development and palate closure. *Nat. Genet*. 22:69-73.

Moon S.K., B.Y. Cha, and C.H. Kim. 2003. In vitro cellular aging is associated with enhanced proliferative capacity, G1 cell cycle modulation, and matrix metalloproteinase-9 regulation in mouse aortic smooth muscle cells. *Arch. Biochem. Biophys*. 418:39-48.

Nasmyth, K. 1999. Separating sister chromatids. *Trends Biochem. Sci.* 24:98-104.

Nasmyth K 2002. Segregating sister genomes: the molecular biology of chromosome separation. *Science* 297:559-565.

Neri, L.M., Y. Raymond, A. Giordano, P. Borgatti, M. Marchisio, S. Capitani, and A.M. Martelli. 1999. Spatial distribution of lamin A and B1 in the K562 cell nuclear matrix stabilized with metal ions. *J. Cell Biochem*. 75:36-45.

Nickerson, J.A. 1998. Nuclear dreams: the malignant alteration of nuclear architecture. *J. Cell. Biochem.* 70: 172-180.

O-charoenrat, P., H. Modjtahedi, Rhys-Evans, W.J. Court, G.M. Box, and S.A. Eccles. 2000. Epidermal growth factor-like ligands differentially up-regulate matrix metalloproteinase 9 in head and neck squamous carcinoma cells. *Cancer Res.* 60: 1121-1128.

O-charoenrat, P., P. Rhys-Evans, W.J. Court, G.M. Box, and S.A. Eccles. 1999. Differential modulation of proliferation, matrix metalloproteinase expression and invasion of human head and neck squamous carcinoma cells by c-erb B ligands. *Clin. Exp. Metastasis,*17: 631-639.

Orr-Weaver, T.L. 1999. The ties that bind: localization of the sister-chromatid cohesin complex on yeast chromosomes. *Cell* 99:1-4.

Ottaviano, Y., and L. Gerace. 1985. Phosphorylation of the nuclear lamins during interphase and mitosis. *J. Biol. Chem*. 260:624-632.

Planas, A.M., S. Solé, C. Justicia, and E. Rodríguez-Farré. 2000. Estimation of gelatinase content in rat brain: effect of focal ischemia. *Biochem. Biophys. Res. Commun*.278:803-807.

Planas A.M., S. Solé, and C. Justicia. 2001. Expression and activation of matrix metalloproteinase-2 and –9 in rat brain after transient focal cerebral ischemia. *Neurobiol. Dis.* 8:834-846.

Planas, AM, C. Justicia, S. Solé, B. Friguls, A. Cervera, A. Adell, and A. Chamorro. 2002. Certain forms of matrix metalloproteinase-9 accumulate in the extracelular space after microdialysis probe implantation and middle cerebral artery occlusion/reperfusion. *J. Cereb. Blood Flow Metab.* 22:918-925.

Price, A., Q. Shi, D. Morris, M.E. Wilcox, P.M. Brasher, N.B. Rewcastle, D. Shalinsky, H. Zou, K. Appelt, R.N. Johnston, V.W. Yong, D. Edwards, and P. Forsyth. 1999. Marked inhibition of tumor growth in a malignant glioma tumor model by a novel synthetic matrix metalloproteinase inhibitor AG3340. *Clin. Cancer Res*. 5:845-854.

Rabbani, S.A., P. Harakidas, Y. Guo, D. Steinman, S.K. Davidsen, and D.W. Morgan. 2000. Synthetic inhibitor of matrix metalloproteases decreases tumor growth and metastases in a synergic model of rat prostate cancer *in vivo*. *Int. J. Cancer* 87: 276-282.

Reynols F.H., G.J. Todaro, C. Fryling, and J.R. Stephenson. 1983. Human transforming growth factors induce tyrosine phosphorylation of EGF receptors. *Nature* 292:259-262.

Reddy, K.B., J.S. Krueger, S.B. Kondapaka, and C.A. Diglio. 1999. Mitogen-activated protein kinase (MAPK) regulates the expression of progelatinase B (MMP-9) in breast epithelial cells. *Int. J. Cancer* 82:268-273.

Rooprai, H.K., G.J. Rucklidge, C. Panou, and G.J. Pilkington. 2000. The effects of exogenous growth factors on matrix metalloproteinase secretion by human brain tumour cells. *Br. J. Cancer* 82:52-55.

Severin, F., A.A. Hyman, and S. Piatti. 2001. Correct spindle elongation at the metaphase/anaphase transition is an APC-dependent event in budding yeast. *J. Cell Biol*. 155:711-718.

Springman, E.B., E.L. Angleton, H. Birkedal-Hansen, and H.E. Van Wart. 1990. Multiple modes of activation of latent human fibroblast collagenase: evidence for the role of a Cys^{73} active-site zinc complex in latency and a "cysteine switch" mechanism for activation. *Proc. Natl. Acad. Sci. U.S.A.* 87: 364-368.

Stetler-Stevenson, W.G. 1990. Type IV collagenases in tumor invasion and metastasis. *Cancer Metastasis Rev*. 9:289-303.

Tonn, J.-C., S. Kerkau, A. Hanke, H. Bouterfa, J.G. Mueller, S. Wagner, G.H. Vince, and K. Roosen. 1999. Effect of synthetic matrix-metalloproteinase inhibitors of invasive capacity and proliferation of human malignant gliomas in vitro. *Int. J. Cancer* 80: 764-772.

Ueda, M., M. Ueki, Y. Terai, A. Morimoto, H. Fujii, K. Yoshizawa, and T. Yanagihara. 1997. Stimulatory effects of EGF and TGF-ζ on invasive activity and 5'-deoxy-5-fluorouridine sensitivity in uterine cervical-carcinoma SKG-IIIb cells. *Int. J. Cancer* 72:1027-1033.

Uhlmann, F., F. Lottspeich, K. Nasmyth. 1999. Sister-chromatid separation at anaphase onset is promoted by cleavage of the cohesin subunit Scc1. *Nature* 400:37-42.

Visscher, D.W., F.H. Sarkar, T.C: Kasunic, and K.B. Reddy. 1997. Clinicopathologic analysis of amphiregulin and heuregulin immunostaining in breast neoplasia. *Breast Cancer Res. Treat*. 45:75-80.

Woessner, Jr.J.F. 1991. Matrix metalloproteinases and their inhibitors in connective tissue remodeling. *FASEB J.* 5:2145-2154.

Yamashita, T., M. Fujii, T. Tomita, R. Ishiguro, M. Tashiro, Y. Tokumaru, Y. Imanishi, M. Kanke, K. Ogawa, K. Kameyama, and Y. Otani. 2003. The inhibitory effect of matrix metalloproteinase inhibitor ONO-4817 on lymph node metastasis in tongue carcinoma. *Anticancer Res.* 23:2297-2302.

Yanagida, M. 1995. Frontier question about sister chromatid separation in anaphase. *Bioessays* 17:519-526.

Yong, V.W., C.A. Krekoski, P.A. Forsyth, R. Bell, and D.R. Edwards. 1998. Matrix metalloproteinases and diseases of the CNS. *Trends Neurosci*. 21:75-80.

Zhang, J.W., and P.E. Gottschall. 1997. Zymographic measurement of gelatinase activity in brain tissue after detergent extraction and affinity-support purification. *J. Neurosci. Meth.* 76:15-20.

Zou, H., O. Stemman, J.S. Anderson, M. Mann, and M.W. Kirschner. 2002. Anaphase specific auto-cleavage of separase. *FEBS Lett.* 528:246-250.

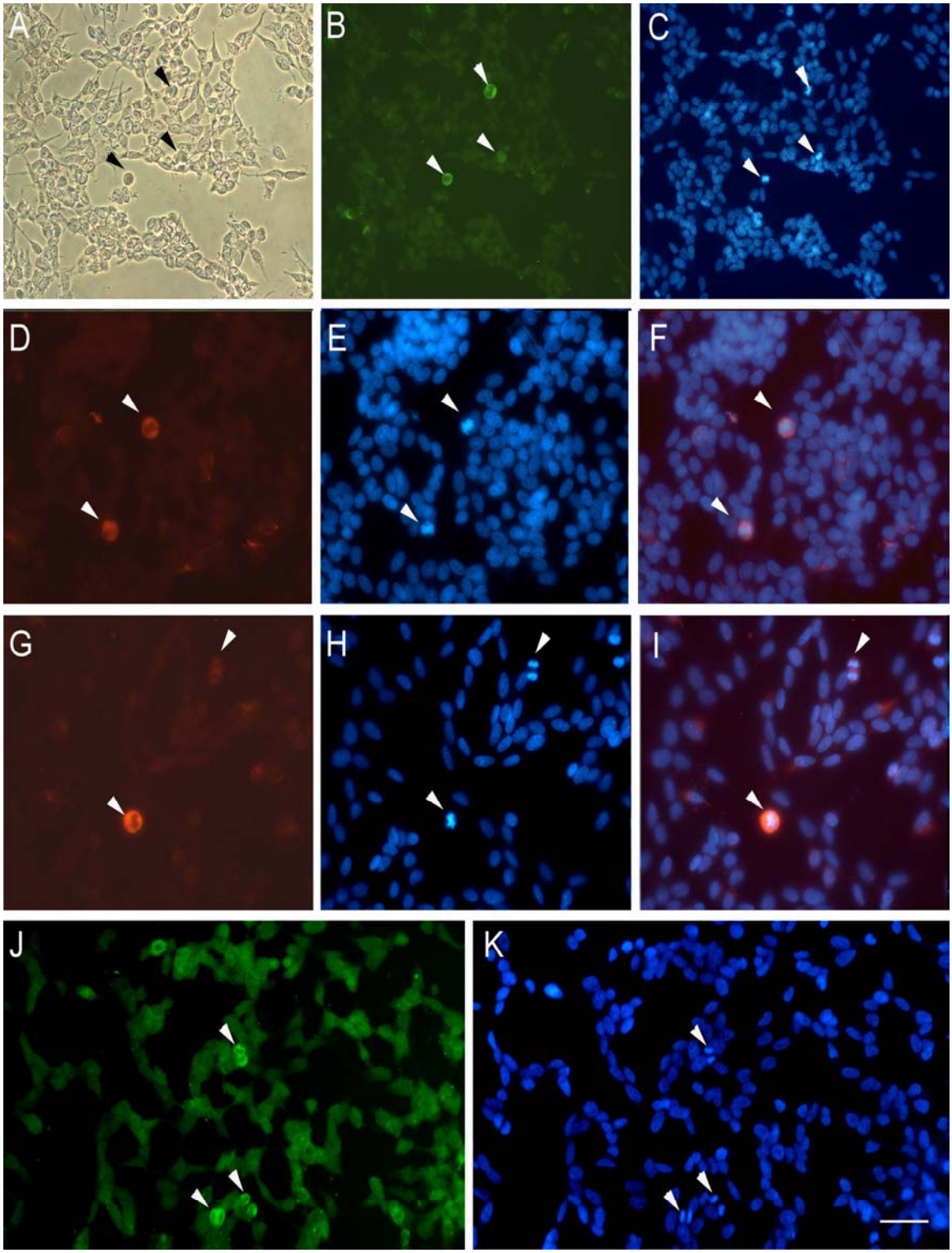

FIG. 1. High expression of an MMP-9-like protein in cells undergoing cell division A) Phase contrast image of SH-SY5Y neuroblastoma cells at the optical microscope. **B)** MMP-9-like immunofluorescent staining with a mouse monoclonal antibody (Chemicon). Arrowheads point to strongly MMP-9-like immunoreactive cells (green), **C)** corresponding to cells undergoing mitosis as revealed with Hoechst 33258 dye (blue), which stains in bright blue the dividing condensed chromosomes (arrowheads). **D)** MMP-9-like staining (red, arrowheads) and **E)** Hoechst 33258 (blue), **F)** showing in the merged image that MMP-9-like immunoreactivity (red) surrounds the DNA (bright blue), in cells at metaphase (arrowheads). **G)** MMP-9-like staining (red, arrowheads) and **H)** corresponding Hoechst 33258 stained mitotic cells (bright blue, arrowheads) at metaphase (bottom-left) and anaphase (top-right), **I)** showing again correspondence in the merged image. **J)** *In situ* gelatin zymography after incubating cultured cells with fluorescein-labeleld gelatin (see Methods). Green-fluorescent staining reveals stronger gelatinase activity in cells undergoing division (arrowheads), as revealed in **K)** with Hoechst 33258 dye (bright blue, arrowheads). Strong gelatinase activity is seen within mitotic cells in the area surrounding the chromosomes. Bar scale: A-C, J-K = 25 σm; D-I = 25 σm.

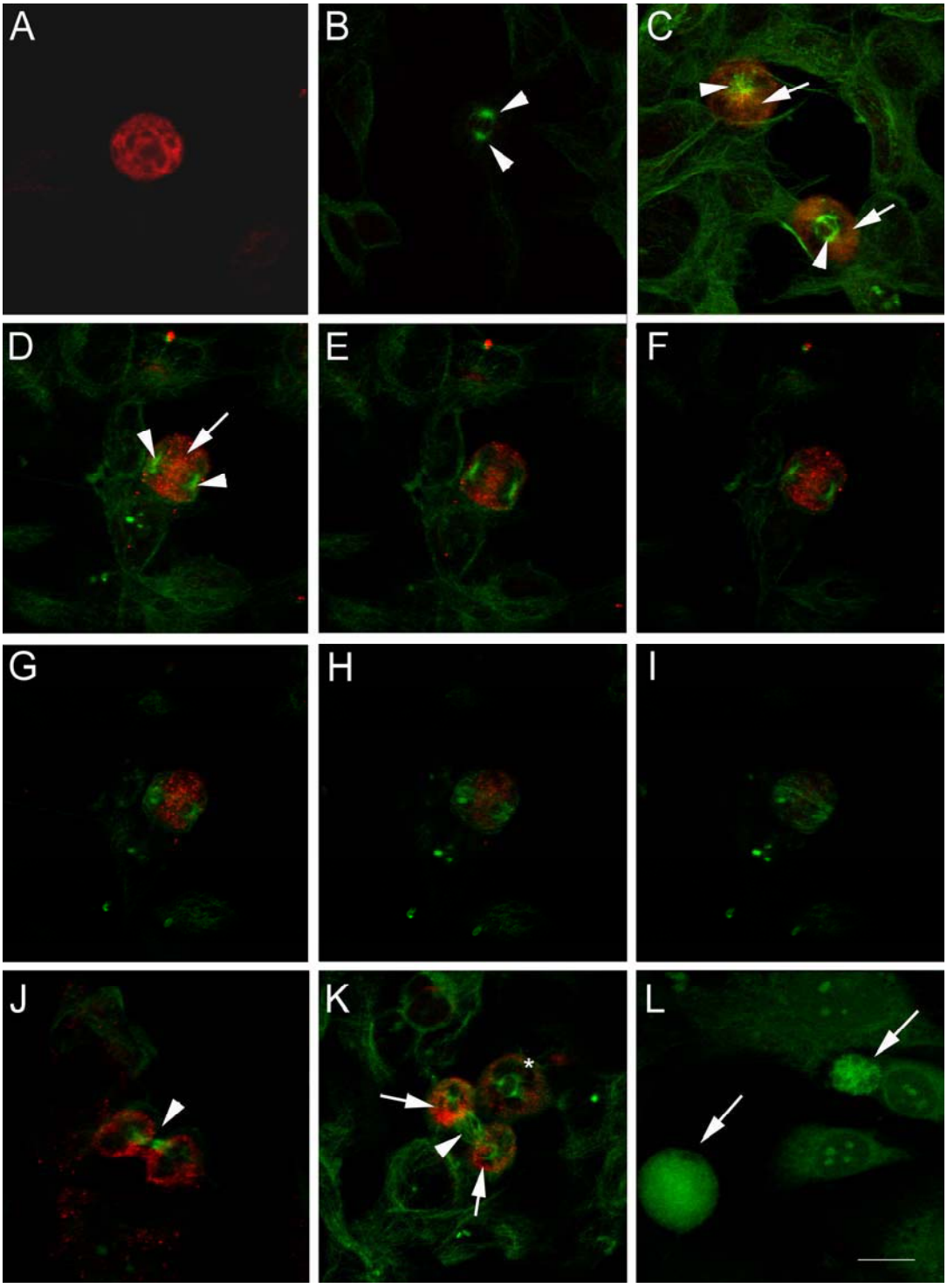

FIG. 2. The MMP-9-like protein and the mitotic spindle labeled with η-tubulin. Confocal microscope images showing MMP-9-like immunoreactivity (red in A-K, and green in L) and/or η-tubulin (green in A-K). The monoclonal antibody against MMP-9 was either from Oncogene (A) or Chemicon (B-L). Cells in A-K are SH-SY5Y neuroblastoma cells, whereas cells in L are mouse fibroblasts. **A)** Single immunocytochemistry against MMP-9 shows strong MMP-9-like staining in a cell at prophase. **B)** Negative control for double immunocytochemistry against MMP-9 and η-tubulin, in which the primary antibody against MMP-9 was omitted. Arrows show the two poles of the mitotic spindle in a dividing cell. **C)** Cells at prophase (top) and metaphase (bottom) showing MMP-9 (red, arrows) located behind the centrosomes (green, arrowheads). **D-I)** Cell at anaphase showing MMP-9 (red, arrow) between the two poles (arrowheads) of the mitotic spindle (green). (D) Shows the projection image whereas (E-I) are sequential 0.5 σm sections through the cell. **J)** Cell at cytokinesis showing the two separated daughter cells surrounded by MMP-9 and connected by the rest of spindle microtubules at the segmentation sulk (arrow). **K)** Cell at prometaphase (asterisk); and cell at cytokinesis showing two clearly distinguished MMP-9-like stained areas (red, arrows) surrounding the two daughter cells, which are connected through the microtubules of the spindle (arrowhead). **L)** MMP-9-like staining (shown in green with a FITC-labeled secondary antibody) is stronger in dividing (arrows) than in resting fibroblasts. Bar scale: 15 σm.

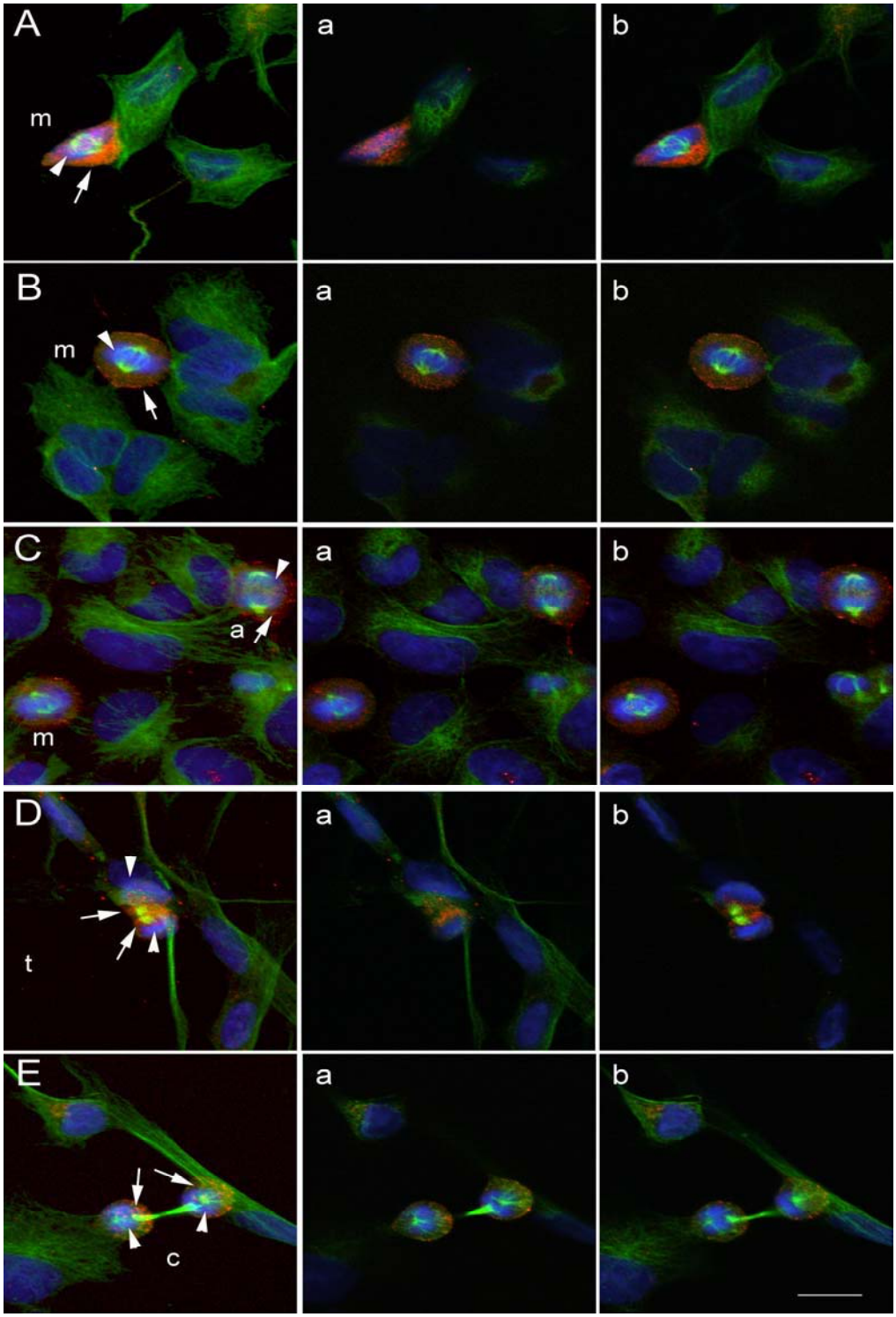

FIG. 3. MMP-9-like immunoreactivity through the different mitotic stages. Staining with antibodies against MMP-9 (Chemicon) (red) and η-tubulin (green), and Hoechst DNA staining (blue). Series A-E show cells at different phases of mitosis. The first picture of each series shows the maximal projection confocal image, while pictures a-b of each series correspond to 0.5 σm -thick sections of the same cell. **A** and **B)** Cells at metaphase (m), showing DNA condensation (blue, arrowhead) and the formation of centrosomes (green), as labeled with η-tubulin, are surrounded by intense red staining against MMP-9 (arrow). **C)** Two mitotic cells, one at metaphase (m) (bottom-left) and one at anaphase (a) (top-right). The cell at anaphase, characterized by a greater separation between the poles of the spindle and chromatid partition (arrowheads), shows MMP-9-like (arrow) staining that is located surrounding the DNA and also between the separating chromatids. **D)** Cell at telophase, showing completed chromatid partition (arrowheads) through the contractile ring, shows MMP-9-like staining (arrows) in between the two chromatids. **F)** Two daughter cells at cytokinesis, which are still connected through the rest of the mitotic spindle or medial corps (green), show MMP-9-like staining (arrows) surrounding the chromatids (arrowheads). Bar scale: 15 σm.

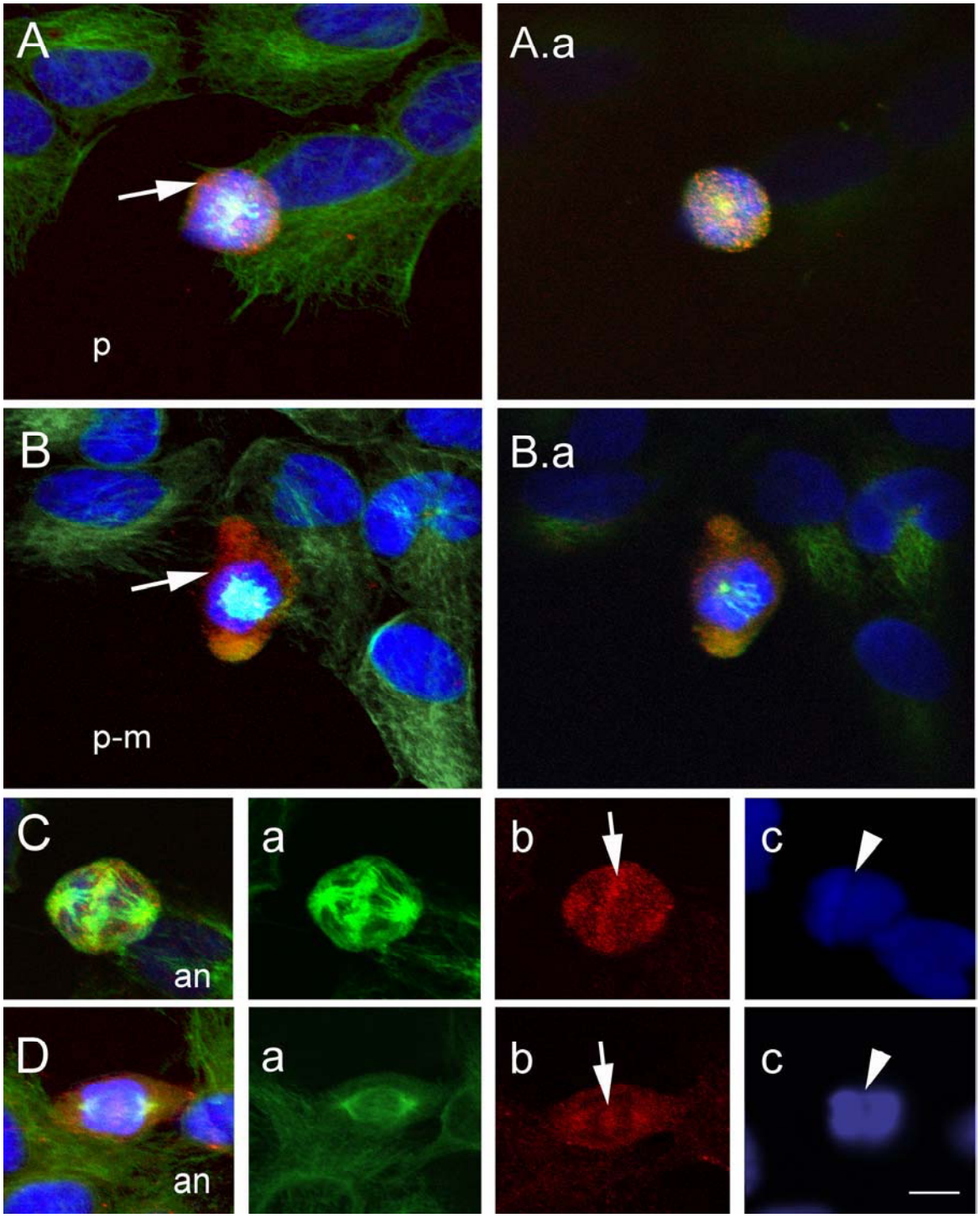

FIG. 4. Confocal microscopy images showing details of the subcellular location of MMP-9-like immunoreactivity at certain mitotic phases. Staining with antibodies against MMP-9 (Chemicon) (red) and η-tubulin (green), and Hoechst DNA staining (blue). **A)** Projection confocal image of a cell at prophase (p) surrounded by MMP-9-like immunoreactivity (arrow). **A.a)** 0.5 σm-thick section of the cell shown in A. The zone of microtubule (green) depolimerization for centrosome formation is in close vicinity with MMP-9-like immunoreactivity (red), as shows the yellow area in the center of the cell. **B)** Projection confocal image of a cell at late prophase-prometaphase, showing a thick wall of intense MMP-9-like staining (arrow) surrounding the DNA (blue). **B.a)** 0.5 σm-thick section of the cell shown in B, showing the centrosome and forming mitotic spindle (light blue) on the top of DNA (dark blue). **C** and **D)** Images of cells at anaphase A (merged image) are composed of corresponding single images of **a)** η-tubulin (green), **b)** MMP-9-like immunoreactivity (red) and **c)** DNA (blue). **C)** Cell at anaphase (an) showing that MMP-9-like staining is in close vicinity with the microtubules (yellow). C.a) Enlargement of the kinetocore microtubules located in between the separating chromatids as marked in C.c) with an arrowhead. At this stage, MMP-9-like staining (arrow in C.b) is apparent between the separating chromatids. **D)** Cell at anaphase (an) showing increased separation between the poles of the spindle, with acquisition of a fusiform shape, and with MMP-9-like staining at the migrating opposite poles of the cells; D.a) shows microtubules; D.b) shows MMP-9-like staining (arrow) between the two separating chromatids (shown in C.c, arrowhead). Bar scale: 10 σm.

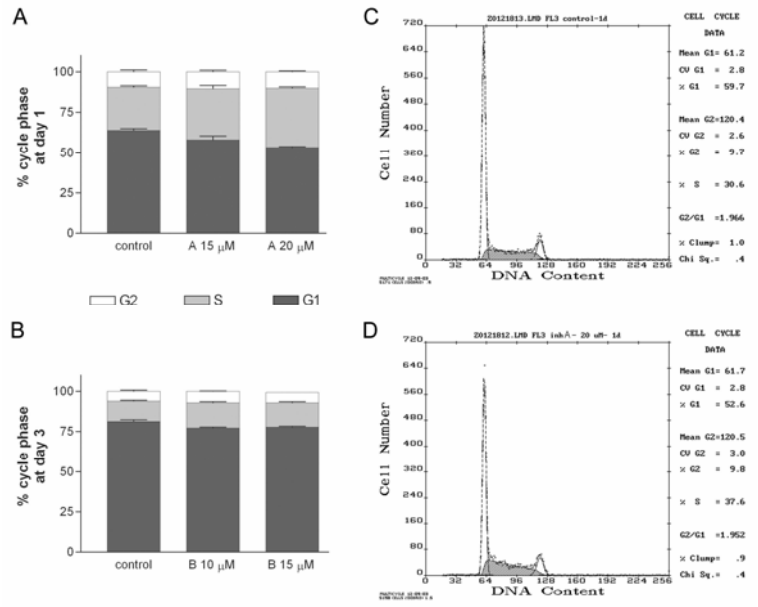

FIG. 5. MMP-9 inhibitors disturb the cell cycle. **A)** After 1-day incubation in the presence or absence of inhibitor A, cells were labeled with propidium iodide and the cell cycle was examined by flow cytometry. The percentage of cells in S phase increases ($p<0.05$ and $p<0.01$ at the doses of 15 σM and 20 σM, respectively) with the inhibitors in relation to vehicle-treated control. The inhibitor also significantly reduces the percentage of cells in G1 phase ($p<0.05$ and $p<0.01$ at the doses of 15 σM and 20 σM, respectively). **B)** Likewise, the percentage of cells in S phase ($p<0.001$) and G2 ($p<0.05$) increase, whereas that of cells in G1 decreased ($p<0.001$) after 3-day exposure to inhibitor B at the doses of 10 and 15 σM. Data is expressed as mean ± SEM (n=6-4) percentage of cells in each cycle phase. Results were analyzed with one-way ANOVA followed by Dunnett's multiple comparison test to evaluate the effects of treatments against the control. Representative examples of the flow cytometry analysis are shown in **C)** and **D)** for a control and for 20 σM inhibitor A, respectively.

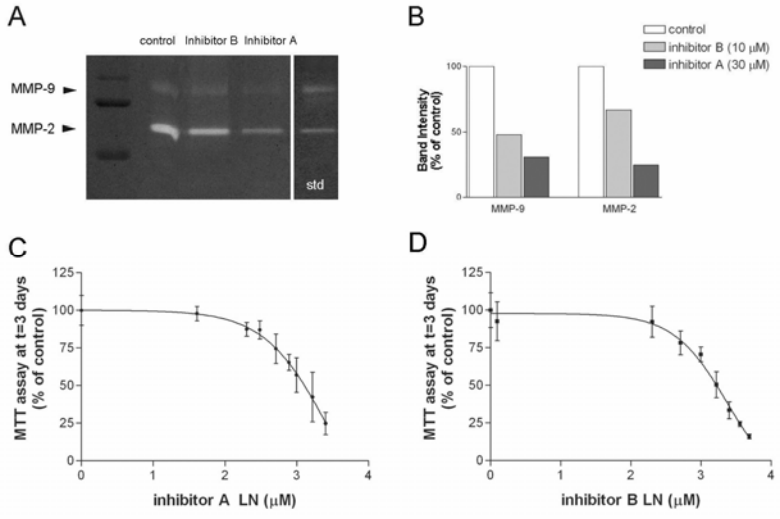

FIG. 6. MMP inhibitors reduce cell growth in a concentration dependent manner. A) Gel zymography shows reduction of gelatinase activity after incubation the cells for 3-days in the presence of the inhibitors. **B)** Inhibitor A reduces MMP-9 and MMP-2 activity, whereas inhibitor B has a higher effect on MMP-9 that on MMP-2 activity. **C, D)** Concentration-response curves where the response is evaluated with the MTT assay as an assessment of cell culture growth. Cultures were exposed to the inhibitor for three days. C) Effect of inhibitor A with concentrations ranging from 0 to 30 σM. D) Effect of inhibitor B with concentrations ranging from 0 to 35 σM. X-axis are expressed as the logarithm (LN) of the inhibitor concentration. Curves are fit with non-linear regression to a sigmoid equation using GraphPad software (Prism). R^2=0.87 and 0.91 for inhibitor A and B, respectively. Each data point is expressed as the percentage of the mean MTT value obtained in the control (3-day vehicle-treated with inhibitor concentration=0) and is the mean ± SD of n (6-18) values obtained in 2-3 independent experiments.

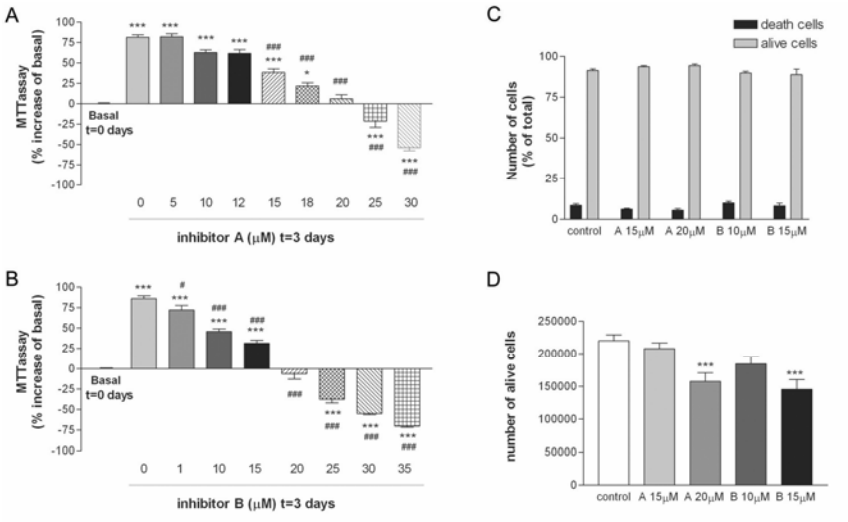

FIG. 7. MMP inhibitors reduce cell growth independently of cell death after 3-day exposure. Cells were exposed to the MMP inhibitors from day 0 to day 3, and then cell growth was assessed with the MTT assay. MTT value was compared to the basal MTT at time 0.* and # indicate comparison versus basal MTT at time 0 and control MTT at 3 days, respectively. After 3 days in culture MTT values increase in the controls by about 75% above basal ($p<0.001$). **A)** From the concentration of 15 σM, inhibitor A reduces the 3-day MTT value in relation to the control (0 σM inhibitor) (#). Increasing concentrations of inhibitor A progressively reduce the 3-day increase in relation to basal MTT (*). No increase above basal MTT is seen at 20 σM, and a reduction below basal is seen from the concentration of 25 σM. **B)** From the concentration of 1 σM, inhibitor B reduces the 3-day MTT value in relation to the control (0 σM inhibitor) (#). Increasing concentrations of inhibitor B progressively reduce the 3-day increase in relation to basal MTT (*). No increase above basal MTT is seen at 20 σM, and a reduction below basal is seen from the concentration of 25 σM. Values in A and B are expressed as percentage of increase or reduction in relation to basal MTT at time 0 and are the mean ± SEM of n (6-18) values per group obtained in 2-3 independent experiments. **C)** The mean ± SEM percentage of death and alive cells in relation to total cell number in the culture is not altered by 3-day exposure to MMP inhibitors (n= 8 values per group obtained in two independent experiments). **D)** In agreement with results of the MTT assay, trypan blue dye exclusion assay shows that the absolute number of alive cells per well (in a 12-well plate) is reduced ($p<0.001$) after exposure to 20 σM inhibitor A or 15 σM inhibitor B. Results were analyzed with one-way ANOVA followed by Dunnett's multiple comparison test to evaluate the effects of treatments against the control. One symbol: $p<0.05$, three symbols: $p<0.001$.

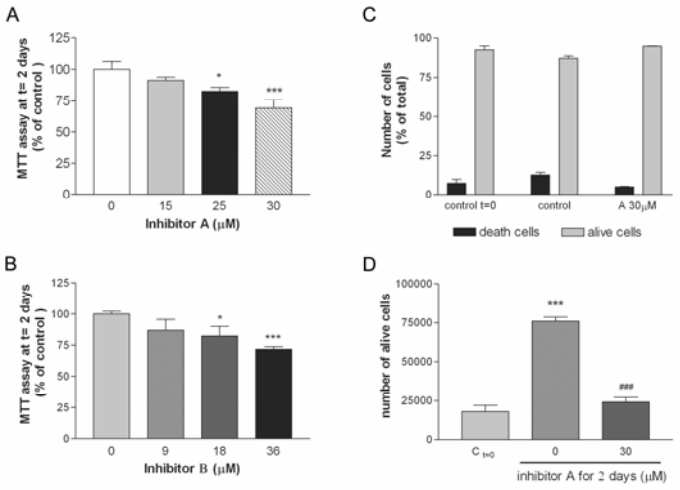

FIG. 8. Two-day exposure to MMP inhibitors reduces cell growth, whilst cell viability is not affected. The MTT assay was carried out after two-day exposure to the MMP inhibitors. **A)** 25 and 30 σM inhibitor A reduce ($p< 0.05$ and 0.001, respectively) MTT values in relation to that in vehicle-treated controls. **B)** 18 and 36 σM inhibitor B reduce ($p< 0.05$ and 0.001, respectively) MTT values in relation to that in vehicle-treated controls. Values in A and B are expressed as the mean ±SEM of 12 values per group obtained in two independent experiments. **C)** The mean ± SEM percentage of death and alive cells, as assessed by the trypan blue dye exclusion assay, in relation to total cell number in the culture is not altered by 2-day exposure to 30 σM MMP inhibitor A in relation to controls exposed to vehicle for 2 days and to basal values obtained at time 0 (n=3 values per group). **D)** The absolute number of alive cells (trypan blue exclusion) increases after two days in culture in vehicle-treated controls (* $p<0.001$). In the presence of 30 σM inhibitor A for 2 days the number of living cells is lower than in vehicle-treated controls (# $p<0.001$). Results were analyzed with one-way ANOVA followed by Dunnett's multiple comparison test to evaluate the effects of treatments against the control. One symbol: $p<0.05$; three symbols: $p<0.001$.

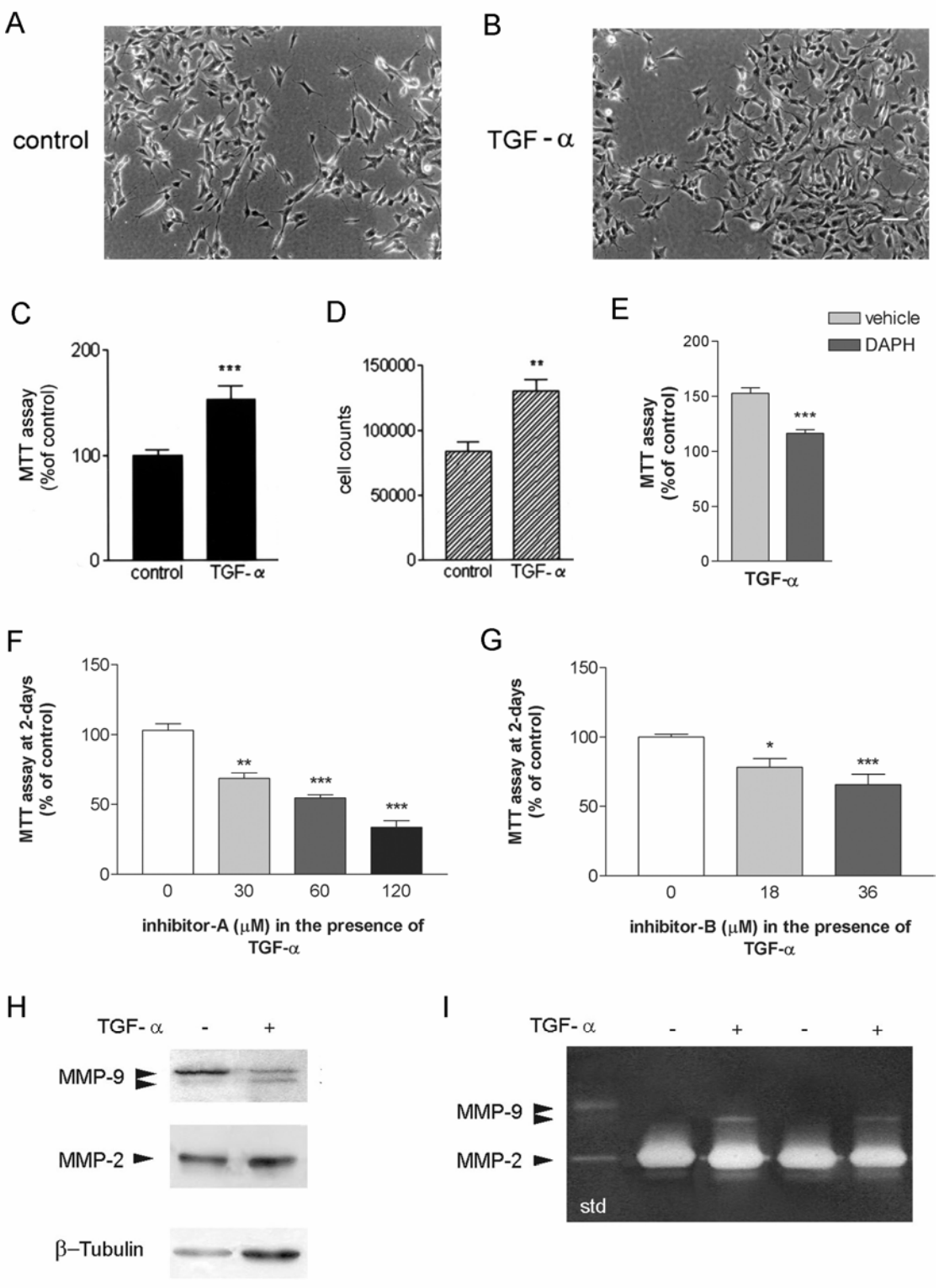

FIG. 9. TGF-ζ enhances cell growth in an MMP-9-dependent manner. A) Microscopic phase contrast images of SH-SY5Y cells after 6 days in culture under control conditions, and **B)** following exposure to 10 ng/ml TGF-ζ, a ligand of EGFR. Bar scale= 50 σm. **C)** MTT-assay (expressed as percentage of control) and **D)** total cell counts per well (trypan blue exclusion assay) show that TGF-ζ increases cell growth. **E)** DAPH, an inhibitor of the tyrosine kinase activity of the EGFR, inhibits TGF-ζ-induced cell growth, showing that the effect of TGF-ζ is mediated through EGFR. **F-G)** MTT assay following exposure to various concentrations of MMP inhibitor A (F) and inhibitor B (G) in the presence of TGF-ζ. TGF-ζ-treated cells are sensitive to the effect of MMP inhibitors as they also reduce cell growth in these cells. **H)** Western blot analysis of cell protein extracts shows a 94-kDa band of MMP-9 corresponding to the proform, together with a faint band at lower molecular weight (around 88-kDa). The intensity of this latter band is enhanced by the presence of TGF-ζ (10 ng/ml), while the intensity of the proform band tends to decrease with this treatment. **I)** Zymographic analysis of cell gelatinase extracts (see Methods) shows that MMP-9 activity is enhanced in the presence of TGF-ζ. *indicates comparison against control, * $p<0.05$, ** $p<0.001$, *** $p<0.0001$.